bruary 1983
nal Report

DOT HS 806 401

US Department of Transportation
National Highway Traffic Safety Administration

Development of Approximating Solutions for CVS Program And of Dummy Design Information

J.T. Fleck

Calspan Corp.
Advanced Technology Center
4455 Genesee Street
Buffalo, N.Y. 14225

Contract Number: DOT-HS-6-01410
Cost: $161,762

TECHNICAL REPORT STANDARD TITLE PAGE

1. Report No.	2. Government Accession No.	3. Recipient's Catalog No.
DOT HS-806-401		

4. Title and Subtitle	5. Report Date
Development of Approximating Solutions For CVS Program and of Dummy Design Information	February 1983
	6. Performing Organization Code W81

7. Author(s)	8. Performing Organization Report No.
J. T. Fleck	ZS-5994-V-1

9. Performing Organization Name and Address	10. Work Unit No.
Calspan Corporation Advanced Technology Center 4455 Genesee Street Buffalo, New York 14225	11. Contract or Grant No. DOT-HS-6-01410
12. Sponsoring Agency Name and Address U. S. Department of Transportation National Highway Traffic Safety Administration 400 Seventh Street, S.W. Washington, D. C. 20590	13. Type of Report and Period Covered Final Report August 1976-February 1983
	14. Sponsoring Agency Code

15. Supplementary Notes

16. Abstract

This report contains results of analytical studies of various aspects of the Crash Victim Simulation (CVS) computer program developed by Calspan. The general objective of the research was to develop, evaluate and recommend means and procedures for evaluating accuracies and sensitivities of various measures of crash victim response to the choice of and to the numerical values of various parameters that are used in crash victim simulations with the CVS computer program. Topics addressed in the analyses include the effect of different levels of sophistication in modelling the shoulders of the Part 572 dummy, the adequacy of the assumption that the dummy segments may be regarded as rigid bodies and vibrational modes neglected, differences between soft and hard (impulsive) contacts, surface compliance in the region of belt or air bag contacts, the effect of air bag stretch, and the need to consider inertial effects for deformations associated with certain types of contacts.

The mathematical formulation and sample application of two computer programs developed in this research project are described and listings of the programs are given in report appendices. The first of these, called the Response Measure Approximating Function Generator, is a multiparameter polynomial interpolating routine which can be useful for parametric studies by providing users with a means of interpolating response measures as a function of several parameters. The other computer program can be used to compute the properties of different chains of connected rigid bodies, each with different mass distributions, that will have identical dynamic responses so as to define dynamically equivalent systems.

17. Key Words	18. Distribution Statement
Crash Victim Simulation Mathematical Modeling Computer Simulation	Document is available to the U. S. Public through the National Technical Information Service, Springfield, Virginia, 22161.

19. Security Classif. (of this report)	20. Security Classif. (of this page)	21. No. of Pages	22. Price
Unclassified	Unclassified	185	

Form DOT F 1700.7 (8-69)

FOREWORD

This document is the final report of the research conducted under Contract No. DOT-HS-6-01410 for the National Highway Traffic Safety Administration. Dr. John T. Fleck of J & J Technologies, Inc. served as Principal Investigator during his earlier tenure as a member of the Calspan Transportation Research Department and was retained as a subcontractor to maintain the continuity necessary to prepare this report.

The Contract Technical Monitor for this project was Dr. Lee Ovenshire of the National Highway Traffic Safety Administration.

This report has been reviewed and approved by:

Anthony L. Russo
Transportation Research
Physical Sciences Department

TABLE OF CONTENTS

TABLE OF CONTENTS (continued)

LIST OF FIGURES

LIST OF TABLES

1.0 INTRODUCTION

The crash victim simulator (CVS) computer program developed by Calspan is a general three-dimensional simulator (Ref. 1). The user must decide the level of detail (i.e., the level of sophistication) that is required to adequately account for all aspects of a particular problem that significantly affect the responses of interest. In the crash victim problem the principal responses of interest are usually those associated with the production of injuries. The presently reported study does not address the problem of identifying injury criteria. Rather, the general objective of the research was to develop, evaluate and recommend means and procedures for evaluating accuracies and sensitivities of various measures of crash victim response to the choice of and to the numerical values of various parameters that are used in crash victim simulations with the CVS computer program.

In particular, many of the studies were confined to the modeling aspects related to a Part 572 dummy. Extensive work to define the parameters of a 15 segment Part 572 dummy model was accomplished in two closely related research programs reported in References 1 and 2. The baseline models used in this study stem from the data obtained in those programs. To facilitate understanding of the analyses and information presented in this report, the reader should be familiar with the CVS program and the results of the comparison studies described in Reference 1.

This research work was divided into eight (8) principal tasks as follows:

1. Plan of Work and Methodology
2. Check the CVS and Input
3. Comparative Study of Levels of Sophistication
4. Response Measure Approximating Function Generator (RMAFG)
5. Study of Response Sensitivity to Model Parameter Variations
6. Reduction of the Number of Inertial Related Parmaters

7. Numerical Verification of the RMAFG
8. The Main Questions.

Comments on the Plan of Work and Methodology, Task 1, are included in the discussions of the individual tasks. The original plan proved overly ambitious. Many of the tasks were much more difficult and required much more time than had originally been proposed. As a result the work was only partially completed.

Task 2, Check the CVS and Input, is discussed in Section 2. This was principally concerned with the joint algorithms in the program since noticeable "drift" of the joint constraints was reported by some users.

Task 3, Comparative Studies of Levels of Sophistication, addresses some of the modeling capabilities of the CVS program. This task is discussed in Sections 3 and 6. Section 6 also addresses Task 8, the Main Questions. These questions are given in Table 1-1 and are intimately related to the levels of sophistication that were to be considered which are given in Table 1-2.

Results of the Study of Response Sensitivity to Model Parameter Variations (Task 5) are presented in Section 3 where a detailed model of a dummy shoulder is studied and in Section 4 where the results of neck and shoulder models are used to demonstrate the Response Measure Approximating Function Generator (RMAFG) developed in Task 4. Table 1-3 lists some of the potential parameters (independent variables) that were considered in the sensitivity studies, and Table 1-4 lists the number of parameters that are associated with various components of a typical model using the CVS program.

Results from Task 7, Numerical Verification of the RMAFG, are also described in Section 4. The RMAFG is a multiparameter polynomial interpolating routine which is useful for parametric studies. The Fortran listing of the RMAFG program is presented in Appendix B.

Table 1-1

QUESTIONS CONCERNING REQUIRED LEVEL OF MODEL DETAIL

1. Is similitude between rigid body characterizations of selected segments adequate or must similitude of one or more vibration modes also be preserved?

2. Are simple ball-and-socket joints an adequate characterization of the shoulder or must the separate motions of the clavicle and scapula be approximated?

3. Is it sufficient to preserve kinematic similitudes that are describable by geometric constraints between the head and the base of the neck or must physical or computer models of the neck include dynamic degrees of freedom that correspond to the human neck?

4. Is a planar model adequate or must a three-dimensional model be used for conditions essentially symmetric to the body?

5. Is it sufficient to preserve similitude of impulses and coefficients of restitution during "hard" impact processes or must similitude of forces also be preserved?

6. Is it necessary to account for the non-symmetric shape of joint stops?

7. Is a sliding/rolling characterization of a particular contact adequate or must similitude of the deflection characteristics be preserved?

8. Is it necessary to provide separate rigid body degrees of freedom for the hands or the feet?

9. Must the similitude of surface compliances be preserved in the region of belt or air bag contacts?

10. It is necessary to preserve similitude of certain dynamic degrees of freedom which include inertial effects for deformations associated with contact?

11. With respect to each of the modeling features, and for various typical crash conditions either:

11.1 what is the simplest level that adequately handles all of the cases, or

11.2 what is the most detailed model that is within the capabilities of the CVS program and that is inadequate for one or more of the cases?

12. What is the simplest and least expensive mechanical idealization, using the CVS, that appears to be adequate for each of several typical crash conditions?

Table 1-2

LEVELS OF SOPHISTICATION

1. Planar, i.e., two-dimensional, motion using planar kinematic constraint option (for symmetric and nearly symmetric crash situations). Include a case where the two sets of planes formed by the upper and lower parts of the arms and legs, respectively, make significant angles with the mid-sagittal plane.

2. Abdomen modeled as several rigid body segments each with independent rotational degrees of freedom. The lumped mass, stiffness, and viscous parameters should be consistent with the Baseline Model (if this is not the Baseline Model itself).

3. Abdomen modeled the same as for item (2) except that the individual abdomen subsegments have orientations with respect to one end that are constrained to be functions of the relative orientations of the opposite end of the abdomen.

4. Neck modeled similar to the treatment described in Item (2) for the abdomen.

5. Neck modeled similar to the treatment described in Item (3) for the abdomen.

6. Shoulder model that includes clavicle, scapula and muscles modeled as tension elements with mass.

7. Globalgraphic descriptions of joint stops that correspond to the human subjects.

8. Impulsive contacts for nominal conditions involving relatively short duration, i.e, hard contacts.

9. Degrees of freedom that approximate certain segment modes of vibration during events that include hard impacts. (This may well involve modeling segments as an assembly of two or more rigid subsegments).

Table 1-3

LIST OF POTENTIAL INDEPENDENT VARIABLES FOR SENSITIVITY STUDIES

1. Components of inertia tensors for body segments.
2. Joint friction torque unlock threshold.
3. Joint moving friction torque.
4. Joint stop parameters.
5. Flexural moment stiffnesses.
6. Joint locations.
7. Initial position and orientation.
8. Contact model parameters.

Table 1-4

SIGNIFICANT PARAMETERS

Significant Parameters	No. of Parameters Required/Element
Segment	
mass	1
inertia	6
contact ellipsoid	9
integrator tests	12
	28 TOTAL
Ball Joint	
location and orientation	12
spring characteristics	10
viscous characteristics	7
	29 TOTAL
Pin Joint	
location and orientation	12
spring characteristics	5
viscous characteristics	7
	24 TOTAL
Euler Joint	
location and orientation	12
spring characteristics	15
viscous characteristics	21
	48 TOTAL
(Globalgraphic joint option requires a minimum of 22 additional parameters)	
Belt	
reference points	9
slack	1
stress-strain zero friction	11 (mimimum)
or infinite friction	(22) (minimum)
	21 (32) minimum TOTAL

Table 1-4 (continued)

Airbag	
basic parameters	38
each additional reaction panel	9
	38 + 9 x number of panels TOTAL
Flexible Element	
for each segment, h function	30
	30 x number of segments TOTAL
Contact Surface	
size, position and orientation	9
force-deflection characteristics	50 typical (minimum 16)
	59 TOTAL

Task 6, the Reduction in the Number of Inertially Related Parameters, is addressed in Section 5 where a theorem is presented which shows that the mass distribution of a set of connected rigid bodies is not unique. A sample case is presented in that section, and the Fortran listing of the computer program for computing dynamically equivalent systems is contained in Appendix C.

2.0 CHECK OF THE CVS PROGRAM

One primary purpose of Task 2 was to make a complete check of the CVS program and the algorithms used to develop the program. A problem that came to light was the failure of the joint constraints, in that, in some runs a noticeable drift occurs in the Pin and Euler joints. This problem was studied in detail and is discussed below.

The CVS program links the segments by imposing forces and torques of constraint at the joints. The program integrates the linear accelerations and velocities of the reference segment(s) to obtain the linear velocity and the position of these segments. It then uses a chaining algorithm to compute the positions and the velocities of the other segments. The use of this chaining procedure insures consistency of the linear variables, i.e., the joints do not pull apart. However, when a joint is locked or pinned (one free axis) or has one locked axis, nothing in the program checks or corrects for any inconsistencies that may occur in the relative angular positions or velocities because of integration or precision errors.

To state the problem: if segments 1 and 2 are connected by a pin joint (IPIN = 1 or IEULER = 4, 5, 6), the angular constraint is that the vector defining the pin axis in segment 1 should remain parallel to the vector defining the pin axis in segment 2. This constraint is imposed on the system by defining a torque of constraint for this joint. The constraint equation is obtained in acceleration form by twice differentiating the equation expressing the equality of the pin axes. Since the orientation of segment 1 is updated by the integrator independently of the orientation of segment 2, errors in integration and lack of infinite precision in the calculations will cause errors in orientation (direction cosine matrices) and hence the pin vectors may not remain parallel. This drift effect has been noticed in some of the computer runs. For simple pin joints the maximum error detected has been less then 1 degree; however, for the Euler joint with one locked axis a very noticeable drift (several degrees) has been reported by Leyland Motors.

Since the typical Part 572 dummy joint is best modeled by the use of the Euler joint, any drift may cause significant errors in the simulation. Thus, considerable effort was expended to determine the cause of the drift. All of the subroutines involving the joint computations were examined in detail to ensure that there were no programming errors or errors in the algorithms. No errors were found; however, it should be noted that a correction had been made to subroutine VISPR in 1979. This correction would make the current version of the program perform differently from previous versions. The correction did not help the drift problem.

A simple three segment-two joint model was used to make tests on the drift. These tests verified that the drift was a function of integrator accuracy. As the ratio test on the integration angular acceleration was reduced, the drift was reduced. In these tests, both joints were Euler joints; one had the precession axis locked and the other had the spin axis locked. It was noticed that although the individual angles drifted from their expected values, the sum of the angles was close to the expected values. The reason for this has not been determined.

Modifications to subroutine PDAUX were tried in an attempt to correct the drift. In particular several methods of correcting the quarternion to insure that the vector part of the quarternion had no component on the effective locked axis were tried. None of these methods has a significant effect on the drift.

It appears that it will be necessary to develop a chaining algorithm for the angular positions and velocities to eliminate the drift problem. Until this is done, it is recommended that the integrator tests be used to hold the drift to an acceptable level. No method of predetermining the best values to use for these tests is known; hence they will have to be determined by trial and error. The tabular time histories of the joint behavior show the values of the angles involved. Examination of these time histories allows the user to detect the drift in any angle that should be constant (locked axis), but unfortunately the drift or error in a time-varying angle cannot be determined.

3.0 COMPARATIVE STUDY OF LEVELS OF SOPHISTICATION

A significant feature of the CVS program is the ability to vary the complexity of the model of a physical system. For most applications simulating the Part 572 dummy, a fifteen-segment model has been used. However, the skeletal structure of the Part 572 dummy consists principally of 33 rigid segments plus the rubber neck and the rubber lumbar spine. Vinyl foam "flesh" surrounds some of these segments to form an approximate human shape. No internal organs are included except for a visceral sac in the lower torso.

Since the CVS program requires that the structure be defined as a set of rigid segments connected by joints, the neck and the spine each must be approximated as a set of rigid segments and the "flesh" is assumed to be rigid and part of the segments to which it is attached. This study did not address the effects of this assumption for the "flesh." The spring and viscous characteristics attributed to the joints are primarily due to the interference between the flesh of the segments connected by each joint. In studies performed in another program (Reference 1) it was found that the visceral sac significantly affected the dynamic motion of the torso and had to be accounted for in defining the properties of the joints representing the lumbar spine.

Many of the 33 rigid segments of the dummy are components of the joints which are modeled by using the "Euler" joint routine in the program. This routine accurately models the kinematics of the joint but ignores the inertial reactions. The inertial reactions are approximated by including the mass and inertia of the joint components as part of the adjoining segments. For example, the elbows are modeled as "Euler" joints and the mass of the joint structure is included in the masses of the upper and lower arms. Thus, by use of the "Euler" joint routine for the elbows, ankles, and hip joints, six of the segments were combined with others to reduce the complexity of the model to 27 segments. The knees were modeled as pin joints and the upper legs as single segments. In addition, the hands were included as part of the lower arms, further reducing the complexity to 21 segments. (In some applications it may be desirable to allow for motion

of the wrist.) Each shoulder structure of the Part 572 dummy includes three segments. Replacement of these by a single "Euler" joint for each shoulder reduces the complexity to 15 segments. A significant part of the effort on this contract was directed toward a study of the shoulder which is discussed in a following section.

3.1 General Discussion of the Levels of Sophistication

Various degrees of complexity in modeling certain of the dummy characteristics, in particular the rubber neck, the rubber lumbar spine (abdomen) and the shoulder were investigated. These degrees of complexity are referred to as "levels of sophistication" and are summarized in Table 1-2. The main questions regarding the required level of model detail are given in Table 1-1.

Level of sophistication 1 of Table 1-2, the study of planar motion, refers to the symmetry options available in the CVS program. There are two symmetry options in the program. The first is the two-dimensional symmetry option whereby all motion perpendicular to the mid-sagittal plane is suppressed. The second option provides mirror symmetry where the motion is reflected in the mid-sagittal plane, e.g., if the right arms and legs move to the right, the left arms and legs will move the same amount to the left. The computer runs that were made using these options showed, in some cases, a reduction in computer time when compared to the same cases run without the symmetry options. This is primarily due to the smoothness of the integration which in turn allowed the use of larger integration steps and, hence, fewer computations. The user is advised to use these options whenever they are applicable to his problem.

Levels of sophistication 2, 3, 4, and 5 of Table 1-2 are concerned with the modeling of the dummy spine and neck. The 15 segment Baseline model of the Part 572 dummy (Ref. 1, Volume 2) uses a single rigid segment to model the abdomen (lumbar-spine) and a single rigid segment to model the neck. Both of these segments are connected to the adjoining segments with ball joints in the model.

The Head/Neck Pendulum tests that are reported in Reference 1, Volume 2 were studied in detail. It was apparent from these results that at least one segment must be used for the neck. For example, the behaviour of the angle of the head with respect to the pendulum in the first ten milliseconds as shown in Figure 4-3 of the cited reference could not be obtained with a model in which the head was connected directly to the upper torso. Results of simulations in which the neck was assumed to be composed of either two or three segments showed no significant differences in response from the one segment model. The Head/Neck Pendulum tests also indicated some extension (stretching) of the neck. Attempts to simulate this effect by replacing the ball joints with sets of springs, thus effectively disconnecting the neck from the upper torso and the head, were unsuccessful. The failure was due primarily to the inability, using the current capabilities of the CVS program, to define a set of springs that would allow extension but would not allow significant lateral motion at the joint. This deficiency could be removed by adding a slip-joint capability to the CVS program. Such a joint could be defined as one imposing a kinematic constraint that would allow relative linear motion at the joint parallel to fixed lines in each of the adjoining segments.

Simulations of torso pendulum impact tests reported in Reference 1, Volume 2 indicated that the principal deficiency of the single-segment model of the abdomen was not in the modeling of the spine but in the lack of modeling of the visceral sac that is in the Part 572 dummy. No significant stretching of the dummy abdomen occurs because of the constraint of the steel cable that passes through the center of the rubber spine. More detailed models of the abdomen were not studied in the current effort.

Level of sophistication 6, as stated, applies to the human victim only since the shoulder of the dummy is a mechanical linkage. The shoulder linkage of the Part 572 dummy is studied in some detail in the next section of this report. The consideration of a model for the human shoulder was not within the scope of this research program.

Level of sophistication 7, dealing with the globalgraphic description of joint stops is applicable whenever there is sufficient motion for a joint to enter a stop. The user is advised to specify this option whenever there is a probability of a joint entering a stop.

Level of sophistication 8, impulsive contacts, can be examined with a simpler model than that of the entire dummy. Question number 5 of Table 1-1 is: Under what conditions is it possible to replace a contact with a hard surface with an idealized impulse? The use of an impulse is justified when there is a change in velocity in a short enough time interval that there is no significant change in position. The problem is the definition of a significant change in position. Section 6.2 of this report presents a more detailed discussion of this problem.

The use of the impulse in relation to question 10 of Table 1-1 should not be overlooked. The program has an inertial spike option which models some of the inertia effects of a contact. It was originally developed for the case of a head striking a windshield where the mass of glass must be accelerated when it shatters. This inertial effect usually lasts only a few milliseconds. The transfer of energy could be approximated by use of an impulse with a negative coefficient of restitution (the program allows this) which would allow the impacting object to continue in the same line of motion without a reversal of velocity.

Level of sophistication 9 is concerned with transverse modes of vibration which may be induced when a hard contact is made with a segment such as a leg and the leg bends due to the severity of the impact. This may be modeled by use of several subsegments but the stiffness of the joints may require a small integrating step and hence make it economically unfeasible. The flexible element option may alleviate this difficulty. The long bones in the dummy are steel shafts and hence are much stiffer than a human bone. Thus, segment transverse vibrations may be a more important consideration for humans than for a dummy model. The consideration of longitudinal modes of vibration are beyond the capabilities of the CVS program.

3.2 Study of the Part 572 Dummy Shoulder

In the Baseline model of the Part 572 dummy (Reference 1), the shoulder is represented as an Euler joint with the spin axis locked. The actual mechanical structure is illustrated in Figure 3-1 and consists of three principal pieces for each shoulder. These are the sterno-clavicular link, the clavicle, and the shoulder yoke. The sterno-clavicular link pivots about an axis which is tilted (pitched) 5 degrees to the x (forward) axis of the upper torso. The motion is constrained by a highly nonlinear viscous damping mechanism and by hard mechanical stops which limit the elevation-depression motion of the shoulder girdle to 15 degrees. The clavicle is pinned to this link with the pin parallel to the nominal z (down) axis of the torso. The motion about this pin is also restricted to approximately plus and minus 15 degrees. The shoulder yoke connects the upper arm to the clavicle. At the clavicle end is a pin joint approximately parallel to the y axis of the torso, and at the upper arm end of the yoke is another pin joint whose axis is approximately parallel to the x axis of the torso. These joints allow flexion-extension and abduction-adduction motion of the upper arm, respectively.

In the Baseline model, the shoulder yoke is modeled by an Euler joint and the sterno-clavicular link and the clavicle are not modeled. The purpose of this study was to examine the effects of using a shoulder model that more closely represents the actual dummy shoulder assembly.

The computer model for investigating the behavior of the shoulder was based on the model used to simulate the torso-pendulum tests described in Reference 1. In the torso-pendulum tests the pendulum is raised to an almost horizontal position and, when released, strikes a honeycomb structure which stops the motion of the pendulum when it reaches a vertical orientation. The torso and associated segments are thus subjected to an impulsive force at the point where the lower torso is attached to the pendulum. The three-piece shoulder structures and the upper and lower arms were added to the torso-pendulum test simulation model to form a fourteen-segment, fourteen-joint model. The segments and joints are listed in Table 3-1 and the configuration is illustrated in Figure 3-2.

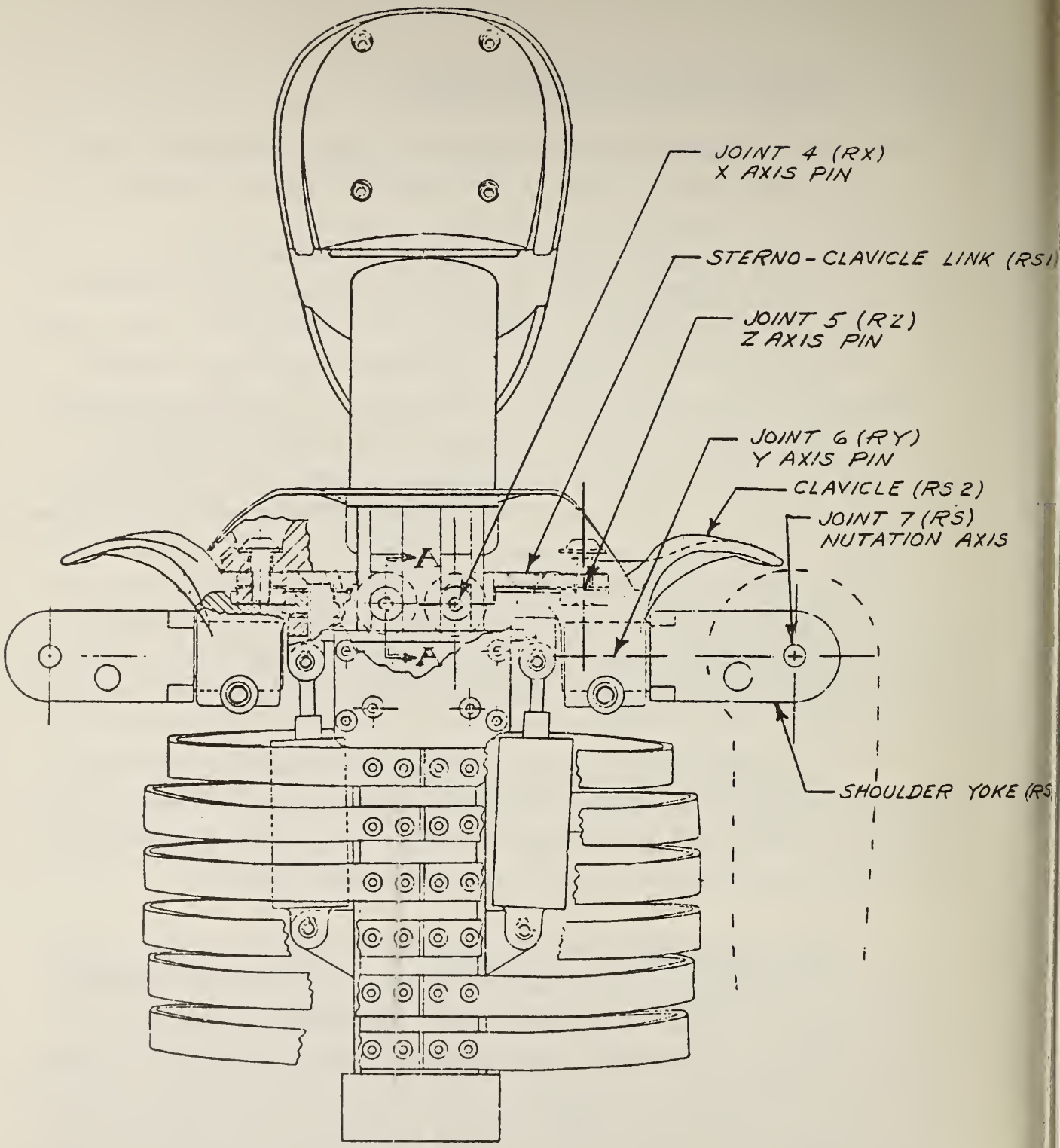

Figure 3-1 SHOULDER JOINT ASSEMBLY - PART 572 DUMMY

Table 3-1

SEGMENTS AND JOINTS OF MODEL USED FOR STUDY OF SHOULDER

SEGMENT			JOINT			
No.	Name	Symbol	No.	Symbol	Type	Connects
1	Pendulum	PEND	1	PP	Ball (Locked)	PEND-LT
2	Lower Torso	LT	2	P	Ball	LT-CT
3	Center Torso	CT	3	W	Ball	CT-UT
4	Upper Torso	UT	4	RX	Pin	UT-RS1
5	Right Sterno-clavicle Link	RS1	5	RZ	Pin	RS1-RS2
6	Right Clavicle	RS2	6	RY	Pin	RS2-RS3
7	Right Shoulder Yoke	RS3	7	RS	Euler	RS3-RUA
8	Right Upper Arm	RUA	8	RE	Euler	RUA-RLA
9	Right Lower Arm	RLA	9	LX	Pin	UT-LS1
10	Left Sterno-clavicle Link	LS1	10	LZ	Pin	LS1-LS2
11	Left Clavicle	LS2	11	LY	Pin	LS2-LS3
12	Left Shoulder Yoke	LS3	12	LS	Euler	LS3-LUA
13	Left Upper Arm	LUA	13	LE	Euler	LUA-LLA
14	Left Lower Arm	LLA	14	PT	Pin	PEND-Ground

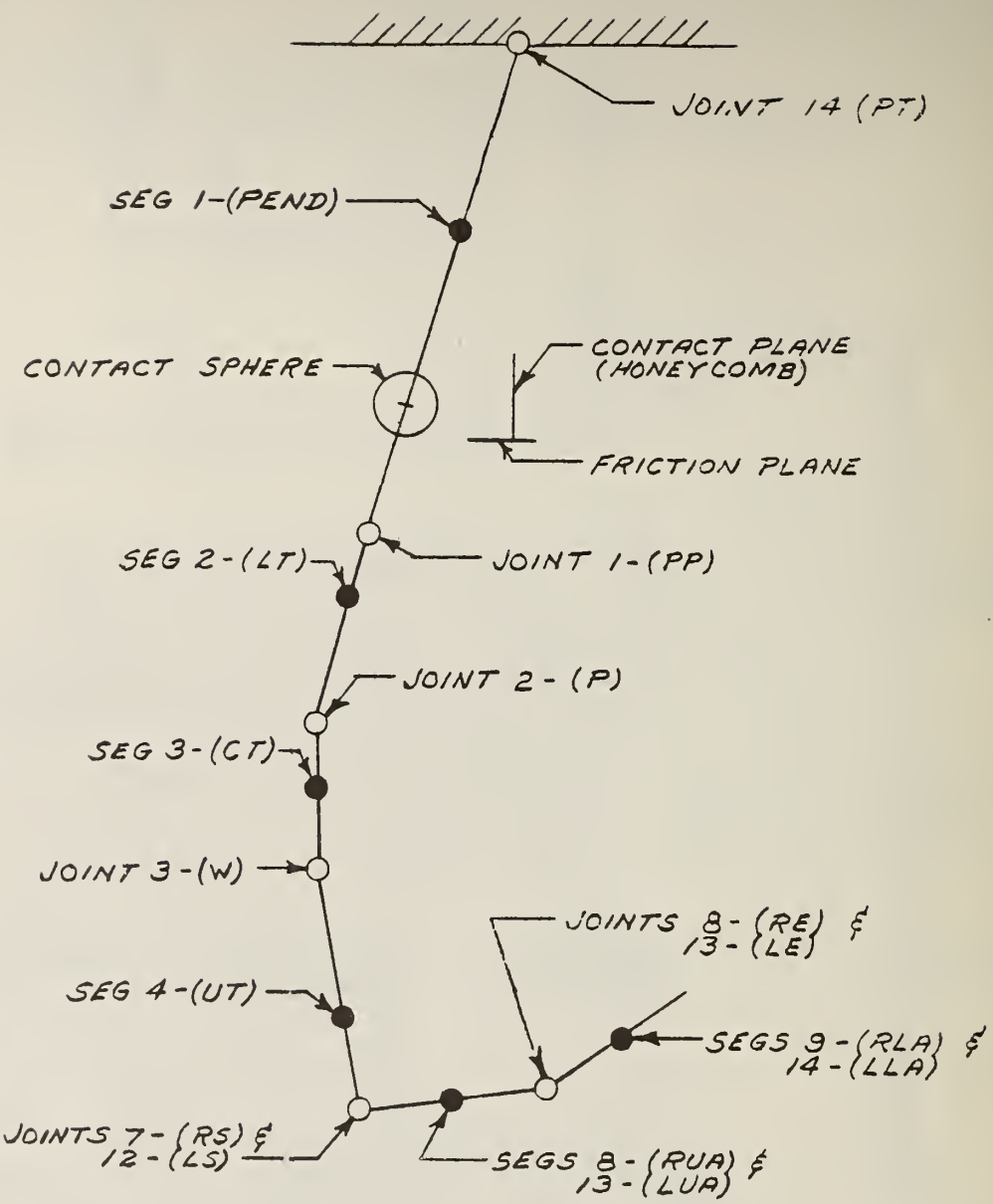

Figure 3-2 MODEL OF PENDULUM TEST OF TORSO WITH SHOULDER AND ARMS

A series of computer simulation runs was made in which selected sets of the shoulder joints were locked or unlocked for three different initial pendulum impact velocities and three different orientations of the torso-shoulder-arm model on the pendulum. A particular set of six runs that was made is tabulated below:

	Joint Status						Level of Sophistication
Run	X	Z	Y	P	N	S	
1	U	U	U	L	U	L	Most sophisticated - all segments active
2	U	U	L	U	U	L	Sterno-clavicle free-Euler for shoulder
3	U	L	L	U	U	L	Clavicle locked-Euler for shoulder
4	L	U	L	U	U	L	Clavicle free-Euler for shoulder
5	L	L	L	U	U	L	Least sophisticated-CVS baseline
6	L	L	U	L	U	L	Sterno-clavicle locked, shoulder yoke-clavicle pivot used instead of Euler

where L indicates that the joint is always locked, and

U indicates that the joint is allowed to unlock at a specified torque.

The column labels for joint status are (see Table 3-1 and Figure 3-1):

X for RX and LX, the joint connecting the sterno-clavicle link to the upper torso,

Z for RZ and LZ, the joint connecting the sterno-clavicle link to the clavicle,

Y for RY and LY, the joint connecting the clavicle to the shoulder yoke.

P the precession axis of the Euler joint. This joint is a direct replacement for Y; when one is locked the other should be unlocked,

N the nutation axis of the Euler joint which should never be permanently locked.

S the spin axis of the Euler joint. This joint is always permanently locked.

The initial angular velocity of the pendulum and all of the segments was 113 degrees per second about the y axis (pitch). This represents an initial linear velocity of 148 inches per second at the cg of the lower torso and 184 inches per second at the shoulder. The arms were initially parallel to the z axis of the torso. All joints except 2, 3 and 14 were initially locked.

Plots of selected response measures for each of the six cases are contained in Appendix A. The response measures plotted are:

(a) The resultant linear acceleration of the right lower arm versus time.
(b) The z versus x displacement of the right lower arm.
(c) The y versus x displacement of the right lower arm.
(d) The flexure angle of the shoulder yoke-clavicle pivot joint versus time.
(e) The precession and nutation of the Euler joint at the shoulder versus time.
(f) The precession and nutation of the Euler joint at the elbow versus time.
(g) The resultant linear acceleration of the upper torso versus time.
(h) The pitch of the upper torso versus time.

The results obtained with the most sophisticated model (Run 1) and with the least sophisticated model (Run 5) of the shoulder are overlaid in Figure 3-3 for comparison. It may be noted in Figure 3-3(d) that the flexure angle at the shoulder when the shoulder-clavicle is free (Run 1 with Y unlocked) seems to reverse direction at approximately 85 milliseconds. This is because the shoulder-clavicle pivot is modeled as a pin joint which is not direction sensitive. The first part of the curve should be reflected about the abscissa so the plot would be much like that of the precession angle of the shoulder for Run 5 (precession axis of the Euler joint unlocked) shown in Figure 3-3(e).

No definitive conclusion was reached from the study except to note that the response of the upper torso is essentially the same in all of the runs. The response of the lower arms is different in each of the runs. The reader should draw his own conclusions as to whether or not the differences are significant.

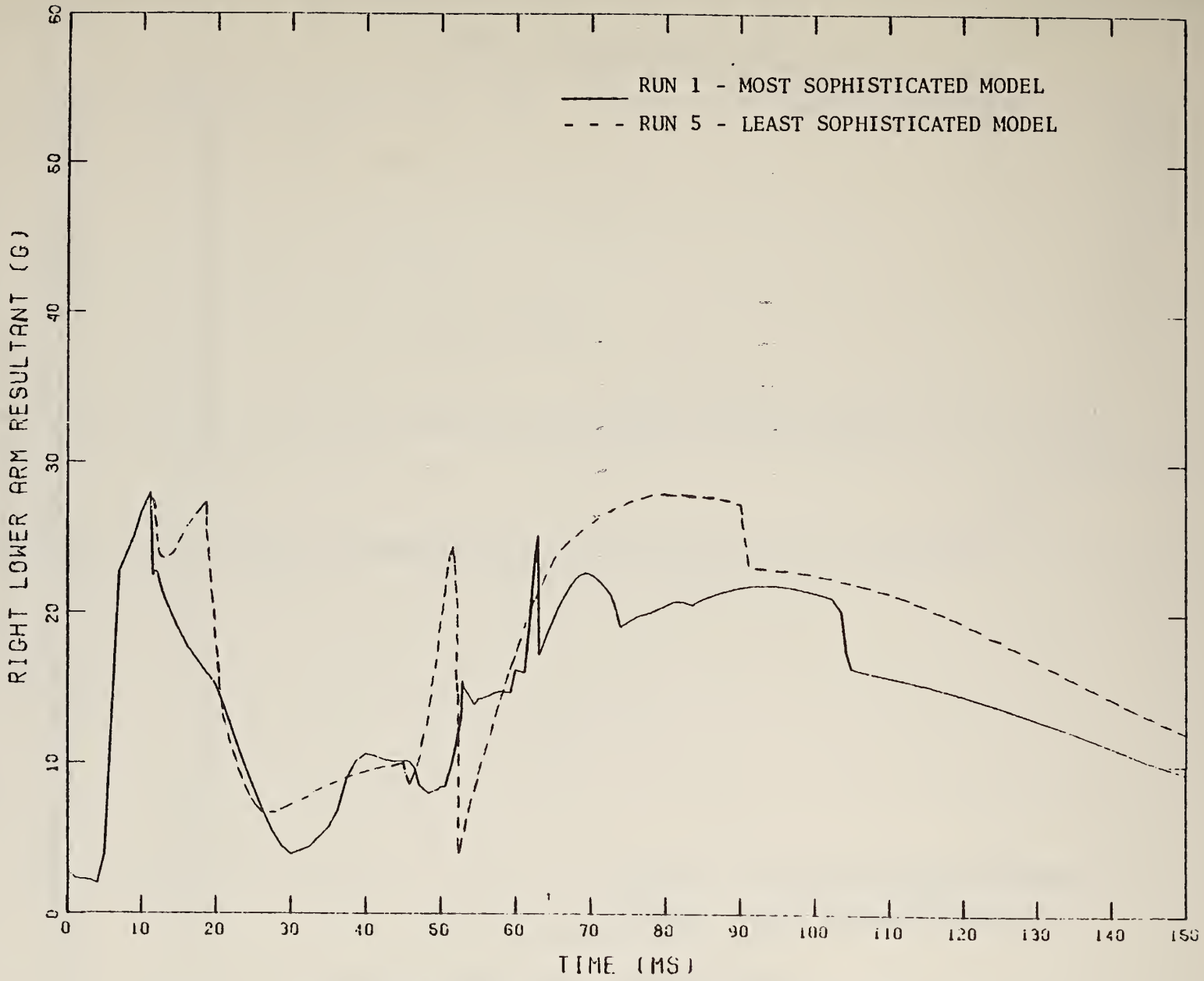

(a) RLA RESULTANT ACCELERATION VS. TIME

Figure 3-3 COMPARISON OF RESPONSES FROM TWO SHOULDER MODELS

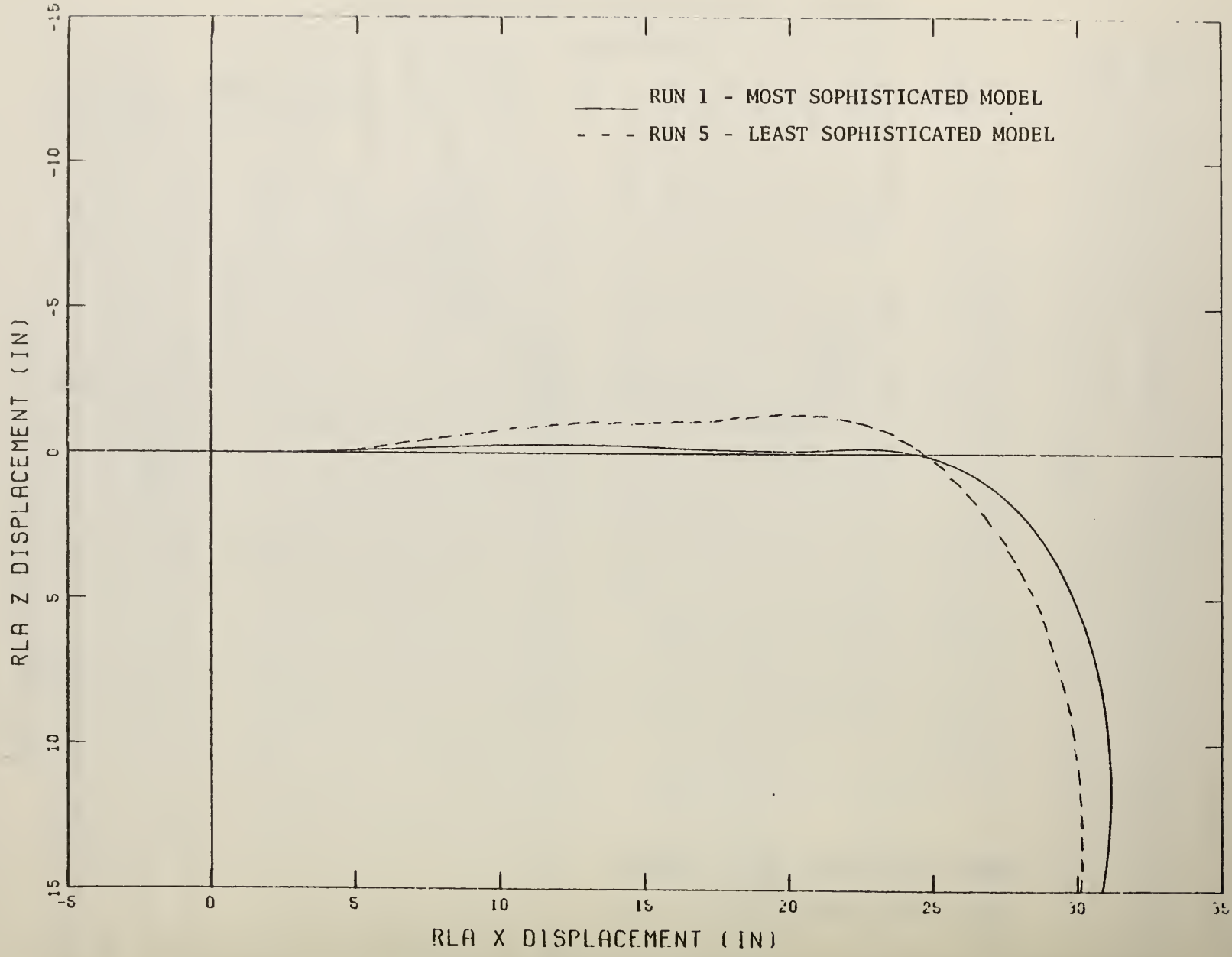

(b) RLA Z VS. RLA X DISPLACEMENT

Figure 3-3 (Cont'd.)

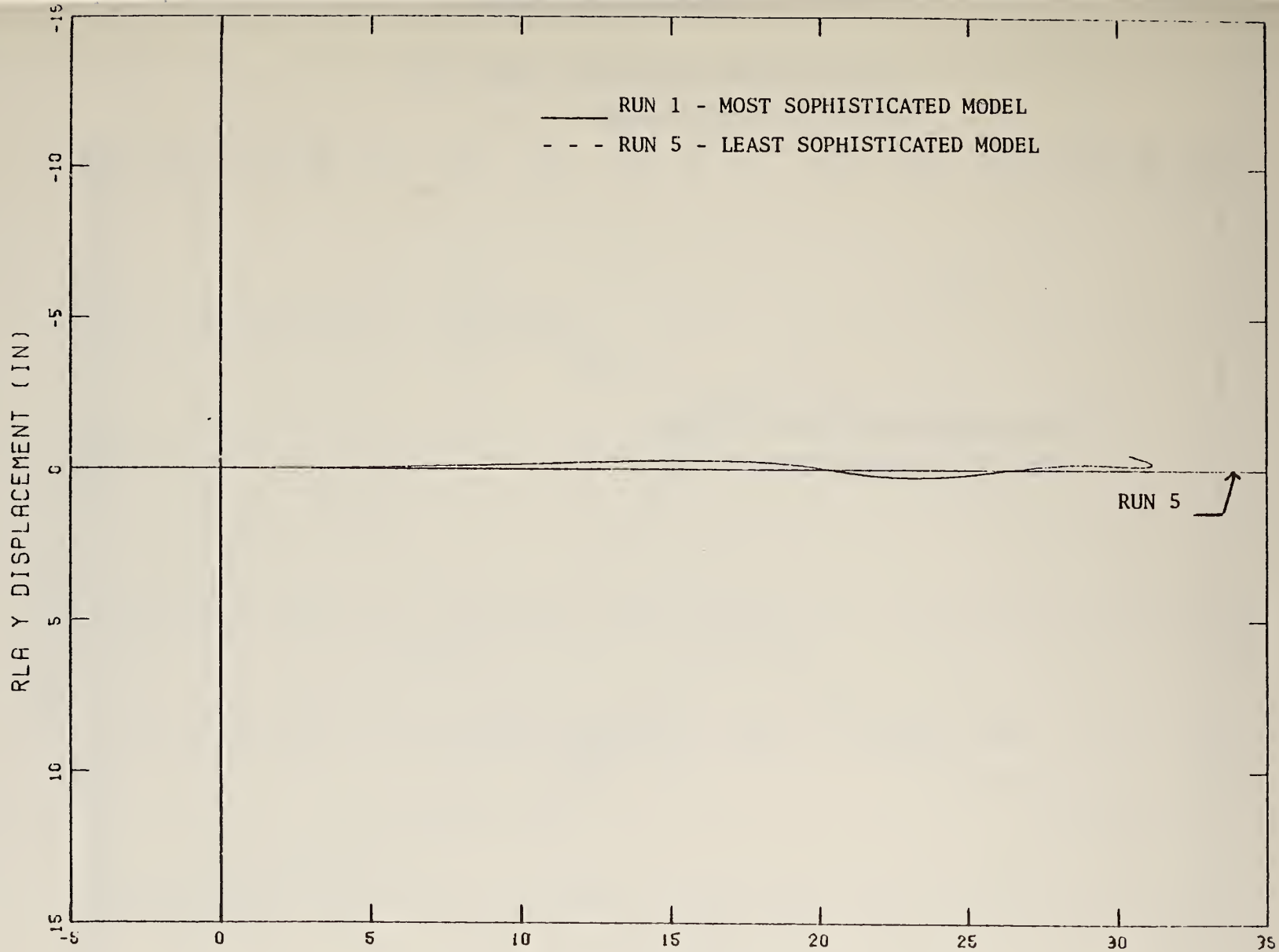

(c) RLA Y VS. RLA X DISPLACEMENT

Figure 3-3 (Cont'd.)

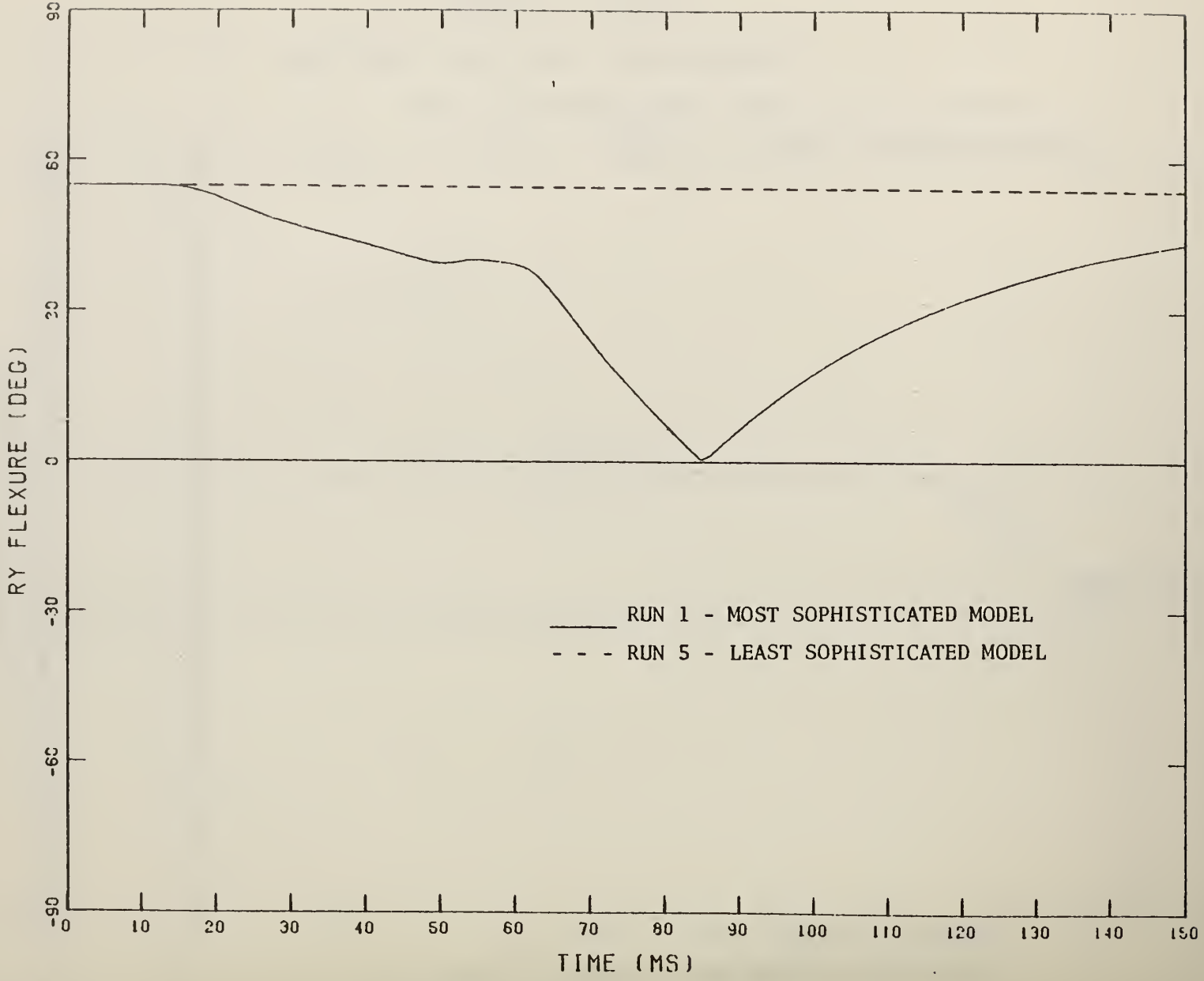

(d) RY FLEXURE VS. TIME

Figure 3-3 (Cont'd.)

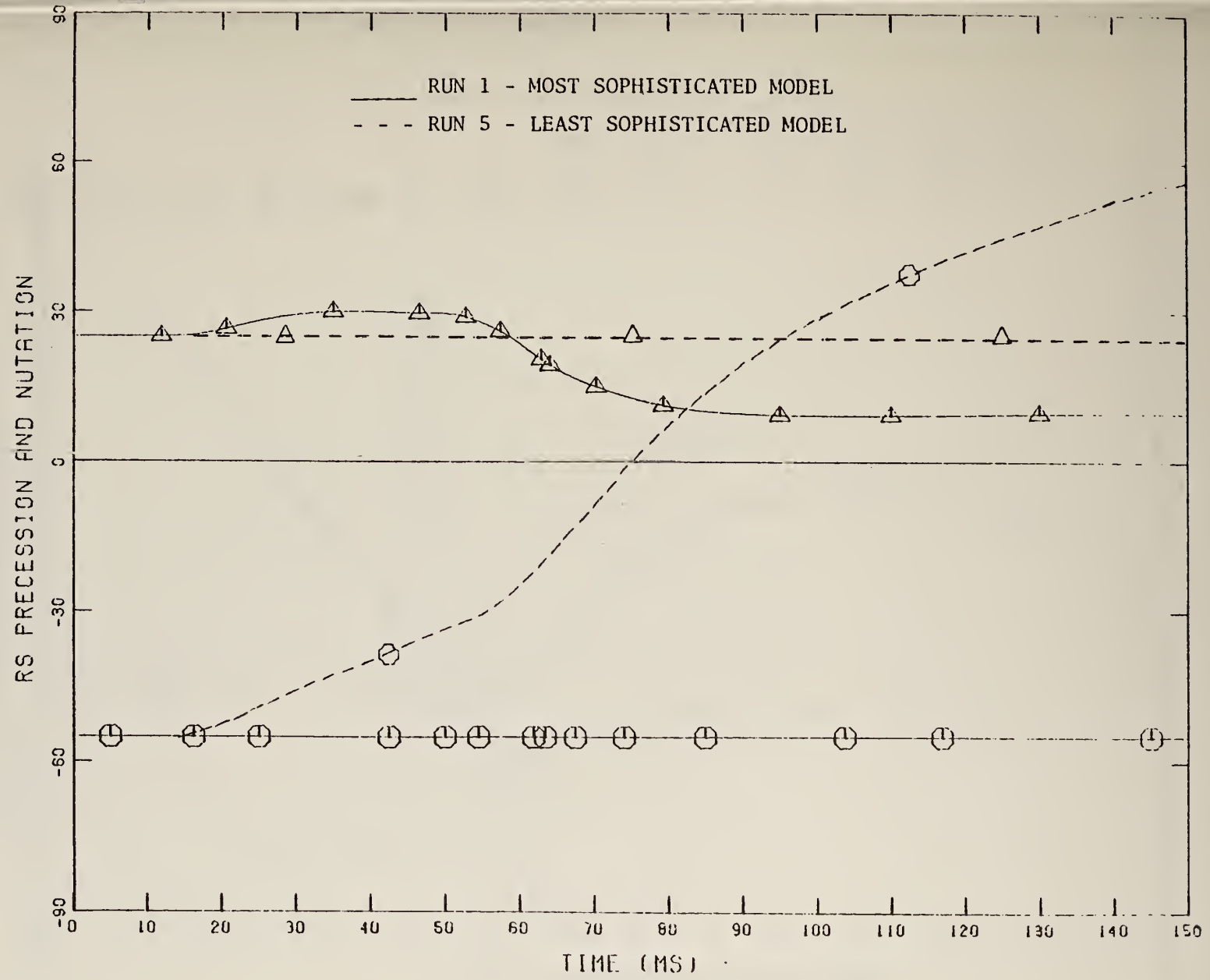

(e) RS PRECESSION AND NUTATION VS. TIME

Figure 3-3 (Cont'd.)

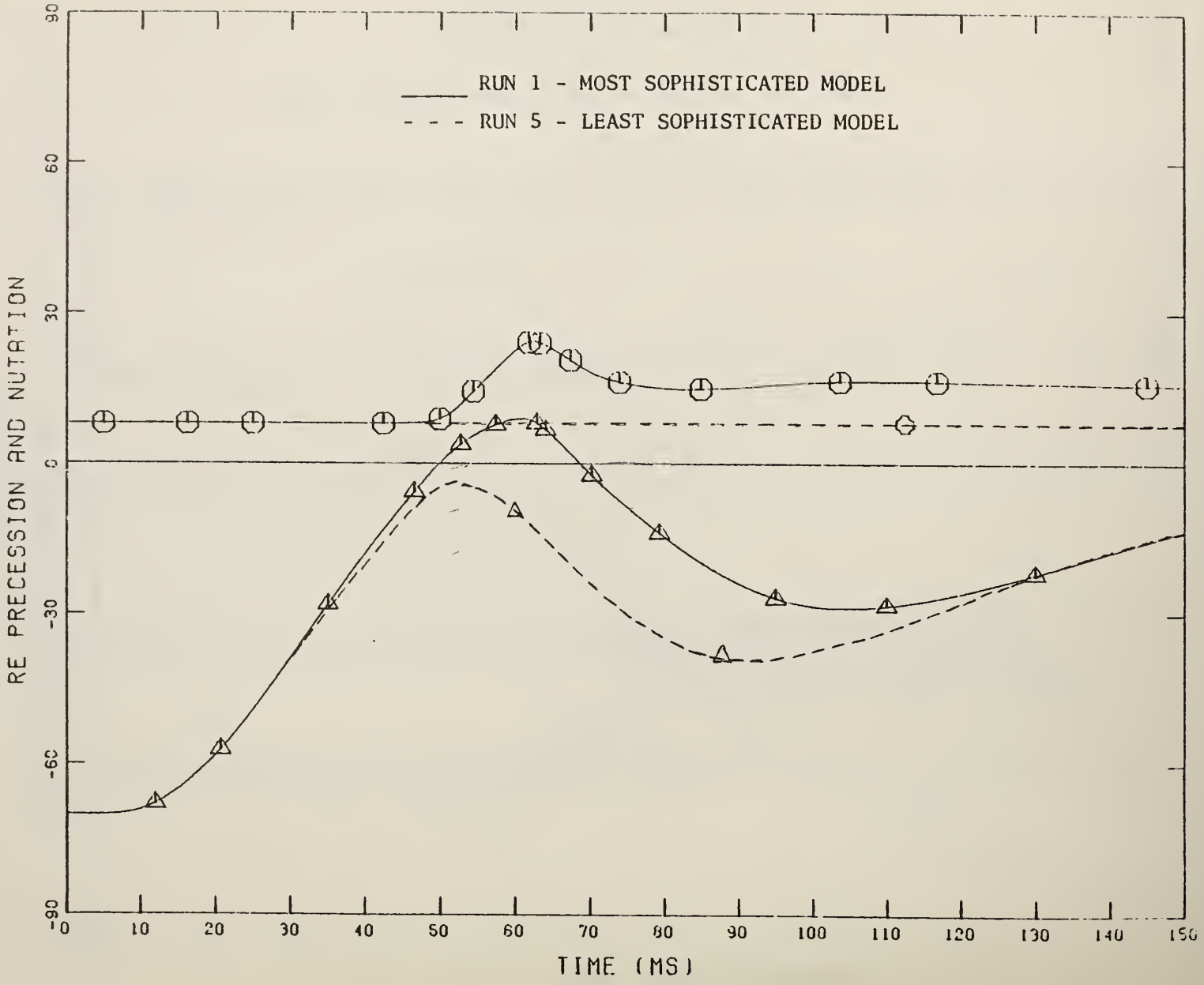

(f) RE PRECESSION AND NUTATION VS. TIME

Figure 3-3 (Cont'd.)

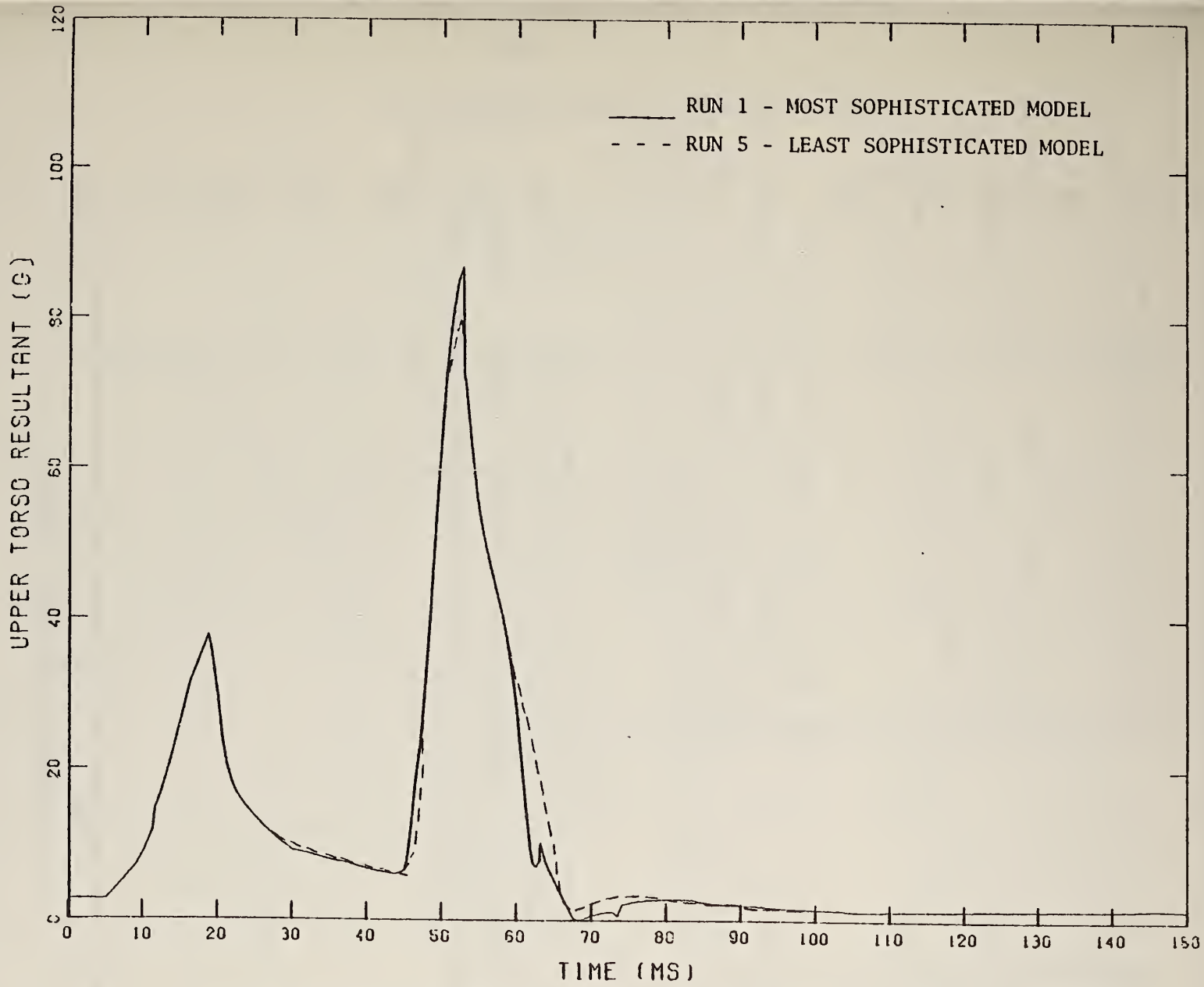

(g) UPPER TORSO RESULTANT ACCELERATION VS. TIME

Figure 3-3 (Cont'd.)

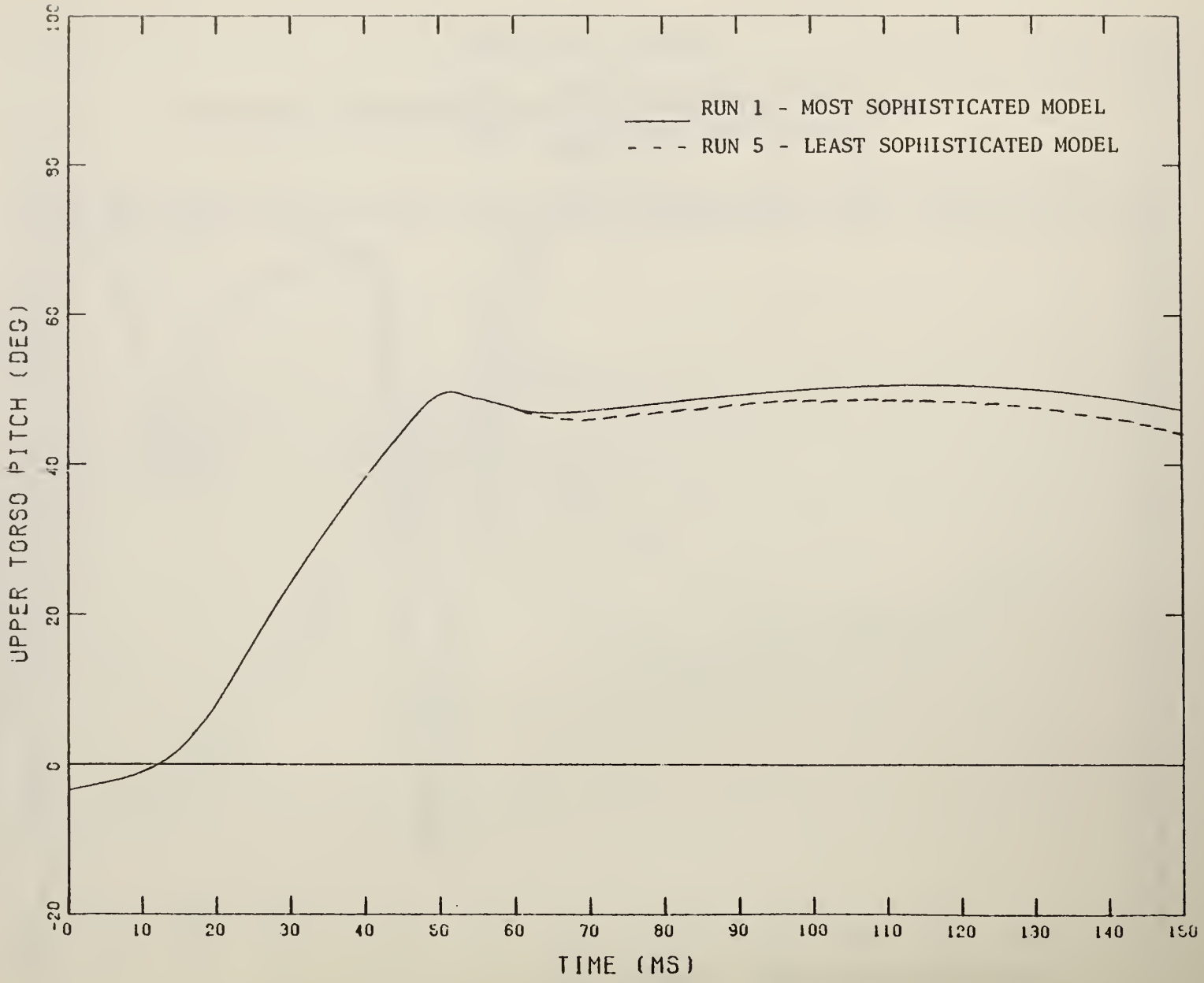

(h) UPPER TORSO PITCH VS. TIME

Figure 3-3 (Cont'd.)

4.0 RESPONSE MEASURE APPROXIMATING FUNCTION GENERATOR

In some applications of the CVS program the user may wish to perform various parameter studies in which he varies one or more parameters in the model and notes the changes in selected response measures. In practice, the resulting response measures are usually plotted and smooth curves drawn to show the variation with the parameters. It is natural to assume that the value of the response measure for any intermediate value of a parameter can be obtained from the curve, i.e., the curve is used as an interpolating function.

The use of a hand drawn curve is quite practical if only one parameter has been varied, but if two parameters are varied a surface must be drawn to use this graphical interpolation approach. If more than two parameters are varied, the interpolation problem usually becomes too complicated to solve using planar graphs.

Hence, a multiparameter interpolating routine was developed to assist the users. This routine is called the Response Measure Approximating Function Generator (RMAFG). The mathematical development and a description of the Fortran program of the RMAFG is contained in the following sections along with a sample application.

4.1 Mathematical Development

Let y be a scalar function of the N parameters X_j, $j = 1, n$, i.e., $y = f(X_1, X_2 \ldots, X_N)$. Assume that this function may be approximated as a polynomial in the N parameters as:

$$
\begin{aligned}
y &= C_0 && \text{Constant Linear} \\
&+ \sum_{i=1}^{N} C_i X_i && \text{Linear} \\
&+ \sum_{i=1}^{N} \sum_{j=1}^{N} C_{ij} X_i X_j && \text{Quadratic} \qquad (4.1) \\
&+ \sum_{i=1}^{N} \sum_{j=1}^{N} \sum_{k=1}^{N} C_{ijk} X_i X_j X_k && \text{Cubic} \\
&+ \text{etc.} && \text{Quartic, etc.}
\end{aligned}
$$

The number of terms of each degree is given by the binomial coefficient $\binom{N-1+K}{K}$ where K is the degree. The total number of terms up to and including degree K is given by $\binom{N+K}{K}$. This is tabulated in Table 4-1 below.

Table 4-1

NUMBER OF TERMS IN MULTINOMIAL EXPANSION

No. of Parameters	Degree K						
N	1	2	3	4	5	6	7
1	2	3	4	5	6	7	8
2	3	6	10	15	21	28	36
3	4	10	20	35	56	84	120
4	5	15	35	70	126	210	330
5	6	21	56	126	252	462	792
6	7	28	84	210	462	924	1716
7	8	36	120	330	792	1716	3432

Note that the first row and the first column of the table are just a sequence of consecutive integers and that the other entries are the sum of the entry above and the entry to the left, i.e., $a_{i,j} = a_{i-1,j} + a_{i,j-1}$.

In a typical sensitivity study some set of parameters, X_j, is varied over a preselected set of values and the values of a response measure, y, are recorded. The values of the response measure may then be plotted as functions of the various variables. However, if one is interested in estimating the value of the response measure for a set of parameters different from one of the preselected sets it is necessary to either compute y for the new set (by running the program) or to estimate y by interpolating the data available. A functional representation such as given by Equation 4.1 provides a means of interpolation. The coefficients, C, can be calculated from the values of y obtained from the preselected sets of X_j's by a least square procedure. The number of independent sets of data must be at least equal to the number of coefficients as given in Table 4-1 but a significantly greater number than this minimum is recommended to achieve a certain degree of smoothing from the least square procedure.

It is difficult, if not impossible, to cite how many values should be used because of the complexity of the problem. It is easier to draw conclusions 'after the fact'; that is, the coefficients are computed for a given set of data and the function evaluated for intermediate points. If there are rapid variations of the function, its use as an interpolation function is in doubt whereas if the function behaves smoothly, then it may be useful. For example, consider a cubic fit to four points of a function of one variable. Both a rapid variation and a smooth variation are illustrated in Figure 4-1. In both cases the cubic goes through all of the data points but the rapidly varying function clearly can result in less accurate interpolated values.

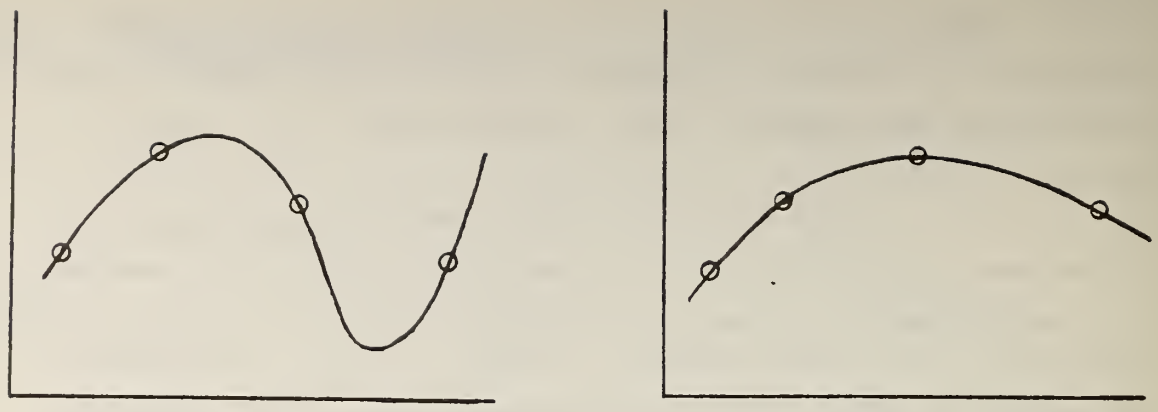

Poor Fit - Rapidly Varying Function

Good Fit - Smoothly Varying Function

Figure 4-1 EXAMPLES OF POOR AND GOOD FITS TO DATA USING CUBIC FUNCTIONS

Returning to Equation 4.1, if the value of each X is replaced by its deviation from some nominal value, i.e., replace X_i by $X_i - X_{i0}$, X_j by $X_j - X_{j0}$, etc., then the coefficients in the expansions may be considered as the terms in a Taylor series. That is, C_o is the value of the function at the nominal point X_{i0}, $i = 1,N$ and the linear terms C_i are the partial derivatives evaluated at the nominal point, etc.

4.2 RMAFG Fortran Program

A Fortran program has been developed to evaluate the coefficients in the expansion of the form given by Equation 4.1. It consists of a Main Program and four subroutines. The basic coding is written in a fashion such that the size of the problem is limited only by the storage assignments made in the dimension statements. In the listing of the program given in Appendix B, the program is dimensioned to handle ten independent variables (X_i) and 100 data points.

Three modes of operation are provided:

Mode 0 -- the expression as given by Equation 4.1 is treated.

Mode 1 -- the X_i of Equation 4.1 are replaced by $X_i - X_{i0}$ where X_{i0} is the average of the given values, i.e.,

$$X_{i0} = \frac{1}{M} \sum_{k=1}^{M} X_i(k), \quad i = 1,N$$

$X_i(k)$ is the value of X_i in the kth data set.

Mode 2 -- The X_i of Equation 4.1 are replaced by $(X_i - X_{i0})/\sigma$

where X_{i0} is as in Mode 1 and

$\sigma = (\frac{1}{M} \sum_{1}^{M} X_i^2(k) - X_{i0}^2)^{1/2}$, is the standard deviation.

Mode 2 has an advantage of normalizing the parameters (independent variables) to a common distribution so that the magnitude of the $C's$ are more readily comparable.

The program allows the degree of parameter to be limited. For example, we may have 3 parameters X_1, X_2 and X_3 and use a cubit fit on all parameters, in which case all 20 coefficients ($C's$) will be evaluated; or, we may limit X_1 to the 1st degree, X_2 to the 2nd degree and X_3 to the 3rd degree. In this case the terms will be $y = C_0 + C_1X_1 + C_2X_2 + C_3X_3 + C_{22}X_2^2 + C_{32}X_2X_3 + C_{33}X_3^2 + C_{333}X_3^3$. The only restriction of the program is that the parameters be labeled so that they are ordered on increasing degrees, as in the example just cited.

The mathematical procedure is most readily described by treating the $C's$ and the combinations of the parameters as components of vectors. In the above example let:

$$\underline{C}^T = (C_0, C_1, C_2, C_3, C_{22}, C_{32}, C_{33}, C_{333})$$

and $$\underline{U}^T = (1, X_1, X_2, X_3, X_2^2, X_2X_3, X_3^2, X_3^3).$$

Equation 4.1 may be written as:

$$y = \underline{U}^T\underline{C}.$$

If we use the subscript m to denote the mth data point then $y_m = \underline{U}_m^T\underline{C}$.

The error of the fit, E_m, is then

$$E_m = y_m - \underline{U}_m^T\underline{C}$$

The mean squared error is:

$$\overline{E^2} = \frac{1}{m}\sum_{1}^{m} E_m^2$$

$$= \frac{1}{M}\sum_{1}^{m} (y_m - \underline{C}^T\underline{U}_m)(y_m - \underline{U}_m^T\underline{C})$$

$$= \overline{y^2} + \underline{C}^T\,\overline{UU^T}\underline{C} - \underline{C}^T\,\overline{Uy} - \overline{yU^T}\,\underline{C}$$

where:

$$\overline{UU^T} = \frac{1}{m}\sum_{m=1}^{m} \underline{U}_m\,\underline{U}_m^T, \text{ an } MxM \text{ matrix}$$

$$\overline{yU^T} = \left(\frac{1}{m}\sum_{1}^{m} y_m,\ \frac{1}{m}\sum_{1}^{m} y_m X_{1m}, \text{ etc.}\right)$$

The mean squared error is minimized when $\underline{C}$ has the value

$$\underline{C} = \overline{(UU^T)}^{-1} \overline{Uy}$$

With this value of $\underline{C}$ the average error $\overline{E}$ is zero and the average squared error is:

$$\overline{E^2} = \overline{y^2} - \overline{yU^T}\,\underline{C}.$$

A special matrix inversion routine was written to compute the $\underline{C}$. It allows the program to output the results obtained by the lower order functions. That is, if a cubic fit is specified it evaluates the best constant, the best linear fit, the best quadratic fit, and finally, the best cubic fit.

The mean squared error is computed for each of these intermediate fits and is printed along with the values of the coefficient $\underline{C}$.

The general flow of the program is as follows.

Read *N, (NDG(J),j=1,N)*

N — number of parameters (independent variables), if *N = 0* program will terminate

NDG(J) — maximum degree of parameter X_1. These must be ordered: *NDG(J-1)* $\leq$ *NDG(J)*.

Call *SET Z*.

Subroutine *SET Z* computes the subscripts used to identify the *C's* and checks whether any storage limits are violated.

Read *NDATA, MODE, IVAL.*

NDATA, number of data sets.

MODE, 0 normal
1 remove mean
2 remove mean, normalize by σ , (the standard deviation).

IVAL, 0 compute fit and go back for another case.
1 read in additional data and evaluate fit at these points.

Read *Y(J), (X(J,I)(J=1,N), I=1, NDATA.*

Y(I) function value at point *I*

X(J,I) parameter value at point *I*

Call *SIGM.*

Subroutine *SIGM* evaluates the mean and sigma of y and the X_j. It modifies X_j depending on the mode selected.

The program then computes the $\overline{UU^T}$ matrix and the $\overline{Uy}$ vector and calls subroutine *SETU* which evaluates the *U* vector for each data point.

Next, subroutine *SOLVE* is called which inverts the $\overline{UU^T}$ matrix and solves for the *C's*. Subroutine *SOLVE* uses a bordering scheme so that the intermediate results are available. As each fit is completed (constant, linear, quadratic, etc.), the main routine evaluates the error of the fit and outputs the error and the values of the coefficients. The routine checks *IVAL* to see if further evaluations are desired. If so, it reads the desired values of the parameter and evaluates y.

4.3 Sample Numerical Evaluation of the RMAFG

Using the Head-Neck Pendulum test simulation (Reference 1, Volume 2) as a baseline run, the linear spring coefficients of the neck joints were varied from 28 to 34.4 in steps of 1.6, the viscous friction of the neck joints was varied from 0.130 to 0.170 in steps of 0.01 and the Coulomb friction of the neck joints was varied from 90 to 110 in steps of 5. This produced a series of 125 runs (each variable has five different values). Several response measures were extracted from the tabular time histories and processed by the RMAFG. The basic results are summarized in Table 4-2.

Table 4-2
SELECTED OUTPUT OF THE RMAFG

Response Measure	Mean	Sigma	Root Mean Square Error For Degree of Fit			
			Constant	Linear	Quadratic	Cubic
1. HIC	91.81	1.65	1.6524	0.4662	0.2697	0.2052
2. HSI	122.85	3.11	3.1068	0.4241	0.3342	0.2971
3. Time of zero head pitch, ms.	103.13	3.16	3.1570	0.1522	0.0135	0.0044
4. Time of max. head resultant acceleration, ms.	33.01	0.05	0.0533	0.0430	0.0275	0.0151
5. Value of max. head resultant acceleration, g	29.88	0.24	0.2352	0.1551	0.1151	0.0750
6. Time of max. head pitch, ms.	55.94	1.17	1.1749	0.0590	0.0221	0.0160
7. Value of max. head pitch, deg.	61.95	2.26	0.2600	0.1099	0.0249	0.0239

The time of zero head pitch was estimated by linearly interpolating the values of pitch just before and just after the pitch passed through zero. In all runs, the tabular time histories were obtained at 2 millisecond intervals. The times of maximums and the values of the maximums were obtained by a quadratic interpolation formula using the three points from the tabular

time histories in the vicinity of the maximum. This quadratic interpolation formula is --

$$f = f_2 + 1/2(f_3 - f_1)(t - t_2)/d + 1/2(f_1 - 2f_2 + f_3)(t - t_2)^2/d^2$$

where f is the value of the function at t and $d = t_1 - t_2$.

The time of the maximum is given by

$$t_{max} = t_2 + [(f_1 - f_3)/(f_1 - 2f_2 + f_3)]d/2$$

and the value of the maximum is

$$f_{max} = f_2 - 1/8(f_1 - f_3)^2/(f_1 - 2f_2 + f_3).$$

In using the RMAFG the three parameters were identified as follows:

x_1	linear spring coefficient
x_2	viscous friction
x_3	coulomb friction.

The mean, m, and the standard deviation, σ, of each of the parameter variations were computed and the normalized variables (mode 2) were used by the RMAFG, i.e., the variables used were $Z_i = (x_i - m)/\sigma$. The use of these normalized variables has the advantage of allowing one to directly compare the significance of the coefficients of the fit obtained by the RMAFG.

With reference to Table 4-2, which shows the root mean square error of the fit as a function of the degree of the fit, we note the following:

1. For all responses except 4 and 5 which deal with the head acceleration there is a dramatic reduction in the rms error when the degree is changed from a constant to a linear fit.

2. The most significant improvement resulting from increasing the degree from a linear to a quadratic fit occurs for responses 3 and 7.

3. Response 3 shows the most significant improvement resulting from changing from a quadratic to a cubic fit.

One conclusion that may be drawn is that, for response 7 (the value of maximum head pitch), a quadratic fit is sufficient since use of a cubic results in a negligible reduction of the error. However, note that the standard deviation of the maximum pitch angle is 2.26 degrees and the mean value is 61.95 degrees (computed from the 125 runs). Thus, even though a quadratic fit reduces the error by a factor of four from the linear fit, the linear fit approximates the data with a rms error of only 0.11 which may be adequate for most purposes.

From a practical point of view, there is not much variation of any of the response measures selected for this set of runs. The most significant deviations are those related to times, responses 3 and 6, and the value of maximum head pitch, response 7. The use of a linear fit in these three cases reduces the error to a small fraction of the standard deviation.

It is recommended that the user use the RMAFG to evaluate the error reduction that results from increasing the degree of the function so that the degree of fit that is adequate for his purpose may be selected. It is further recommended that interpolated results at intermediate points (points other than the inputted data used for the fit) be checked to ensure that the degree selected does not give a 'poor' fit as illustrated in Figure 4-1.

4.4 Example of RMAFG Program Output

Data from a set of computer runs made as a part of the shoulder model studies (see Section 3.2) were used to illustrate the output provided by the RMAFG computer program. In this set of simulations, the shoulders were represented as EULER joints with the precession and nutation axes initially locked and allowed to unlock at specified torque levels. The coulomb friction and the unlocking torques were varied over preselected ranges and the unlocking torque for each axis was arbitrarily set as 110 percent of the coulomb friction. The response measures selected for determining approximating functions with the RMAFG using the coulomb friction of the precession and nutation axes as the independent variables were: the maximum pitch angle of the right lower arm, the time at which this maximum pitch occurred, and the pitch and the yaw angles of the right lower arm at the end of each 300 millisecond run. The data from the shoulder simulations that were input to the RMAFG program are given in Table 4-3.

The output from the RMAFG routine for each of the four response measures evaluated is presented in Figure 4-2(a) through (d). Note that, for each case, a quadratic fit of the data using MODE = 2 (see Section 4.2) was specified. Also, the values of the functions for two intermediate values of the independent variables were calculated.

A sample plot of the pitch angle of the lower arm at 300 msec as a function of the coulomb friction on the precession and nutation axes that results from the quadratic fit obtained with the RMAFG is depicted in Figure 4-3.

Table 4-3

RESULTS OF SHOULDER SIMULATIONS INPUT TO THE RMAFG

Run No.	Precession Axis Coulomb Friction In.-Lb.	Precession Axis Unlocking Torque In.-Lb.	Nutation Axis Coulomb Friction In.-Lb.	Nutation Axis Unlocking Torque In.-Lb.	Max. Pitch Degree	Time of Max. Pitch msec.	Pitch @ 300 msec. Degree	Yaw @ 300 msec. Degree
BASE	163	180	122	134	-3.91	45	-71.66	10.91
A	122	134	163	180	1.02	85	-62.82	8.04
B	140	154	110	121	-1.90	65	-63.28	8.28
C	110	121	140	154	1.90	85	-64.15	7.87
D	180	198	130	143	-4.25	40	-77.14	14.80
E	130	143	180	198	-0.01	85	-62.57	8.30
F	180	198	180	198	-4.25	40	-77.00	14.61
G	110	121	110	121	1.90	85	-64.18	8.03

```
SHLD25 RUNS TO DEMONSTRATE RMAFG, PENDULUM TEST 14 SEGMENT SHOULDER ARMS,EULER
ND.VAR. COULOMB TORQUE; DEP. MAX PITCH, TIME MAX PITCH, PITCH(300MS),YAW(300MS)

   Mean              -1.18750  Sigma              2.54957  for Function Y

  J   Degree        Mean       Sigma:  for Parameters X( )
  1     2       141.87500       27.21414
  2     2       143.25000       25.81061

MEAN removed from Parameters X( ) and normalized

The error using     1 coefficients is        2.54957
Coefficients            Value                                    Constant

        0.           -1.187500


The error using     3 coefficients is         .39268
Coefficients            Value                                    Linear

        0.           -1.187500
        1.           -2.527440
        2.             .307646


The error using     6 coefficients is         .15472
Coefficients            Value

        0.           -2.098679                                   Quadratic
        1.           -2.752310
        2.             .256477
       11.             .768566
       21.            -.247936
       22.             .164377

Error Distribution - Histogram
  Sigma       # Points                    Point IndeX
 -2.50        0.
 -2.00        0.
 -1.50        1. *                       2
 -1.00        0.
  -.50        3. ***                     3   5   8
  0.00        1. *                       7
   .50        1. *                       6
  1.00        0.
  1.50        2. **                      1   4
  2.00        0.
  2.50        0.
```

(a) Function For Maximum Pitch Angle

Figure 4-2 SAMPLE OUTPUT OF THE RMAFG ROUTINE APPLIED TO SHOULDER MODEL RESPONSE MEASURES

Function 1 Evaluations at Given Input Points

Point	Y(Input)	Y(Fit)	Parameters X( )	
1	-3.910	-3.713	163.000	122.000
2	1.020	.752	122.000	163.000
3	-1.900	-1.985	140.000	110.000
4	1.900	2.113	110.000	140.000
5	-4.250	-4.356	180.000	130.000
6	-.010	.101	130.000	180.000
7	-4.250	-4.242	180.000	180.000
8	1.900	1.830	110.000	121.000

Function 1 Evaluations at Specified Input Points

Point	Y(Fit)	Parameters X( )	
1	-.895	130.000	130.000
2	-2.793	150.000	150.000

Figure 4-2(a) (Cont'd.)

```
SHLD25 RUNS TO DEMONSTRATE RMAFG, PENDULUM TEST 14 SEGMENT SHOULDER ARMS,EULER
ND.VAR. COULOMB TORQUE; DEP. MAX PITCH, TIME MAX PITCH, PITCH(300MS),YAW(300MS)

   Mean              66.25000  Sigma              20.11685  for Function Y

  J   Degree        Mean        Sigma:  for Parameters X( )
  1     2       141.87500        27.21414
  2     2       143.25000        25.81061

MEAN removed from Parameters X( ) and normalized

The error using     1 coefficients is        20.11685
Coefficients             Value

        0.           66.250000


The error using     3 coefficients is         3.17906
Coefficients             Value

        0.           66.250000
        1.          -19.816600
        2.            3.955115


The error using     6 coefficients is         1.43056
Coefficients             Value

        0.           54.792162
        1.          -21.930729
        2.            2.442389
       11.            5.207368
       21.           -5.730120
       22.            6.753447

Error Distribution - Histogram
  Sigma        # Points                    Point IndeX
 -2.50         0.
 -2.00         0.
 -1.50         1. *                       2
 -1.00         1. *                       3
  -.50         1. *                       5
  0.00         2. **                      7   8
   .50         0.
  1.00         2. **                      4   6
  1.50         1. *                       1
  2.00         0.
  2.50         0.
```

(b) Function For Time of Occurrence of Maximum Pitch Angle

Figure 4-2 (Cont'd.)

Function 2 Evaluations at Given Input Points

Point	Y(Input)	Y(Fit)	Parameters X( )	
1	45.000	47.135	163.000	122.000
2	85.000	82.611	122.000	163.000
3	65.000	63.881	140.000	110.000
4	85.000	86.577	110.000	140.000
5	40.000	38.936	180.000	130.000
6	85.000	86.082	130.000	180.000
7	40.000	40.028	180.000	180.000
8	85.000	84.750	110.000	121.000

Function 2 Evaluations at Specified Input Points

Point	Y(Fit)	Parameters X( )	
1	64.596	130.000	130.000
2	49.362	150.000	150.000

Figure 4-2(b) (Cont'd.)

```
SHLD25 RUNS TO DEMONSTRATE RMAFG, PENDULUM TEST 14 SEGMENT SHOULDER ARMS,EULER
ND.VAR. COULOMB TORQUE; DEP. MAX PITCH, TIME MAX PITCH, PITCH(300MS),YAW(300MS)

   Mean              -67.85000  Sigma              5.97668  for Function Y

  J   Degree        Mean       Sigma:  for Parameters X( )
  1     2       141.87500       27.21414
  2     2       143.25000       25.81061

MEAN removed from Parameters X( ) and normalized

The error using     1 coefficients is        5.97668
Coefficients            Value

        0.          -67.850000


The error using     3 coefficients is        2.41994
Coefficients            Value

        0.          -67.850000
        1.           -5.470639
        2.             .071163


The error using     6 coefficients is         .56663
Coefficients            Value

        0.          -66.643753
        1.           -4.942339
        2.             -.132234
       11.           -2.443365
       21.            -.556155
       22.            1.285935

Error Distribution - Histogram
  Sigma       # Points                    Point IndeX
 -2.50        0.
 -2.00        0.
 -1.50        1. *                       3
 -1.00        1. *                       2
  -.50        1. *                       5
  0.00        2. **                      4   7
   .50        1. *                       6
  1.00        1. *                       8
  1.50        0.
  2.00        1. *                       1
  2.50        0.
```

(c) Function For Pitch Angle @ 300 msec.

Figure 4-2 (Cont'd.)

Function 3 Evaluations at Given Input Points

Point	Y(Input)	Y(Fit)	Parameters X( )	
1	-71.660	-70.617	163.000	122.000
2	-62.820	-63.375	122.000	163.000
3	-63.280	-64.060	140.000	110.000
4	-64.150	-64.252	110.000	140.000
5	-77.140	-77.556	180.000	130.000
6	-62.570	-62.188	130.000	180.000
7	-77.000	-77.054	180.000	180.000
8	-64.180	-63.699	110.000	121.000

Function 3 Evaluations at Specified Input Points

Point	Y(Fit)	Parameters X( )	
1	-64.670	130.000	130.000
2	-68.327	150.000	150.000

Figure 4-2(c) (Cont'd.)

```
SHLD25 RUNS TO DEMONSTRATE RMAFG, PENDULUM TEST 14 SEGMENT SHOULDER ARMS,EULER
ND.VAR. COULOMB TORQUE; DEP. MAX PITCH, TIME MAX PITCH, PITCH(300MS),YAW(300MS)

   Mean              10.10500  Sigma              2.80935  for Function Y

  J   Degree        Mean        Sigma:  for Parameters X( )
  1     2       141.87500       27.21414
  2     2       143.25000       25.81061

MEAN removed from Parameters X( ) and normalized

The error using     1 coefficients is        2.80935
Coefficients            Value

        0.            10.105000


The error using     3 coefficients is         .98164
Coefficients            Value

        0.            10.105000
        1.             2.603300
        2.              .223047


The error using     6 coefficients is         .10535
Coefficients            Value

        0.             7.943752
        1.             2.052303
        2.              .070976
       11.             1.855552
       21.             -.310125
       22.              .332918

Error Distribution - Histogram
  Sigma       # Points                    Point IndeX
 -2.50        0.
 -2.00        0.
 -1.50        1. *                       2
 -1.00        0.
  -.50        3. ***                     3   5   8
  0.00        1. *                       7
   .50        1. *                       6
  1.00        1. *                       1
  1.50        1. *                       4
  2.00        0.
  2.50        0.
```

(d) Function For Yaw Angle @ 300 msec.

Figure 4-2 (Cont'd.)

Function 4 Evaluations at Given Input Points

Point	Y(Input)	Y(Fit)	Parameters X( )	
1	10.910	11.020	163.000	122.000
2	8.040	7.857	122.000	163.000
3	8.280	8.245	140.000	110.000
4	7.870	8.036	110.000	140.000
5	14.800	14.735	180.000	130.000
6	8.300	8.370	130.000	180.000
7	14.610	14.618	180.000	180.000
8	8.030	7.959	110.000	121.000

Function 4 Evaluations at Specified Input Points

Point	Y(Fit)	Parameters X( )	
1	7.383	130.000	130.000
2	8.739	150.000	150.000

Figure 4-2(d) (Cont'd.)

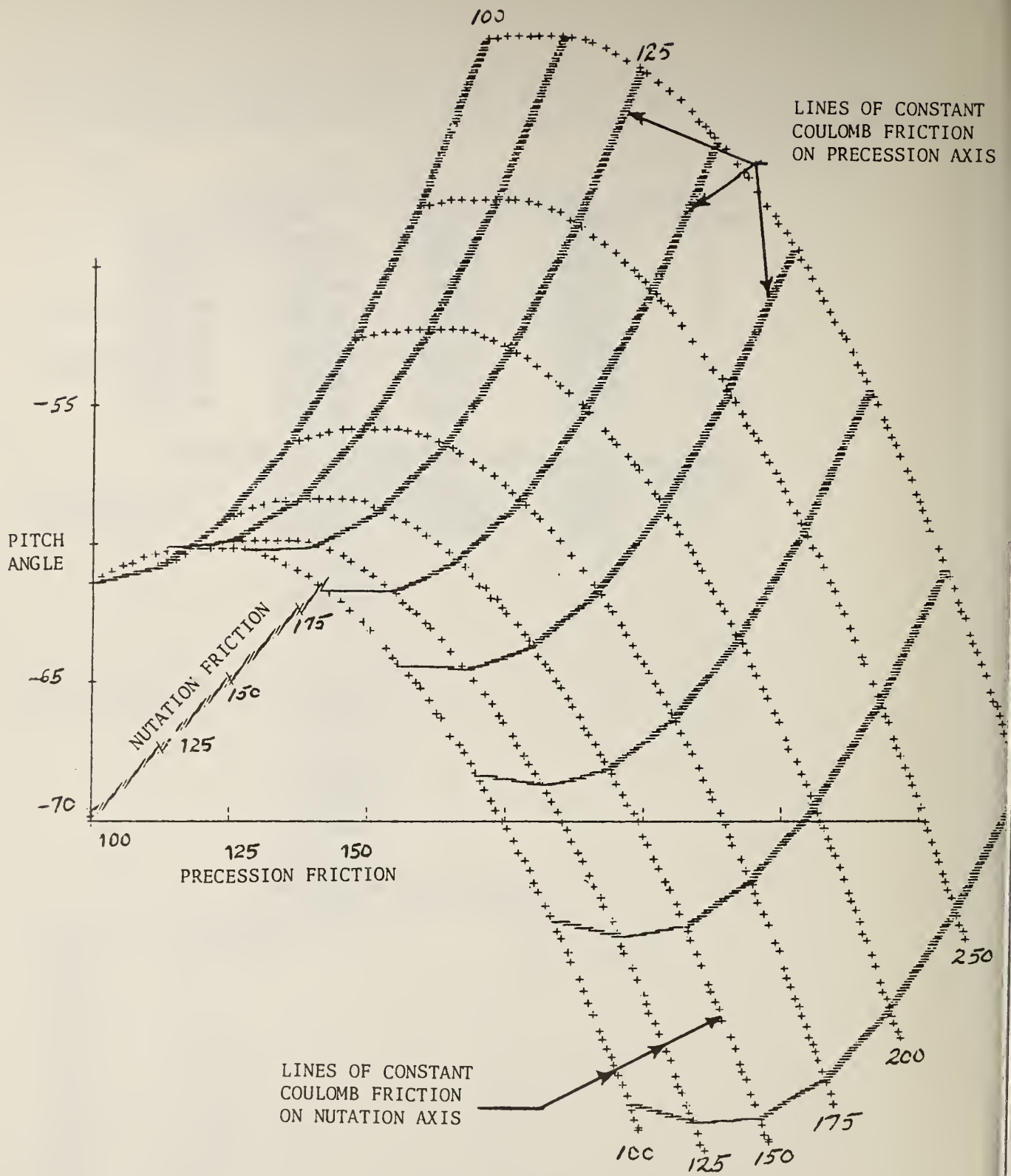

Figure 4-3 SAMPLE PLOT OF RMAFG QUADRATIC FUNCTION FOR PITCH ANGLE @ 300 MSEC.

5.0 REDUCTION OF THE NUMBER OF INERTIA RELATED PARAMETERS

A fact that is not widely appreciated is that there is an infinite number of different chains of connected rigid bodies, each with different mass distributions, that all have identical dynamic responses and may be considered as "dynamically equivalent." In particular, it is possible to add or subtract an arbitrary amount from each mass in a connected chain of rigid bodies and obtain a dynamically equivalent system. The only constraint is that the sum of the mass perturbations be zero, i.e., the total mass must not be changed. It is, in fact, possible to make one or more of the masses in the chain zero, or negative, and still define an equivalent system.

The purpose of this task was to develop a computer program to compute dynamically equivalent systems. The basic theorem and the questions are given on pages 113-117 of Volume 1 - Engineering Manual of Reference 1.

Theorem:

Given a system of N rigid bodies connected by joints in a tree structure, make the following transformations:

$$M_k^* = M_k + d_k, \quad \text{where} \quad \sum_{k=1}^{N} d_k = 0 \quad \text{mass equation,}$$

$$P_k^* = P_k + \sum_j d_{k_j} \left[r_{k_j}^* \times (r_{k_j} \times) \right], \quad \text{inertia equation,}$$

$$X_k^* = X_k - C_k, \quad \text{transformation of c.g.,}$$

$$M_k^* C_k = \sum_j d_{k_j} r_{k_j}, \quad \text{evaluation of } C_k,$$

$$r_{k_j}^* = r_{k_j} + C_k, \quad \text{transformation of joint locations,}$$

(The notation $[s \times (r \times]$ denotes the matrix $r s^T - s^T r I$, where s^T is the transpose of s and I is the identity matrix.)

where:

M_k is the mass of segment k and M_k^* is the perturbed mass,

d_k is the mass perturbation of segment k,

d_{k_j} is the sum of the d_k of the segments which may be reached through joint j from segment k,

P_k is the inertia matrix of segment k and P_k^* is the perturbed inertia,

X_k is the location of the c.g. of segment k and X_k^* is the perturbed location,

C_k is the perturbation of the c.g. and joint locations of segment k,

r_{k_j} is the location of the j'th joint associated with segment k and

$r_{k_j}^*$ is the perturbed joint location. Joint locations are relative to the c.g. of the segment.

The theorem states that this perturbed system has the same motion as the unperturbed system. This implies that, even if one had complete knowledge of the motion, i.e., positions, velocities and orientations of the segments, one would not be able to compute the masses of the individual segments (the M_k) or determine the location of the center of mass of the segments (the X_k). Note that the geometry is the same. The mass, inertia matrix and location of the

center of mass are the only quantities that are changed. (Of course, the location of a joint relative to the c_m will change because the c_m will change, but the distance between joints attached to the same segment is not changed.)

5.1 Description of the Delta Algorithm Fortran Program

The listing of the Fortran program called the "Delta Algorithm" which will compute an equivalent system is given in Appendix C. Figure 5-1 is a flow diagram of the main program.

The routine to compute an equivalent system has been written so that it accepts the segment cards (B2) and the joint cards (B3) with the same information and format as the main CVS program (see Reference 1, Volume 3). A lead card with the number of segments (NSEG), the number of joints (NJNT) and the value of G (to convert weight to mass units) is required. A final card(s) containing the weight (mass) perturbations is also read.

All of the computations are made in subroutine DELTA. The key to the procedure is the computation of the d_{k_j} from the information in JNT(J). The logic of the computation is in the DO 35 loop of the subroutine. Although it has only about 25 Fortran statements, this logic is quite involved and hence is difficult to follow. It is based on the following properties of the JNT vector.

$$0 < JNT(J) \leq J$$

(This assumes all segments are connected and any flexible elements are considered as regular segments.)

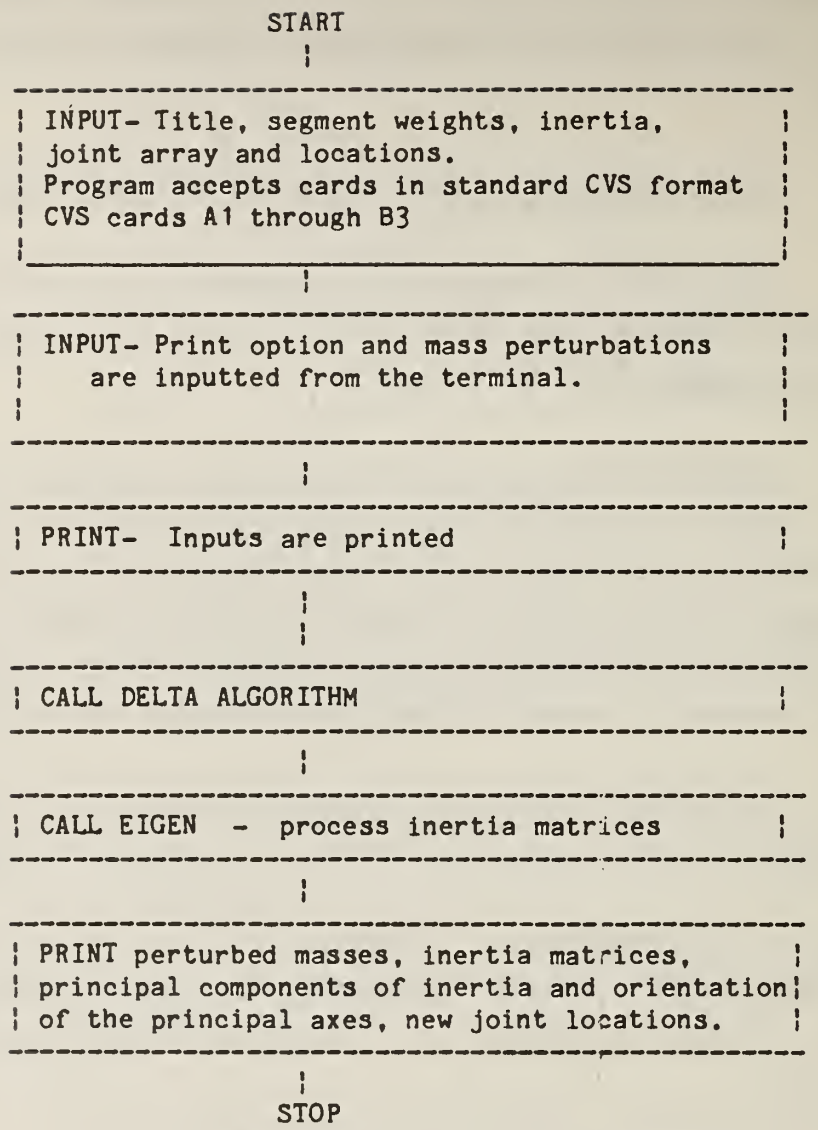

Figure 5-1 FLOW DIAGRAM OF DELTA ALGORITHM COMPUTER PROGRAM

If $JNT(J) = N$, the segment $J+1$ is in the branch emanating from segment N via joint J. All segment numbers which are not in the vector $JNT(J)$ are the end of a branch (except for segment 1). For example, consider the JNT vector of the standard 15 segment crash victim model:

J	1	2	3	4	5	6	7	8	9	10	11	12	13	14
JNT	1	2	3	4	1	6	7	1	9	10	3	12	3	14

Segments 5, 8, 11, 13, 15 are not in the vector. These are the head, feet and the lower arms.

In this example, for segment 1

$$d_{1_1} = d_2 + d_3 + d_4 + d_5 + d_{12} + d_{13} + d_{14} + d_{15}$$

$$d_{1_5} = d_6 + d_7 + d_8$$

$$d_{1_8} = d_9 + d_{10} + d_{11}$$

Note: $d_1 + d_{1_1} + d_{1_5} + d_{1_8} = 0$, since $\Sigma\, d_n = 0$.

In the routine the sums required to compute c_k and P_k^* are accumulated as c_k, and the d_{k_j} are determined in the DO 35 loop. The formula for P_k^* is written in a modified form as follows:

$$P_k^* = P_k + \sum_j d_{k_j} [r_{k_j} \times (r_{k_j} \times] + \sum_j d_{k_j} [C_k \times (r_{k_j} \times]$$

$$= P_k + \sum_j d_{k_j} [r_{k_j} \times (r_{k_j} \times] + M_k^* [C_k \times (C_k \times]$$

(The notations $[s \times (r \times]$ denotes the matrix $r\, s^T - s^T r I$, where s^T is the transpose of s and I is the identity matrix.)

The $r_{k_j}^*$ are computed in subroutine DELTA. When subroutine DELTA has finished, the main program calls subroutine EIGEN to determine the principal moments of inertia from P_k^* and the relative direction cosine matrix. The main routine then computes the yaw, pitch and roll angles of the system for P^* with respect to the original system for P_k.

Finally, the M_k^*, P_k^*, C_k, principal moments of inertia, yaw pitch and roll, and the $r_{k_j}^*$ are printed. This is sufficient information to form an input deck for the latest version of the CVS program which allows for a rotated inertia matrix.

5.2 Sample Application of the Delta Algorithm Program

The Delta algorithm computer program was executed to illustrate how it can be used to compute dynamically equivalent systems. For this example, an old data deck for a 15 segment-14 joint model of a crash victim was used. The printout from the routine, presented in Figure 5-2, shows the values of the original physical system and the weight perturbations of the various segments that were input to the program, and the computed characteristics of the segments and joints of the dynamically equivalent system.

```
DYNAMICALLY EQUIVALENT SYSTEM
 15 NOV 1979    TEST RUN OF EQUIVALENT SYSTEM ROUTINE , CVS TEST CASE 3 CARD A1
 TEST CASE 3. INITIAL EQUILIBRIUM AND AIRBAG. RUN UNDER CVS-III (VER. 19A)
 15 SEGMENTS. CAR-TO-CAR CRASH. FRONT SEAT DUMMY WITH SEAT BELT AND AIRBAG.
IN. LB.SEC.      0.0         0.0      386.088                          CARD A3
  6  30  0.002  0.00025  0.001 0.000125                                CARD A4
0 0 5 2 5 5                                                           CARD A5

SEGMENTS   15  JOINTS   14
```

SEGMENT			WEIGHT	SEGMENT MOMENT OF INERTIA			SEGMENT CONTACT ELLIPSOID SEMIAXES			CENTER		
1	LT	5	35.750	1.78000	1.14000	1.71000	4.94	6.94	7.60	0.00	0.00	0.00
2	CT	4	9.380	.32500	.31400	.14900	4.91	6.35	7.03	0.00	0.00	-2.00
3	UT	3	31.750	2.32000	1.65000	1.33000	4.41	6.78	4.94	0.00	0.00	0.00
4	N	2	3.130	.04000	.04000	.00660	2.57	2.28	3.28	0.00	0.00	0.00
5	H	1	10.130	.25900	.31100	.20000	3.99	3.10	4.59	0.00	0.00	0.00
6	RUL	6	17.440	.72700	.70300	.15400	2.99	3.74	12.40	0.00	0.00	-2.60
7	RLL	7	6.970	.44000	.44200	.01900	2.36	2.23	9.07	0.00	0.00	-.45
8	RF	8	2.750	.03830	.04340	.01320	1.52	1.80	5.22	0.00	0.00	.95
9	LUL	9	17.440	.72700	.70300	.15400	2.99	3.74	12.40	0.00	0.00	-2.60
10	LLL	A	6.970	.44000	.44200	.01900	2.36	2.23	9.07	0.00	0.00	-.45
11	LF	B	2.750	.03830	.04340	.01320	1.52	1.80	5.22	0.00	0.00	.95
12	RUA	C	5.260	.16400	.16600	.01410	2.07	1.64	6.88	0.00	0.00	0.00
13	RLA	D	4.790	.25500	.25900	.01150	1.30	1.11	8.38	0.00	0.00	0.00
14	LUA	E	5.260	.16400	.16600	.01410	2.07	1.64	6.88	0.00	0.00	0.00
15	LLA	F	4.790	.25500	.25900	.01150	1.30	1.11	8.38	0.00	0.00	0.00

JOINT					LOCATION			SEG(JNT)	LOCATION		SEG(J+1)	PRIN. AXIS(DEG) - SEG(JNT)			PRIN. AXIS(DEG) - SEG(J+1)		
J	SYM	PLOT	JNT	PIN	X	Y	Z		X	Y	Z	YAW	PITCH	ROLL	YAW	PITCH	ROLL
1		P	1	-2	-1.60	0.00	-2.50		-1.50	0.00	2.50	0.00	0.00	0.00	0.00	0.00	0.00
2		O	2	-2	-1.50	0.00	-2.30		-1.50	0.00	6.80	0.00	0.00	0.00	0.00	0.00	0.00
3	P	N	3	-2	-.90	0.00	-2.20		0.00	0.00	3.80	0.00	0.00	0.00	0.00	0.00	0.00
4	P	M	4	-2	0.00	0.00	-1.20		-1.10	0.00	3.30	0.00	0.00	0.00	0.00	0.00	0.00
5	H	Q	1	0	2.10	4.45	2.50		0.00	0.00	-7.31	0.00	0.00	0.00	0.00	-66.50	5.72
6	K	R	6	1	0.00	0.00	6.79		0.00	0.00	-7.48	0.00	0.00	0.00	0.00	56.80	0.00
7	A	S	7	-2	0.00	0.00	8.69		1.54	0.00	-1.28	0.00	0.00	0.00	0.00	-81.00	0.00
8	H	T	1	0	2.10	-4.45	2.50		0.00	0.00	-7.31	0.00	0.00	0.00	0.00	-66.50	-5.72
9	K	U	9	1	0.00	0.00	6.79		0.00	0.00	-7.48	0.00	0.00	0.00	0.00	56.80	0.00
10	A	V	10	-2	0.00	0.00	8.69		1.54	0.00	-1.28	0.00	0.00	0.00	0.00	-81.00	0.00
11	S	W	3	-2	-.80	7.60	-1.60		0.00	0.00	-5.25	0.00	0.00	0.00	0.00	-57.50	10.19
12	E	X	12	-1	0.00	0.00	5.45		0.00	0.00	-6.58	0.00	0.00	0.00	0.00	-64.30	0.00
13	S	Y	3	-2	-.80	-7.60	-1.60		0.00	0.00	-5.25	0.00	0.00	0.00	0.00	-57.50	-10.19
14	E	Z	14	-1	0.00	0.00	5.45		0.00	0.00	-6.58	0.00	0.00	0.00	0.00	-64.30	0.00

```
WEIGHT PERTURBATIONS

   -1.5000  0.0000   .5000 -1.0000   .5000  -.2500   .2500   .5000  -.2500   .2500   .5000  -.2500   .5000  -.2500   .5000
```

Figure 5-2 SAMPLE OUTPUT FROM THE DELTA ALGORITHM COMPUTER PROGRAM

COMPUTATIONS OF DELTA ALGORITHM

1	1	0	0.0000	0.0000	0.0000
1	1	2	.5000	.5000	.5000
1	1	3	-1.0000	-.5000	-.5000
1	1	4	.5000	0.0000	0.0000
1	1	11	-.2500	-.2500	-.2500
1	1	12	.5000	.2500	.2500
1	1	13	-.2500	0.0000	0.0000
1	1	14	.5000	.5000	.5000
1	5	0	-.2500	-.2500	.2500
1	5	6	.2500	0.0000	.5000
1	5	7	.5000	.5000	1.0000
1	8	0	-.2500	-.2500	.7500
1	8	9	.2500	0.0000	1.0000
1	8	10	.5000	.5000	1.5000
2	2	0	.5000	.5000	.5000
2	2	3	-1.0000	-.5000	-.5000
2	2	4	.5000	0.0000	0.0000
2	2	11	-.2500	-.2500	-.2500
2	2	12	.5000	.2500	.2500
2	2	13	-.2500	0.0000	0.0000
2	2	14	.5000	.5000	.5000
3	3	0	-1.0000	-1.0000	-1.0000
3	3	4	.5000	-.5000	-.5000
3	11	0	-.2500	-.2500	-.7500
3	11	12	.5000	.2500	-.2500
3	13	0	-.2500	-.2500	-.5000
3	13	14	.5000	.2500	0.0000
4	4	0	.5000	.5000	.5000
6	6	0	.2500	.2500	.2500
6	6	7	.5000	.7500	.7500
7	7	0	.5000	.5000	.5000
9	9	0	.2500	.2500	.2500
9	9	10	.5000	.7500	.7500
10	10	0	.5000	.5000	.5000
12	12	0	.5000	.5000	.5000
14	14	0	.5000	.5000	.5000

Figure 5-2 (Cont'd.)

SEGMENT 1 WEIGHT 24.250

INERTIA MATRIX			OFFSET	EIGENVALUES	DIRECTION COSINE			Y-P-R
1.70431	0.00000	.01890	.03796	1.70973	.961230	0.000000	-.275747	0.00000
0.00000	1.10073	0.00000	0.00000	1.10073	0.000000	1.000000	0.000000	16.09652
.01890	0.00000	1.64384	.03650	1.63842	.275747	0.000000	.961230	0.00000

SEGMENT 2 WEIGHT 9.380

INERTIA MATRIX			OFFSET	EIGENVALUES	DIRECTION COSINE			Y-P-R
.32465	0.00000	.00932	0.00000	.32515	.998602	0.000000	-.052861	0.00000
0.00000	.31365	0.00000	0.00000	.31365	0.000000	1.000000	0.000000	3.03012
.00932	0.00000	.14900	-.25586	.14851	.052861	0.000000	.998602	0.00000

SEGMENT 3 WEIGHT 32.250

INERTIA MATRIX			OFFSET	EIGENVALUES	DIRECTION COSINE			Y-P-R
2.30726	0.00000	.01210	.02481	2.30740	.999933	0.000000	-.011536	0.00000
0.00000	1.71515	0.00000	0.00000	1.71515	0.000000	1.000000	0.000000	.66099
.01210	0.00000	1.25828	-.09612	1.25814	.011536	0.000000	.999933	0.00000

SEGMENT 4 WEIGHT 2.130

INERTIA MATRIX			OFFSET	EIGENVALUES	DIRECTION COSINE			Y-P-R
.01738	0.00000	0.00000	0.00000	.01738	1.000000	0.000000	0.000000	0.00000
0.00000	.01738	0.00000	0.00000	.01738	0.000000	1.000000	0.000000	0.00000
0.00000	0.00000	.00660	.61033	.00660	0.000000	0.000000	1.000000	0.00000

SEGMENT 5 WEIGHT 10.630

INERTIA MATRIX			OFFSET	EIGENVALUES	DIRECTION COSINE			Y-P-R
.27244	0.00000	.00448	.05174	.27272	.998028	0.000000	-.062771	0.00000
0.00000	.32593	0.00000	0.00000	.32593	0.000000	1.000000	0.000000	3.59887
.00448	0.00000	.20149	-.15522	.20121	.062771	0.000000	.998028	0.00000

SEGMENT 6 WEIGHT 17.190

INERTIA MATRIX			OFFSET	EIGENVALUES	DIRECTION COSINE			Y-P-R
.69511	0.00000	0.00000	0.00000	.69511	1.000000	0.000000	0.000000	0.00000
0.00000	.67111	0.00000	0.00000	.67111	0.000000	1.000000	0.000000	0.00000
0.00000	0.00000	.15400	.50887	.15400	0.000000	0.000000	1.000000	0.00000

SEGMENT 7 WEIGHT 7.220

INERTIA MATRIX			OFFSET	EIGENVALUES	DIRECTION COSINE			Y-P-R
.41534	0.00000	0.00000	0.00000	.41534	1.000000	0.000000	0.000000	0.00000
0.00000	.41734	0.00000	0.00000	.41734	0.000000	1.000000	0.000000	0.00000
0.00000	0.00000	.01900	1.37881	.01900	0.000000	0.000000	1.000000	0.00000

SEGMENT 8 WEIGHT 3.250

INERTIA MATRIX			OFFSET	EIGENVALUES	DIRECTION COSINE			Y-P-R
.04010	0.00000	.00216	-.23692	.04029	.996132	0.000000	-.087871	0.00000
0.00000	.04779	0.00000	0.00000	.04779	0.000000	1.000000	0.000000	5.04111
.00216	0.00000	.01580	.19692	.01561	.087871	0.000000	.996132	0.00000

Figure 5-2 (Cont'd.)

SEGMENT 9 WEIGHT 17.190

INERTIA MATRIX			OFFSET	EIGENVALUES	DIRECTION COSINE			Y-P-R
.69511	0.00000	0.00000	0.00000	.69511	1.000000	0.000000	0.000000	0.00000
0.00000	.67111	0.00000	0.00000	.67111	0.000000	1.000000	0.000000	0.00000
0.00000	0.00000	.15400	.50887	.15400	0.000000	0.000000	1.000000	0.00000

SEGMENT 10 WEIGHT 7.220

INERTIA MATRIX			OFFSET	EIGENVALUES	DIRECTION COSINE			Y-P-R
.41534	0.00000	0.00000	0.00000	.41534	1.000000	0.000000	0.000000	0.00000
0.00000	.41734	0.00000	0.00000	.41734	0.000000	1.000000	0.000000	0.00000
0.00000	0.00000	.01900	1.37881	.01900	0.000000	0.000000	1.000000	0.00000

SEGMENT 11 WEIGHT 3.250

INERTIA MATRIX			OFFSET	EIGENVALUES	DIRECTION COSINE			Y-P-R
.04010	0.00000	.00216	-.23692	.04029	.996132	0.000000	-.087871	0.00000
0.00000	.04779	0.00000	0.00000	.04779	0.000000	1.000000	0.000000	5.04111
.00216	0.00000	.01580	.19692	.01561	.087871	0.000000	.996132	0.00000

SEGMENT 12 WEIGHT 5.010

INERTIA MATRIX			OFFSET	EIGENVALUES	DIRECTION COSINE			Y-P-R
.13495	0.00000	0.00000	0.00000	.13495	1.000000	0.000000	0.000000	0.00000
0.00000	.13695	0.00000	0.00000	.13695	0.000000	1.000000	0.000000	0.00000
0.00000	0.00000	.01410	.80589	.01410	0.000000	0.000000	1.000000	0.00000

SEGMENT 13 WEIGHT 5.290

INERTIA MATRIX			OFFSET	EIGENVALUES	DIRECTION COSINE			Y-P-R
.30577	0.00000	0.00000	0.00000	.30577	1.000000	0.000000	0.000000	0.00000
0.00000	.30977	0.00000	0.00000	.30977	0.000000	1.000000	0.000000	0.00000
0.00000	0.00000	.01150	.62193	.01150	0.000000	0.000000	1.000000	0.00000

SEGMENT 14 WEIGHT 5.010

INERTIA MATRIX			OFFSET	EIGENVALUES	DIRECTION COSINE			Y-P-R
.13495	0.00000	0.00000	0.00000	.13495	1.000000	0.000000	0.000000	0.00000
0.00000	.13695	0.00000	0.00000	.13695	0.000000	1.000000	0.000000	0.00000
0.00000	0.00000	.01410	.80589	.01410	0.000000	0.000000	1.000000	0.00000

SEGMENT 15 WEIGHT 5.290

INERTIA MATRIX			OFFSET	EIGENVALUES	DIRECTION COSINE			Y-P-R
.30577	0.00000	0.00000	0.00000	.30577	1.000000	0.000000	0.000000	0.00000
0.00000	.30977	0.00000	0.00000	.30977	0.000000	1.000000	0.000000	0.00000
0.00000	0.00000	.01150	.62193	.01150	0.000000	0.000000	1.000000	0.00000

Figure 5-2 (Cont'd.)

JOINT	LOCATION X	Y	SEG(JNT) Z	LOCATION X	Y	SEG(J+1) Z
1	-1.56	0.00	-2.46	-1.50	0.00	2.24
2	-1.50	0.00	-2.56	-1.48	0.00	6.70
3	-.88	0.00	-2.30	0.00	0.00	4.41
4	0.00	0.00	-.59	-1.05	0.00	3.14
5	2.14	4.45	2.54	0.00	0.00	-6.80
6	0.00	0.00	7.30	0.00	0.00	-6.10
7	0.00	0.00	10.07	1.30	0.00	-1.08
8	2.14	-4.45	2.54	0.00	0.00	-6.80
9	0.00	0.00	7.30	0.00	0.00	-6.10
10	0.00	0.00	10.07	1.30	0.00	-1.08
11	-.78	7.60	-1.70	0.00	0.00	-4.44
12	0.00	0.00	6.26	0.00	0.00	-5.96
13	-.78	-7.60	-1.70	0.00	0.00	-4.44
14	0.00	0.00	6.26	0.00	0.00	-5.96

END OF DELTA PROGRAM.

Figure 5-2 (Cont'd.)

6.0 ANSWERS TO SPECIFIC QUESTIONS

Task 8 of the research effort was to answer a series of questions designed to address the problem of determining the required level of model detail (level of sophistication) that would be adequate to simulate typical crash situations and the problems related to the development of techniques for performing simulation studies. The principal questions were listed earlier in Table 1-1 and the levels of sophistication in Table 1-2.

The following subsections describe the analytical studies that were performed to answer several of the questions of Table 1-1. It was originally intended to supplement these studies with sample runs of the CVS model but these runs were not completed.

6.1 Table 1-1, Question 1

Question 1 in Table 1-1 is: Is similitude between rigid body characteristics of selected segments adequate or must similitude of one or more vibration modes also be preserved?

Our answer to this question is a qualified yes; rigid body characteristics are adequate for all segments except the lumbar spine and neck. The spine and neck are discussed elsewhere in this report. The context in which we are answering this question is one where the concern is with the gross motion of the dummy or the human and not with more sophisticated details such as the effects on internal organs like the brain or those contained in the torso. Thus, we interpret this question as one concerned with the long bone segments which are the arms and legs and answer the question accordingly.

To substantiate our answer we rely on the following development which is based on the simple beam theory given in Reference 3.

Consider a simply supported beam (one in which the ends are held by pin or ball joints) as depicted in Figure 6-1. The frequencies of free oscillation of such a beam are given by (Reference 3, page 83):

$$f_n = \frac{n^2 \pi}{2\ell^2} \sqrt{\frac{EIg}{\rho A}}$$

where f_n = frequency, Hz

n = mode number (1, 2, - - - -)

ℓ = length of beam, in.

E = Young's modulus (30×10^6 lb/in^2 for steel)

I = second moment of area, in^4

ρ = density (0.28 lb/in^3 for steel)

A = cross sectional area, in^2

g = 386 in/sec^2

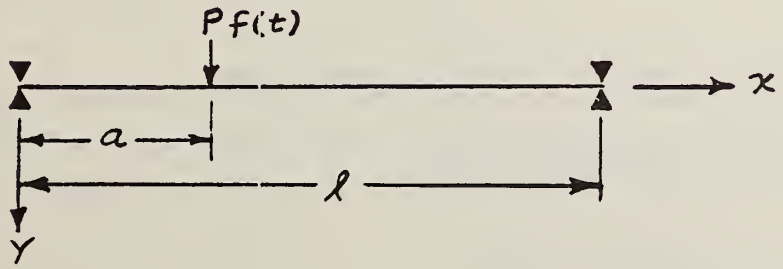

Figure 6-1 SIMPLY SUPPORTED BEAM

For a circular rod $I = 0.5\ \pi\ r^4$ and $A = \pi\ r^2$ where r is the radius. Hence,

$$f_n = 2.25 \times 10^5\ n^2\ r/\ell^2.$$

If ℓ = 12 in. and r = 1/4 in., $f_n = 390\ n^2$. Thus, the fundamental frequency of oscillation ($n = 1$) is 390 Hertz, or a 2.6 millisecond period. The first harmonic ($n = 2$) would be 1560 Hertz or a 0.64 millisecond period. The mode shape (displacement of rod) is sinusoidal;
$\phi\ (x) = \sqrt{2}\ \sin\ (n\pi x/\ell),\ 0 \leq x \leq \ell.$

If the beam is subjected to an axial compressive load of Q lbs. (tensile load $-Q$), the frequency is reduced (increased) by the factor $\sqrt{1-Q/Q_c}$ where Q_c is the Euler critical load (Reference 3, page 136). The Euler critical load is given by $Q_c = \pi^2 EI/\ell^2$. For a steel circular rod 12 inches long and 0.25 inch radius; Q_c = 12600 lb.

Response to Disturbing Force

If the beam is subjected to a normal disturbing force located at one point (see Figure 6-1) the displacement y is given by:

$$y = \sum_n \phi_n\ (x)\ q_n(t)$$

where:

$$\ddot{q}_n + \omega_n^2\ q_n = P\ \phi_n(a)\ f(t)/m$$

$\phi_n(x) = \sqrt{2}\ \sin\ (n\pi x/\ell)$, mode shape

$P\ f(t)$, disturbing force

$m = \rho A \ell$, mass of beam.

If the disturbing force is sinusoidal, $f(t) = \sin \omega t$, the solution is $q_n = a_n \sin \omega_n t + b_n \cos \omega_n t + P \phi_n(a) \sin \omega t/(m(\omega_n^2 - \omega^2))$ where a_n and b_n are constants depending on the initial conditions.

The steady state response will be

$$y = y(x) \sin \omega t \quad \text{where}$$

$$y(x) = (P/M)\sum_n \phi_n(a)\, \phi_n(x)/(\omega_n^2 - \omega^2).$$

When the frequency is small ($\omega^2 << \omega_n^2$), $y(x)$ will approach the deflection due to a static force P at a as given by:

$$y(x) = (P\ell^3/EI)\, h(x) \tag{6.1}$$

where:

$$h(x) = (\ell-a)\, x\, (2\ell a - a^2 - x^2)/(6\ell^4)\ ,\ 0 \leq x \leq a$$

$$= (\ell-x)\, a\, (\ell^2 - a^2 - (\ell - x)^2)/(6\ell^4)\ ,\ a \leq x \leq \ell$$

The maximum static deflection occurs at $x = a$ and is

$$y(a) = (P\ell^3/EI)(a^2(\ell-a)^2/3\ell^4)$$

$$= (P\ell^3)/48\ EI \quad \text{if} \quad a = \ell/2$$

For example, for a circular steel rod 12 inches long and 0.25 inch radius, if the force is applied at the mid point the static deflection is 0.2 inches per 1000 lbs of force.

Force and Moment

The moment M acting at the point x is:

$$M = -EI \frac{\partial^2 y}{\partial x^2}$$

and the shear force S is:

$$S = \frac{\partial M}{\partial x} = -EI \frac{\partial^3 y}{\partial x^3} .$$

From the equation 6.1, the moment M is zero at the end points and equal to $P(\ell-a)$ at $x = a$. The shear force S is $P(\ell-a)/\ell$ from $x = 0$ to $x = a$; and $-Pa/\ell$ from $x = a$ to $x = \ell$. The discontinuity at $x = a$ is due to the applied load P at that point. For the case of free oscillations where the mode shape is sinusoidal we have for a unit peak displacement:

$$M = -EI \frac{\partial^2}{\partial x^2} \sin\left(\frac{n\pi x}{\ell}\right) = EI \left(\frac{n\pi}{\ell}\right)^2 \sin\left(n\pi x/\ell\right) \quad \text{and}$$

$$S = \frac{\partial M}{\partial x} = EI \left(\frac{n\pi}{\ell}\right)^3 \cos\left(n\pi x/\ell\right) = n^3 Q_c \frac{\pi}{\ell} \cos\left(n\pi x/\ell\right)$$

where Q_c is the Euler critical load. At $x = 0$ for a circular steel rod 12 inches long and 0.25 inch radius, S = 3300 lb per inch peak displacement of the first mode ($n = 1$).

Discussion

The preceding development was concerned with effects of transverse loading. Axial loads will be propagated with the speed of sound. In steel the speed of sound is 2×10^5 inches per second. This is 60 microseconds per foot. Since the typical minimum time interval of interest in the gross motion simulation is the order of 1 millisecond and typical dimensions are of the

order of 1 foot, propagation time delays can reasonably be ignored. The compression or expansion due to axial loads will be negligible for loads experienced in typical situations. The reduction in length due to bending from a transverse load will be of the order of d^2/ℓ where d is the peak displacement and ℓ is the length.

The transverse loading considered assumed a simply supported beam which implies that the ends of the beam are held by a pin or a ball to adjoining segments which are held fixed. In the typical situation this is not true but they may be partially 'fixed' by contact loading and/or inertial loading. Any of these situations will reduce the peak displacement. These may be estimated from the shear forces which exist at the ends of the beam.

Conclusion

For the long bone segments in the Part 572 dummy the deformation due to axial loading is negligible and the deformation due to transverse loading will probably not exceed a small fraction of an inch per 1000 pounds of load. It is believed that errors caused by ignoring these effects will be much smaller than the errors caused by other simplifying assumptions in the model.

6.2 Table 1-1, Questions 5 and 7

Questions 5 and 7 of Table 1-1 concerning required level of model detail are:

5: Is it sufficient to preserve similitude of impulses and coefficients of restitution during 'hard' impact processes or must simulitude of forces also be preserved?

7: Is a sliding/rolling characterization of a particular contact adequate or must similitude of the deflection characteristics be preserved?

To answer these questions consider the idealized problem of a hard sphere contacting a deformable planar surface where the force-deflection characteristic of the contact is linear and the coefficient of friction is a constant. The geometry of the contact is illustrated in Figure 6-2 below.

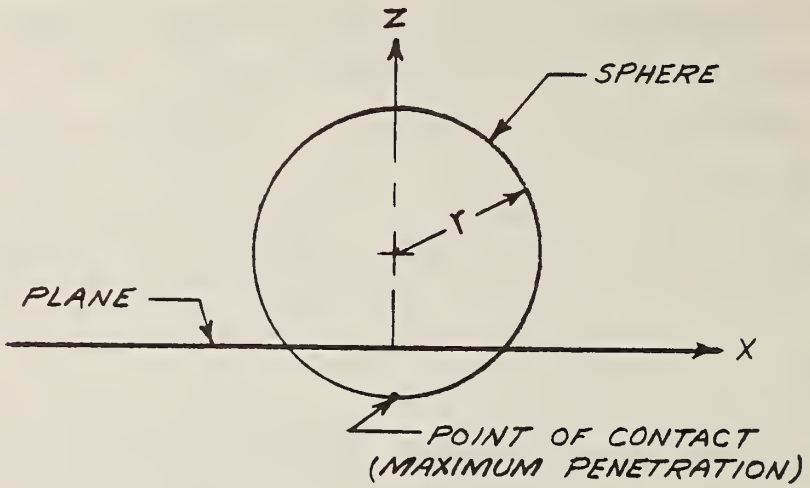

Figure 6-2 SPHERE-PLANE CONTACT

Let the motion be in the X-Z plane. The equations of motion are:

$$M\ddot{X} = -\mu k\,(r-z) \tag{6.2}$$

$$M\ddot{Z} = k\,(r-z)$$

$$M\rho^2\ddot{\theta} = \mu k r\,(r-z)$$

where

M	=	mass	lb-sec^2/in
ρ	=	radius of gyration	in
X	=	X position of center of sphere	in
Z	=	Z position of center of sphere	in
$\dot{X}, \dot{Z}$	=	linear velocities	in/sec
$\ddot{X}, \ddot{Z}$	=	linear accelerations	in/sec^2
θ	=	angular position of sphere	radians
$\dot{\theta}$	=	angular velocity	rad/sec
$\ddot{\theta}$	=	angular acceleration	rad/sec^2
r	=	radius of sphere	in
k	=	spring constant	lb/in
μ	=	friction coefficient	

The solutions of equations 6.2 are:

$$
\begin{array}{lll}
 & & \text{initially at } t = 0 \\
\dot{X} = \dot{X}_0 + \mu\dot{Z}_0\,(1 - \cos(\Omega t)) & , & \dot{X}_0 \\
\dot{Z} = \dot{Z}_0 \cos \Omega t & , & \dot{Z}_0 \\
\dot{\theta} = \dot{\theta}_0 - \mu r\dot{Z}_0\,(1 - \cos(\Omega t))/\rho^2 & , & \dot{\theta}_0 \\
X = \dot{X}_0 t + \mu\dot{Z}_0\,(t - \sin(\Omega t)/\Omega) & , & 0 \\
Z = r + \dot{Z}_0 \sin \Omega t/\Omega & , & r \\
\theta = \dot{\theta}_0 t - \mu r\dot{Z}_0\,(t - \sin(\Omega t)/\Omega)/\rho^2 & , & 0
\end{array}
\qquad (6.3)
$$

where $\Omega = \sqrt{k/M}$

At time equal to zero, the time of initial contact, assume that $\dot{Z}_0$ is negative and $\dot{X}_0$ is positive. The motion in the Z direction is not affected by the friction. At time $t = \pi/2\Omega$, $\dot{Z} = 0$ and the value of Z is $r + \dot{Z}_0/\Omega$; this is the time of maximum penetration which is $\dot{Z}_0/\Omega$ giving a maximum spring force of $k(r-z) = -k\dot{Z}_0/\Omega$. At time $t = \pi/\Omega$, the sphere has rebounded and leaves the surface with a Z velocity of $\dot{Z} = -\dot{Z}_0$. This is analogous to an impulsive impact with a coefficient of restitution of unity.

The behavior in the X direction is dependent on the coefficient of friction. The tangential (X direction) velocity, V, at the point of contact is given by

$$V = \dot{X}_0 - r\dot{\theta}_0 + \mu\,(1 + r^2/\rho^2)\,\dot{Z}_0\,(1 - \cos(\Omega t)) \qquad (6.4)$$

The sign of the friction coefficient μ is selected to agree with the sign of V, i.e., the frictional force opposes the tangential motion. Initially $V_0 = \dot{X}_0 - r\dot{\theta}_0$. We must distinguish between several cases which are:

Case 1: The tangential velocity, V, is initially positive and remains positive throughout the interval $0 \leq t \leq \pi/\Omega \equiv T$.

Case 2: The tangential velocity, V, is initially positive and becomes zero at time $t = \upsilon T$ where $0 < \upsilon < 1$ and υT satisfies the equation

$$V = \dot{X}_0 - r\dot{\theta}_0 + \mu\,(1 + r^2/\rho^2)\,\dot{Z}_0\,(1 - \cos(\upsilon T)) = 0.$$

Case 3: The tangential velocity, V, is initially zero. In this case (and also in Cases 2 and 5 when the tangential velocity becomes zero) the tangential velocity remains zero since $\ddot{X} = \ddot{\theta} = 0$ and the sphere rolls on the plane.

Case 4: The tangential velocity, V, is initially negative and remains negative throughout the interval $0 \leq t \leq T$. In this case and in Case 5, $-\mu$ is substituted for μ in equations 6.2, 6.3 and 6.4.

Case 5: The tangential velocity, V, is initially negative and becomes zero at time $t = \upsilon T$, where $0 \leq \upsilon \leq 1$ and υT satisfies the equation

$$V = \dot{X}_0 - r\dot{\theta}_0 - \mu\,(1 + r^2/\rho^2)\,\dot{Z}_0\,(1 - \cos(\upsilon T)) = 0.$$

The solution to all five cases at $t = T$, the time when the sphere leaves the surface, can be written as:

$$\dot{X} = \dot{X}_0 + \mu\dot{Z}_0\,(1 - \cos(\upsilon\pi))$$

$$\dot{Z} = -\dot{Z}_0$$

$$\dot{\theta} = \dot{\theta}_0 - \mu r\dot{Z}_0\,(1 - \cos(\upsilon\pi))/\rho^2 \qquad (6.5)$$

$$X = (\dot{X}_0 + \mu\dot{Z}_0)\,T - \mu\dot{Z}_0 T\,(\sin(\upsilon\pi)/\pi + (1-\upsilon)\cos(\upsilon\pi))$$

$$Z = r$$

$$\theta = (\dot{\theta}_0 - \pi r\dot{Z}_0/\rho^2)T + \mu r\dot{Z}_0 T\,(\sin(\upsilon\pi)/\pi + (1-\upsilon)\cos(\upsilon\pi))/\rho^2$$

where μ is replaced by $-\mu$ if $V_0 = (\dot{X}_0 - r\dot{\theta}_0) < 0$,

$\mu = 0$ if $V_0 = \dot{X}_0 - r\dot{\theta}_0 = 0$,

and υ is the solution of the equation:

$$V = \dot{X}_0 - r\dot{\theta}_0 + \mu\,(1 + r^2/\rho^2)\,\dot{Z}_0\,(1 - \cos(\upsilon\pi)) = 0 \qquad (6.6)$$

providing the solution is in the range $0 \leq \upsilon \leq 1$,

$\upsilon = 0$ if $\dot{X}_0 - r\dot{\theta}_0 = 0$,

$\upsilon = 1$ if $\dot{X}_0 + r\dot{\theta}_0 \neq 0$ and equation 6.6 does not have a solution in the range $0 \leq \upsilon \leq 1$.

Impulsive Solutions

Consider the case of the sphere contacting the plane where we apply an impulse at the time of first contact. The equations are:

$$M\Delta\dot{X} = -\mu I$$

$$M\Delta\dot{Z} = I$$

$$M\rho^2\Delta\dot{\theta} = \mu r I$$

where $\Delta\dot{X}$, $\Delta\dot{Z}$, and $\Delta\dot{\theta}$ are the instantaneous changes in velocity due to the impulse of strength I (lb-sec).

Letting I be equal to $-2M\dot{Z}_0$ we have at $t = 0+$ (just after the impulse)

$$\dot{X}_+ = \dot{X}_0 + 2\mu\dot{Z}_0$$

$$\dot{Z}_+ = -\dot{Z}_0$$

$$\dot{\theta}_+ = \dot{\theta}_0 - 2\mu r\dot{Z}_0/\rho^2$$

where the sign of the friction coefficient is the same as the sign of the relative velocity $V_0 = \dot{X}_0 - r\dot{\theta}_0$ at the time of contact. If $V_0 = 0$, μ is taken as equal to zero. At a time T we have

$$\dot{X} = \dot{X}_0 + 2\mu\dot{Z}_0$$

$$\dot{Z} = -\dot{Z}_0$$

$$\dot{\theta} = \dot{\theta}_0 - 2\mu r\dot{Z}_0/\rho^2 \qquad (6.7)$$

$$X = (\dot{X}_0 + 2\mu\dot{Z}_0)T$$

$$Z = r - \dot{Z}_0 T$$

$$\theta = (\dot{\theta}_0 - 2\mu r\dot{Z}_0/\rho^2)T$$

Comparison of Solutions

The results of the 'soft' contact are given by Equations 6.5 and of the 'hard' contact by Equations 6.7 at time T when the 'soft' contact has left the surface. For the case of pure roll (Case 3), $V_0 = 0$, we have:

	'soft'	'hard' (impulse)
$\dot{X}$	$\dot{X}_0$	$\dot{X}_0$
$\dot{Z}$	$-\dot{Z}_0$	$-\dot{Z}_0$
$\dot{\theta}$	$\dot{\theta}_0$	$\dot{\theta}_0$
X	$\dot{X}_0 T$	$\dot{X}_0 T$
Z	r	$r-\dot{Z}_0 T$
θ	$\dot{\theta}_0 T$	$\dot{\theta}_0 T$

We note that the only difference is in the Z position. As the 'soft' contact becomes harder (k increases), T gets smaller. In the limit, $T \to 0$ and the results are identical. For Cases 1 and 4 where $\upsilon = 1$ we have

	'soft'	'hard'
$\dot{X}$	$\dot{X}_0 + 2\mu\dot{Z}_0$	$\dot{X}_0 + 2\mu\dot{Z}_0$
$\dot{Z}$	$-\dot{Z}_0$	$-\dot{Z}_0$
$\dot{\theta}$	$\dot{\theta}_0 - 2\mu r\dot{Z}_0/\rho^2$	$\dot{\theta}_0 - 2\mu r\dot{Z}_0/\rho^2$
X	$(\dot{X}_0 + \mu\dot{Z}_0)T$	$(\dot{X}_0 + 2\mu\dot{Z}_0)T$
Z	r	$r - \dot{Z}_0 T$
θ	$(\dot{\theta}_0 - \mu r\dot{Z}_0/\rho^2)T$	$(\dot{\theta}_0 - 2\mu r\dot{Z}_0/\rho^2)T$

We note that the velocities are the same but the positions are different. The differences in X and θ vanish as $\mu \to 0$ or as $T \to 0$. The difference in Z vanishes only when $T \to 0$.

In Cases 2 and 5 where the slide becomes a roll at some point in the time interval T $(0 < \upsilon < 1)$ there will be a difference in both the velocities and positions. For example for $\upsilon = 1/2$

	'soft'	'hard'
$\dot{X}$	$\dot{X}_0 + \mu\dot{Z}_0$	$\dot{X}_0 + 2\mu\dot{Z}_0$
$\dot{Z}$	$-\dot{Z}_0$	$-\dot{Z}_0$
$\dot{\theta}$	$\dot{\theta}_0 - \mu r\dot{Z}_C/\rho^2$	$\dot{\theta}_0 - 2\mu r\dot{Z}_0/\rho^2$
X	$(\dot{X}_0 + \mu\dot{Z}_C)T - \mu\dot{Z}_0 T/\pi$	$(\dot{X}_0 + 2\mu\dot{Z}_0)T$
Z	r	$r - \dot{Z}_0 T$
θ	$(\dot{\theta}_0 - \mu r\dot{Z}_0/\rho^2)T$ $+ \mu r\dot{Z}_0 T/(\pi\rho^2)$	$(\dot{\theta}_0 - 2\mu r\dot{Z}_0/\rho^2)T$

Numerical Considerations

The time interval T is given by $T = \pi/\Omega$ and $\Omega = \sqrt{k/m}$. The mass m is the weight, w, in pounds divided by the acceleration of gravity g (in/sec^2). Values of T and Ω for a range of stiffness to weight ratio are given below:

k/w (1/in)	T (milliseconds)	Ω (rad/sec)
1	160	19.6
10	50.6	62
100	16	196
1000	5.1	621
10000	1.6	1960

Consider, for example, an impact with $k/w = 1000$. In this case the sphere would lose contact with the planar surface at $T = 5.1$ milliseconds. If, on the other hand, an impulsive contact was assumed and the impact occurred at a velocity of 30 mph ($\dot{Z}_0 = 528$ in/sec), the Z position of the sphere at that time would be 528 (.0051) = 2.7 inches above the planar surface.

Integrator Considerations

For the case of a 'soft' impact, the time T represents a half cycle of a sinusoid. If we assume that at least 10 integration steps are needed to achieve a reasonable precision in the numerical integration, then the maximum step size of the integrator must be $T/10$. The use of a 'hard' impact imposes no restrictions on the integration step size.

Injury Criteria

A commonly used injury criterion is the HIC number which is defined by the formula

$$HIC = \max_{t_2, t_1} \; (t_2 - t_1) \left[\frac{1}{(t_2 - t_1)} \int_{t_1}^{t_2} |a| \; dt \right]^{2.5} \qquad (6.8)$$

where $|a|$ is the magnitude of the acceleration expressed in g's. For the 'soft' contact we have

$$|a| = \Omega |\dot{Z}_0| \sqrt{1 + \mu^2} \; \sin(\Omega t)/g$$

The HIC number is computed for $\Omega t_1 = 0.518$ and $t_2 = T - t_1$. From Equation 6.8 we get

$$HIC = 1.3 \; (|\dot{Z}_0| \sqrt{1 + \mu^2}/g)^{2.5} \; \Omega^{1.5}$$

For the 'hard' impact the HIC number is not defined since by definition of an impulse the integral in Equation 6.8 is finite and the HIC varies inversely as $(t_2 - t_1)^{1.5}$. Thus the HIC number would be infinite.

Another commonly used criterion is the Severity Index which is defined as

$$SI = \int_{t_1}^{t_2} |a|^{2.5} \; dt.$$

For the 'soft' impact this is given by

$$SI = (|\dot{Z}_0| \sqrt{1 + \mu^2}/g)^{2.5} \; \Omega^{1.5} \int_0^{\pi} d\mu \; (\sin \mu)^{2.5}$$

where $\int_0^{\pi} d\mu \; (\sin \mu)^{2.5} \approx 1.44$

Thus, for a half sine wave acceleration the HIC and the SI are essentially equal. For a 'hard' impact the SI is infinite.

For a specified HIC number we can compute Ω as a function of $\dot{Z}_0$ and μ. The results for a HIC = 1000 and $\mu = 0$ are shown below.

$\dot{Z}_0$ (in/sec)	$\dot{Z}_0 T$ (in)	Ω (rad/sec)	k/w (1/m)
50	0.062	2532	16612
100	0.393	799	1653
150	1.161	406	427
200	2.500	251	163
250	4.534	173	78
300	7.370	128	42

Conclusions and Answers to Questions 5 and 7 of Table 1-1

The only definite answers we can make to the questions is that if the contact involves a segment where the HIC number or the severity index is required the impulse option or the slide/roll option must not be used. (Proper use of the slide/roll option requires the use of an impulse to reduce the normal velocity to zero at the time of first contact, hence the slide/roll option is subject to the same restrictions as the impulse option.) In contacts where the HIC number or the severity index are not important for the segment involved in the contact, the user must make the decision based on evaluation of the differences, primarily in positions, of the variables involved and the computing time. It should be remembered that the principal advantage of the impulse options in the CVS program is that they place no restriction on the step size of the integrator whereas the use of a 'soft' impact restricts the step size.

6.3 Table 1-1, Question 9

Question 9 of those listed in Table 1-1 is:

Must the similitude of surface compliances be preserved in the region of belt or air bag contacts?

The answer to this question is yes. To support this answer we refer to the analytic studies presented in subsections 6.3.1 and 6.3.2 which follow.

A simple model of a belt passing over a deformable spherical surface is analyzed in Section 6.3.1. In this analysis it is shown that the effective stress is significantly reduced from what would be computed if the compliance of the surface was ignored. When using the belt algorithm in the CVS program the user must define a stress-strain function which accounts for the effect of the compliance.

The analysis also solves the equations for a belt on a nondeformable spherical surface with friction, and shows that the belt will not necessarily lie in a plane if there is friction perpendicular to the belt line. It also shows that the tension decreases exponentially along the belt line. The belt algorithm in the CVS program should not be used if the effects of friction are important (this algorithm assumes either zero or infinite friction). However, the harness algorithm allows for surface compliance and finite friction.

For air bag restraints, the nominal pressure in the uncontacted bag is usually a few inches of water and contacts by body segments reduce the volume of the bag so that pressures of a few pounds per square inch are produced. The compliance of the bag must be considered to predict these pressures. Also, the effective area is larger than the actual area of contact as illustrated in Figure 6-3.

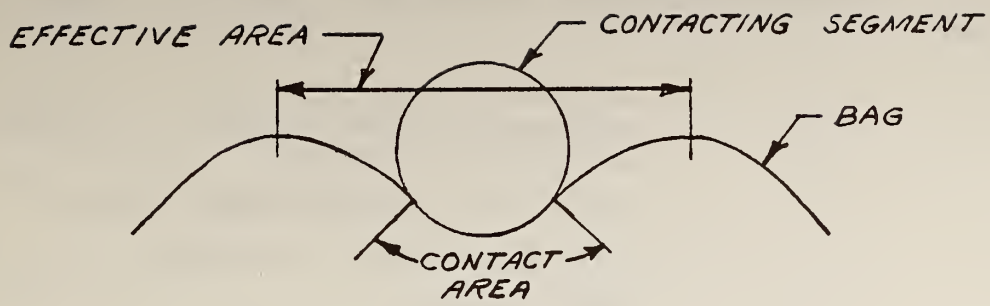

Figure 6-3 EFFECTIVE AREA OF SEGMENT CONTACT WITH AIR BAG

The air bag algorithm in the program estimates the reduction in volume and the effective area assuming that the contacting segment is rigid and that the bag material does not stretch. Actual experiments with an air bag (Reference 1 - Volume 2) indicated that although the fibers in the cloth of the bag do not stretch the material effectively stretches at an angle to the weave so as to produce undulations of the bag surface in the vicinity of the contact by an object. The analyses described in Section 6.3.2 show this effect. One of the studies shows how a fabric with a rectangular weave will lie on a sphere. The other study shows the effect of bag stretch.

6.3.1 Belt Analyses

(a) Belt With Friction

Consider a belt lying on a surface as shown in the following sketch.

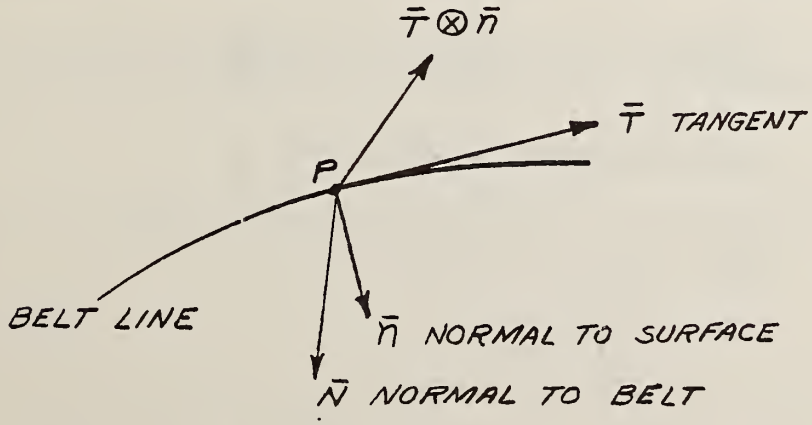

Assume the belt may be treated as a curve in space. At the point P let:

$\overline{T}$	=	unit vector tangent to belt (in direction of decreasing tension)
$\overline{N}$	=	unit vector principal normal to belt
$\overline{n}$	=	unit vector normal to surface
q	=	tension in belt
f	=	magnitude of force along $\overline{n}$
μ	=	coefficient of friction along $\overline{T}$
υ	=	coefficient of friction along $\overline{T} \otimes \overline{n}$, ($\otimes$, vector cross product)
ds	=	differential length of belt
ϕ	=	angle between n and N.

We have the equation:

$$\frac{d(q\overline{T})}{ds} = f\overline{n} - \mu f\overline{T} - \upsilon f\,(\overline{T} \otimes \overline{n}) \tag{6.9}$$

From the properties of surface curves, Reference 4, page 283, we have:

$$\frac{d\overline{T}}{ds} = K\overline{N}, \text{ where } K \text{ is the curvature of the belt} \tag{6.10}$$

$$\overline{N} = \overline{n} \cos\phi\,(\overline{T} \otimes \overline{n}) \sin\phi \tag{6.11}$$

$$\overline{T} \otimes \overline{N} = \overline{B} = \overline{n} \sin\phi + (\overline{T} \otimes \overline{n}) \cos\phi$$

From Equations 6.9, 6.10 and 6.11

$$\frac{dq}{ds} = -\upsilon f \tag{6.12}$$

$K \sin \phi = \upsilon f/q$, the geodesic curvature of the belt γ (6.13)

$K \cos \phi = f/q$, the normal curvature of the belt k (6.14)

Thus, from 6.13 and 6.14

$\tan \phi = \upsilon$.

We make the following observations:

1. If the coefficient of friction, μ, is zero along the belt line the tension in the belt, q, is a constant.

2. If the coefficient of friction, υ, perpendicular to the belt line is constant, the angle, ϕ, between the normals to the surface and the belt is constant. If υ is zero the normals are the same and the belt is a geodesic.

Thus, for a frictionless belt:

$$\frac{dq}{ds} = 0$$

$$\phi = 0 \text{ and} \qquad (6.15)$$

$$K = f/q.$$

The equation of a belt on a nondeformable surface may be derived as follows:

Let $\overline{r}$ = vector from origin to point P on the belt. We have

$$\overline{T} = \frac{d\overline{r}}{ds}$$

$$\frac{d\bar{T}}{ds} = K\bar{N} = k\bar{n} = \gamma\ (\bar{T} \circledast \bar{n}) \qquad (6.16)$$

$$\frac{d\bar{n}}{ds} = \bar{T} \cdot grad\ \bar{n} = -k\bar{T} + t(\bar{T} \circledast \bar{n})$$

(t is the geodesic torsion)

At the point P, $\bar{r}$ and $\bar{T}$ are known, $\bar{n}$ and $grad\ \bar{n}$ are functions of the equations describing the surface. The normal curvature k may be computed from $\bar{n}$ as:

$$k = -\bar{T} \cdot \frac{d\bar{n}}{ds}\ .$$

From Equations 6.13 and 6.14, $\gamma = \upsilon k$. Hence Equation 6.16 becomes:

$$\frac{d\bar{T}}{ds} = \frac{d^2\bar{r}}{ds^2} = k\bar{n} - \upsilon k\ (\bar{T} \circledast \bar{n}) \qquad (6.17)$$

Equation 6.17 is the equation for the belt. For a unit sphere we have:

$$\bar{n} = -\bar{r}$$

$$grad\ \bar{n} = -I \quad \text{(the identity)}$$

$$\frac{d\bar{n}}{ds} = -\bar{T}$$

$k = 1$, normal curvature of all curves on a unit sphere is 1

$t = 0$, geodesic torsion is zero, all curves on a sphere are lines of curvature.

Equation 6.17 for a sphere is:

$$\frac{d^2\bar{r}}{ds^2} + \upsilon\left(\bar{r} \circledast \frac{d\bar{r}}{ds}\right) + \bar{r} = 0 \qquad (6.18)$$

Crossing this equation with $\bar{r}$ yields:

$$\bar{r} \circledast \frac{d^2\bar{r}}{ds^2} + \upsilon\left(\bar{r} \cdot \frac{d\bar{r}}{ds} - \frac{d\bar{r}}{ds}\right) = 0$$

but $\bar{r} \circledast \frac{d^2\bar{r}}{ds^2} = \frac{d}{ds}\left(\bar{r} \circledast \frac{d\bar{r}}{ds}\right)$ and $r \cdot \frac{d\bar{r}}{ds}$ is zero for the sphere. Hence,

$$\frac{d}{ds}\left(\bar{r} \circledast \frac{d\bar{r}}{ds}\right) = \upsilon \frac{d\bar{r}}{ds}. \qquad (6.19)$$

For constant υ, Equation 6.19 may be integrated to give:

$$\bar{r} \circledast \frac{d\bar{r}}{ds} = \upsilon\left(\bar{r}-\bar{r}_0\right) + \bar{r}_0 \circledast \frac{d\bar{r}_0}{ds}$$

$$\bar{r} \circledast \frac{d\bar{r}}{ds} = \upsilon\left(\bar{r}-\bar{r}_0\right) + \bar{r}_0 \circledast \bar{T}_0 \qquad (6.20)$$

Substituting 6.20 into 6.18 yields:

$$\frac{d^2\bar{r}}{ds^2} + \left(1 + \upsilon^2\right)\bar{r} = \upsilon^2\bar{r}_0 - \upsilon\bar{r}_0 \circledast \bar{T}_0 \qquad (6.21)$$

Letting $K^2 = 1 + \upsilon^2 = r_0$ and noting that

$$\overline{T} = \overline{T}_0 \quad \text{at} \quad s = 0,$$

solution of Equation 6.21 yields:

$$\overline{r} = \frac{\overline{r}_0}{K^2} [\upsilon^2 + \cos Ks] + \overline{T}_0 \frac{\sin Ks}{K} + \frac{\upsilon}{K^2} \overline{r}_0 \circledast \overline{T}_0 (\cos Ks - 1) \tag{6.22}$$

$$\overline{T} = \frac{d\overline{r}}{ds} = -\frac{\overline{r}_0}{K} \sin Ks + \overline{T}_0 \cos Ks - \frac{\upsilon}{K} \overline{r}_0 \circledast \overline{T}_0 \sin (Ks) \tag{6.23}$$

$$K\overline{N} = \frac{d\overline{T}}{ds} = -\overline{r}_0 \cos Ks - \overline{T}_0 K \sin Ks - \upsilon \overline{r}_0 \circledast \overline{T}_0 \cos Ks \tag{6.24}$$

From Equation 6.14, $f = kq$, and from Equation 6.12

$$\frac{dq}{ds} = -\mu k q = -\mu q \quad (k = 1 \text{ on unit sphere})$$

If μ is a constant, this equation may be integrated to give

$$q = q_0 e^{-\mu s} \tag{6.25}$$

Thus, for the case of a belt lying on a unit sphere with constant coefficients of friction, Equations 6.22, 6.23 and 6.24 describe the geometry and Equation 6.25 gives the tension as a function of the arc length s.

To complete the analysis, let $L(s)$ be the variable describing the length of the constrained belt. Let the stress-strain relation of the belt be $q = F$ (strain), where the strain is $\frac{ds}{dL}$. If the function is linear, we have

$$q = a \frac{ds}{dL} \quad \text{where} \quad a = \frac{\delta F}{\delta strain} \quad \text{is a constant.}$$

Thus, $\frac{dL}{ds} = \frac{a}{q} = \frac{a}{q_0} e^{\mu s}$

$$L = \frac{a}{q_0} \frac{(e^{\mu s} - 1)}{\mu} \tag{6.26}$$

or $$s = \frac{1}{\mu} \ln[1 + \frac{\mu q_0}{a} L]$$

where $L = 0$ for $s = 0$.

We may rewrite Equation 6.26 in terms of q as:

$$L = \frac{a}{q_0 \mu} [\frac{q_0}{q} - 1],$$

or $$q = q_0/(1 + \mu \frac{q_0}{a} L)$$

If the quantity $\frac{\mu q_0}{a} L$ is small compared to one, we have from Equation 6.26:

$$s \approx \frac{q_0}{a} L \quad \text{or} \quad q_0 = as/L$$

(b) Belt on Deformable Surface

Consider a belt lying on a surface as shown in the following sketch.

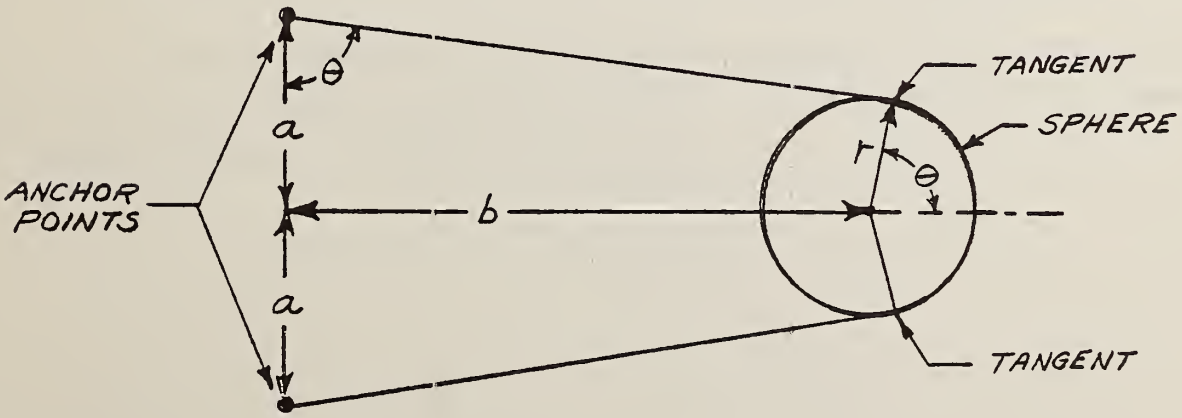

Assume the belt lies in a plane and the surface is circular (spherical). From the geometry:

$$\sin\theta = (\phi\sqrt{a^2 + b^2 - r^2} + ar)/(a^2 + b^2)$$

$$\cos\theta = (a\sqrt{a^2 + b^2 - r^2} - br)/(a^2 + b^2) \qquad (6.27)$$

The total length, L, of the belt is:

$$L = 2\,[a\sec\theta + r\,(\theta - \tan\theta)]$$

$$= 2\,[r\theta + \sqrt{a^2 + b^2 - r^2}\,] \qquad (6.28)$$

Let $q = \ell\,(L/L_0 - 1)$, tension in belt,

$f = k\,(r_0 - r)$, normal force per unit length

ℓ = strain coefficient, lbs. per unit stress

k = force coefficient for surface (lbs. per inch length per inch deformation)

r_0 = undeformed radius

From Equation 6.15 we have:

$q = rf$, or

$$\ell\,(L/L_0 - 1) = kr\,(r_0 - r) \qquad (6.29)$$

In the case where the surface is rigid ($k = \infty$) Equation 6.29 is not applicable; the value of r does not change and L is computed from Equation 6.28 as a function of b. When the surface is not rigid ($k < \infty$) Equations 6.27, 6.28 and 6.29 must be solved simultaneously to evaluate L, θ and r as a function of b.

Consider the strains:

$$s = L/L_0 - 1$$

$$\frac{ds}{db} = \frac{1}{L_0} \frac{\delta L}{\delta r} \frac{dr}{db} + \frac{\delta L}{\delta b}$$

but $\frac{\delta L}{\delta r} = 2\theta$ and from Equation 6.29

$$\ell \frac{ds}{db} = k\,[r_0 - 2r] \frac{dr}{db},$$

Hence,

$$\frac{ds}{db} = \frac{\delta L/\delta b}{1 + 2\ell\theta/(kL_0(2r - r_0))} \tag{6.30}$$

$$\frac{dq}{db} = \ell \frac{ds}{db} = \frac{\ell\, \delta L/\delta b}{1 + 2\ell\theta/(kL_0\,(2r - r_0))}$$

Thus, the effective slope of the stress-strain curve is reduced by the factor in the denominator of Equation 6.30. Note that for $k = \infty$ (non-deformable surface) the denominator is 1.

Numerical Example

Consider a case where $a = r_0 = 7''$, $b = 20''$. We have $\theta = \pi/2$ and when $r = r_0$

$$1 + 2\ell\theta/(k\, L_0\, (2r - r_0)) = 1 + \frac{\ell}{k}\ \frac{\pi}{7\ (40 + 7\pi)}$$

If a belt produces a stress (tension) of 1000 lbs. for a strain of 0.1, then $\ell = 10000$. If the 7" radius is reduced to 6" by the 1000#, then $k = 1000/6$ (Equation 6.29). Thus, $\ell/k = 60$ and the slope of the stress-strain is reduced by the factor 1.43. Failure to allow for the compliance of the surface would produce a 30% error $(\frac{1}{1.43} = .70)$ in the computed stress. As b increases, r is reduced and the reduction factor becomes even greater.

6.3.2 Air Bag Analyses

(a) Technique for Generating a Set of Equally Spaced Points on a Sphere

Assume that along any two great circles of a sphere we are given a set of equally spaced points, $\bar{X}_{1k}$, and $\bar{X}_{k1}$, as illustrated in the sketch below.

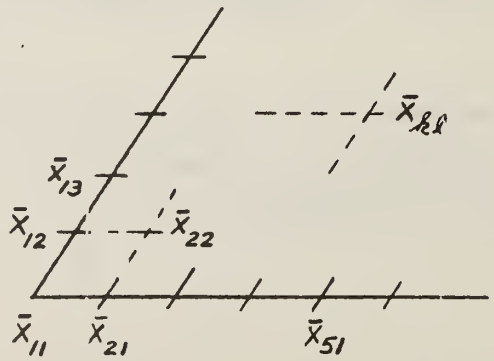

Let the spacing (arc length) be ℓ and the angle between the vectors from the origin to any two adjacent points be $\Delta = \ell/r$, where r is the radius of the sphere.

We wish to complete the array $\overline{X}_{k\ell}$ such that the spacing of any two adjacent points is ℓ. This can be done by starting with $\overline{X}_{12}$ and $\overline{X}_{21}$ and finding $\overline{X}_{22}$. Then from $\overline{X}_{22}$ and $\overline{X}_{31}$ finding $\overline{X}_{32}$, etc.

This may be done by using the relation:

$$\overline{X} = \frac{1}{1 + \cos \delta} \left[\cos \Delta \, (\overline{X}_1 + \overline{X}_2) + \sqrt{\left(\frac{\sin \Delta}{\sin \delta/2}\right)^2 - 1} \; \frac{\overline{X}_2 \circledcirc \overline{X}_1}{r}\right]$$

where $\cos \delta = \overline{X}_1 \cdot \overline{X}_2/r^2$.

Letting $\overline{X}_1 = \overline{X}_{12}$, $\overline{X}_2 = \overline{X}_{21}$, then $\overline{X}$ is $\overline{X}_{22}$.

Consider the segment of the surface of the sphere depicted in the following sketch where $\overline{X}_+$ is the value of $\overline{X}$ using the plus square root and $\overline{X}_-$ is the value for the negative square root.

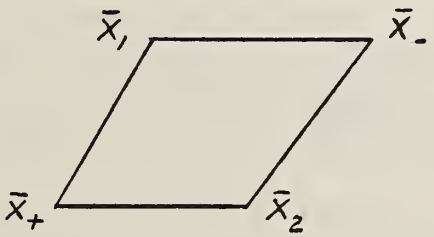

We have

$$\cos \delta = \overline{X}_1 \cdot \overline{X}_2/r^2$$

$$\cos \theta = \overline{X}_+ \cdot \overline{X}_-/r^2 = \tan^2\left(\frac{\delta}{2}\right) \cos 2\Delta \, \sec^2\left(\frac{\delta}{2}\right).$$

The arc $\overline{X_- X_+}$ is thus $r\theta$ and the arc $\overline{X_1 X_2}$ is $r\delta$. The arc of the undistorted figure (when $\delta = \theta$) of length

$$\ell_0 = \overline{X_- X_+} = \overline{X_1 X_2} = 2r \sin^{-1} \sqrt{1-\cos \Delta} \, .$$

In this case $\cos^2(\frac{\delta}{2}) = \cos \Delta = \cos^2(\frac{\theta}{2})$.

Thus, the elongation is

$$\frac{\overline{X_- X_+}}{\ell_0} = \frac{\sin^{-1} \sqrt{\frac{1-\cos \theta}{2}}}{\sin^{-1} \sqrt{1-\cos \Delta}}$$

Proof:

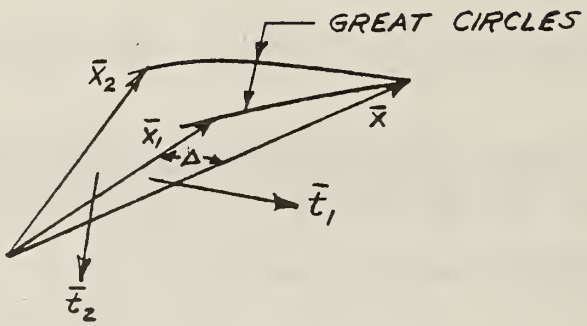

Let the unit normal to the great circle containing $\bar{X}_1$ and $\bar{X}$ be $\bar{t}_1$, and the unit normal to the great circle containing $\bar{X}_2$ and $\bar{X}$ be $\bar{t}_2$ as shown in the sketch above. Then

$$\bar{t}_1 \cdot \bar{X}_1 = 0 \quad \text{and} \quad \bar{t}_2 \cdot \bar{X}_2 = 0 \quad \text{and}$$

$$\bar{X} = \cos \Delta \, \bar{X}_1 + \sin \Delta \, \bar{t}_1 \circledast \bar{X}_1 = \cos \Delta \, \bar{X}_2 + \sin \Delta \, \bar{t}_2 \circledast \bar{X}_2 \qquad (6.31)$$

Let $\bar{t}_1 = \alpha\bar{X}_1 + \beta\bar{X}_2 + \gamma\bar{X}_1 \circledast \bar{X}_2$

We have $\bar{t}_1 \cdot \bar{X}_1 = 0 = \alpha\bar{X}_1 \cdot \bar{X}_1 + \beta\bar{X}_1 \cdot \bar{X}_2 = 0$

We note from Equation 6.31 that

$$\cos\Delta\, \bar{X}_1 \cdot \bar{X}_2 + \sin\Delta\, \bar{t}_1 \cdot \bar{X}_1 \circledast \bar{X}_2 = \cos\Delta\, \bar{X}_2 \cdot \bar{X}_2$$

Hence, $\bar{t}_1 \cdot \bar{X}_1 \circledast \bar{X}_2 = \cos\Delta\,(\bar{X}_2 \cdot \bar{X}_2 - \bar{X}_1 \cdot \bar{X}_2) = \gamma\, \bar{X}_1 \circledast \bar{X}_2 \cdot \bar{X}_1 \circledast \bar{X}_2$

Thus,

$$\bar{t}_1 = \beta\left(\bar{X}_2 - \frac{\bar{X}_1 \cdot \bar{X}_2}{\bar{X}_1 \cdot \bar{X}_1}\bar{X}_1\right) + \frac{\cos\Delta\,(\bar{X}_2 \cdot \bar{X}_2 - \bar{X}_1 \cdot \bar{X}_2)}{\left|\bar{X}_1 \circledast \bar{X}_2\right|^2}\bar{X}_1 \circledast \bar{X}_2$$

Since $\bar{t}_1 \cdot \bar{t}_1 = 1$, we have

$$\beta \sin\Delta = \frac{1}{1+\cos\delta}\sqrt{\frac{1}{\bar{X}_2 \cdot \bar{X}_2}}\sqrt{\left(\frac{\sin\Delta}{\sin\delta/2}\right)^2 - 1}$$

Collecting terms we obtain

$$\bar{X} = \frac{1}{1+\cos\delta}\left[\cos\Delta\,(\bar{X}_1 + \bar{X}_2) + \sqrt{\left(\frac{\sin\Delta}{\sin\delta/2}\right)^2 - 1}\,\frac{\bar{X}_2 \circledast \bar{X}_1}{r}\right]$$

where $\bar{X}_1 \cdot \bar{X}_1 = \bar{X}_2 \cdot \bar{X}_2 = r^2$ and $\cos \delta = \bar{X}_1 \cdot \bar{X}_2 / r^2$

Note that, for a solution to exist, $\sin \Delta \geq \sin \delta/2$, i.e., the arc length between the points must not be greater than $2 \Delta r$.

(b) Effect of Bag Stretch

The sketch below depicts a half-cross section of the contact of a penetrator of radius r_a with a bag of radius r_b. The deformed bag shape is assumed to consist of two circular arcs A-B and B-C. If the bag does not stretch, the length of line A-B-C is $r_b \psi$.

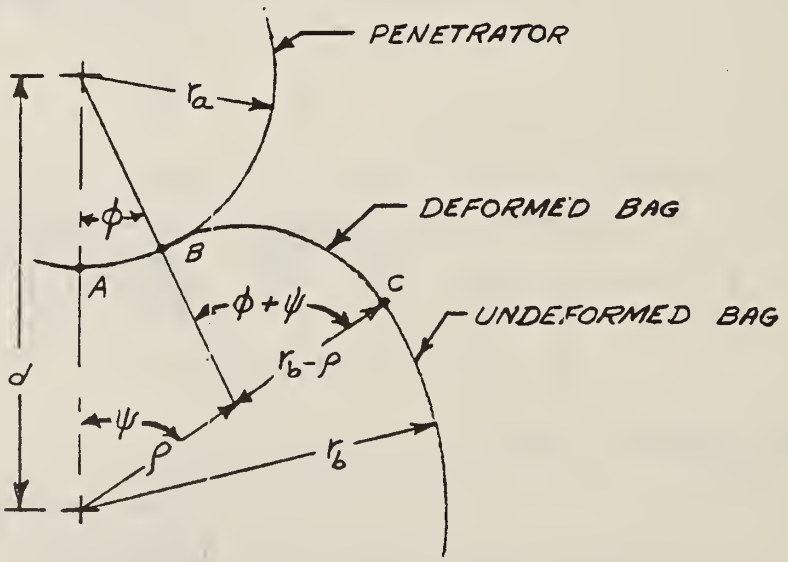

Assume the bag stretches by a factor μ over the arcs A-B-C.

Then,

$$\mu r_b \psi = r_a \phi + (r_b - \rho)(\phi + \psi)$$

$$\rho \cos \psi + (r_a + r_b - \rho) \cos \phi = d \qquad (6.32)$$

$$\rho \sin \psi - (r_a + r_b - \rho) \sin \phi = 0$$

The unknowns are ρ, ϕ and ψ.

If $\mu = 1$ (no stretch) the solution reduces to

$$\phi = \psi, \quad \cos \phi = \frac{d}{r_a + r_b}, \quad \rho = \frac{r_a + r_b}{2}.$$

We have $$\rho = \frac{(r_a + r_b) \sin \phi}{\sin \psi + \sin \phi} = \frac{d - (r_a + r_b) \cos \phi}{\cos \psi - \cos \phi}$$

$$\sin \psi = \sin \phi \; \frac{(r_a + r_b)^2 - d^2}{d^2 + (r_a + r_b)^2 - 2d(r_a + r_b) \cos \phi} =$$

$$\sin \phi \; \frac{(r_a + r_b)^2 - d^2}{2(r_a + r_b)(r_a + r_b - d \cos \phi) - ((r_a + r_b)^2 - d^2)}$$

$$\rho = r_a + r_b - \frac{(r_a + r_b)^2 - d^2}{2[r_a + r_b - d \cos \phi]}$$

$$[(\mu - 1) r_b + \rho] \psi = (r_a + r_b - \rho) \phi$$

These equations may be solved using an iterative type procedure. As μ increases $\rho \to r_b$. This is a limiting case for this model. At this limit:

$$\mu = \frac{r_a}{r_b} \quad \frac{\phi}{\psi} \quad ; \quad \frac{\sin \phi}{\sin \psi} = \frac{r_b}{r_a} \; ; \; \cos \phi = \frac{d}{2r_a} - \frac{r_b^2 - r_a^2}{2r_a d}$$

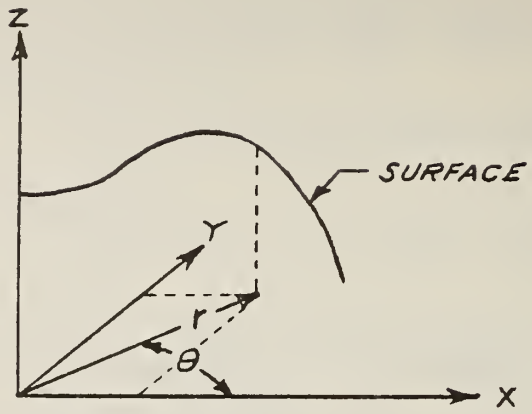

In a cylindrical coordinate system (see sketch above) the surface of the bag may be described as:

$$r^2 + z^2 = r_b^2 \quad \text{for} \quad r \geq r_b \sin \psi$$

$$r^2 + (z-d)^2 = r_a^2 \quad \text{for} \quad r \leq r_a \sin \phi$$

$$(r - p \sin \psi)^2 + (z - p \cos \psi)^2 = (r_b - p)^2, \quad \text{for} \quad r_a \sin \phi \leq r \leq r_b \sin \psi$$

where $x = r \cos \theta$, $y = r \sin \theta$

and the penetration, $p = r_a + r_b - d$

Assume the bag does not stretch in the planes $\theta = 0$ and $\theta = \pi/2$ which represent the warp and fill directions of the fabric. Let the stretch factor be represented by the first term of a Fourier Series as

$$\mu = 1 + (\beta/2)(1 - \cos(2\theta)) = 1 + \beta \sin^2(\theta)$$

Thus, ρ, ψ and ϕ determined by Equations 6.32 are functions of θ.

Sample calculations based on the foregoing analysis were performed to illustrate how the bag volume and the effective contact area vary with the stretch factor β. The effective area is the area obtained by projecting the curve defined by $\frac{\partial z}{\partial r} = 0$ onto the XY plane. For these calculations a 4 inch radius rigid sphere was assumed to penetrate 2.5 inches into two different size bags having radii of curvature of 10.38 and 21.33 inches, respectively.* The results of the computations are presented in Table 6-1. Note that the volumes and the effective areas decrease significantly as the stretch factor increases. The current version of the CVS program does not allow for this effect and it would be difficult to account for it since it is a function of the local properties of the bag at the point of contact.

Table 6-1

EFFECT OF STRETCH FACTOR ON AIR BAG VOLUME AND EFFECTIVE CONTACT AREA

	Volume - $in.^3$		Area - $in.^2$	
Stretch Factor, β	$r_b = 10.38$ in.	$r_b = 21.33$ in.	$r_b = 10.38$ in.	$r_b = 21.33$ in.
0	71.24	139.92	54.44	100.60
0.05	62.84	102.52	52.36	92.72
0.10	58.84	88.72	49.80	83.88
0.15	56.72	81.56	47.56	77.68
0.20	N/A	77.32	45.40	71.24

*These values are the approximate maximum radii of curvature of the ellipsoidal bag used for the static tests described in Volume 2 of Reference 1.

6.4 Table 1-1, Question 10

Question 10 of Table 1-1 is:

Is it necessary to preserve similitude of certain dynamic degrees of freedom which include inertial effects for deformations associated with contact?

To answer this question consider the simple dynamic systems illustrated in Figure 6-4 below. In the system depicted in part (a) of the figure, mass m moving with velocity v contacts mass m_1 which is coupled to mass m_2 with a linear spring. Mass m_2, is coupled to a fixed reference with a linear spring. Masses m_1 and m_2 are initially at rest. Part (b) of the figure shows an equivalent system if masses m_1 and m_2 are negligible.

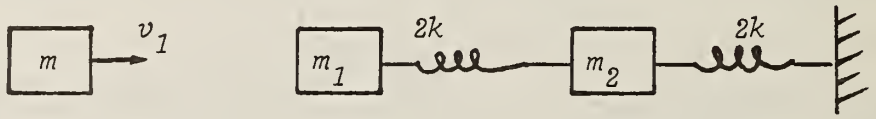

(a)

k - spring constant

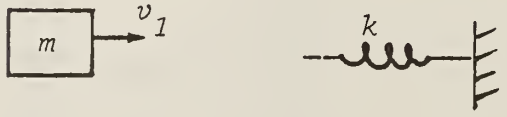

(b)

Figure 6-4 SPRING MASS CONTACT MODELS

Assume that the initial contact is sufficiently 'soft' so that the effects of an impulsive contact need not be considered. (Impulsive contacts are discussed in Section 6.2 of this report.) Further, assume that mass m combines with mass m_1 and that they move as a single unit. The initial velocity is then (from conservation of momentum) $V_1^* = V_1 \, m/m^*$ where $m^* = m + m_1$.

The equations of motion are:

$$m^* \ddot{X} = 2k \, (X_2 - X - (X_2 - X)_0)$$

$$m_2 \ddot{X}_2 = -2k \, (X_2 - X - (X_2 - X)_0) + 2k \, (X_3 - X_2 - (X_3 - X_2)_0)$$

where: X = position of combined mass m^*

X_2 = position of mass m_2

X_3 = position of fixed reference.

Solving these equations for, $\ddot{X}$, the acceleration of X, yields:

$$\ddot{X} = -\frac{k}{m^*} V_1^* \left[\left[1 - \frac{\rho}{\sqrt{4+\rho^2}} \right] \frac{\sin \omega_1 t}{\omega_1} + \left[1 + \rho / \sqrt{4+\rho^2} \right] \frac{\sin \omega_2 t}{\omega_2} \right] \quad (6.33)$$

where: $$\omega_1^2 = \frac{k}{m^*} \, \frac{4}{2 + \rho + \sqrt{4+\rho^2}}$$

$$\omega_2^2 = \frac{k}{m^*} \, \frac{2 + \rho + \sqrt{4+\rho^2}}{\rho}$$

$$\rho = m_2/m^*$$

The solution for the system shown in Figure 6-4(b) may be obtained from Equation 6.33 by letting $\rho = 0$ and $m^* = m$. Thus for this system:

$$\ddot{X} = -\frac{k}{m} V_1 \frac{\sin \omega t}{\omega} = V_1 \sqrt{\frac{k}{m}} \sin \left(t \sqrt{\frac{k}{m}}\right) \tag{6.34}$$

where $\omega^2 = k/m$.

We only show the solution for the acceleration of X since in the crash environment most injury criteria are based on accelerations or forces. For simplicity let us normalize Equation 6.33 by dividing by the amplitude factor of Equation 6.34. We have

$$\begin{aligned} a &= \ddot{X}/(-\frac{k}{m} V_1/\omega_1) \\ &= \frac{m}{m^*} \frac{V_1^*}{V_1} \left[\left(1 - \rho/\sqrt{4+\rho^2}\right) \frac{\omega}{\omega_1} \sin \omega_1 t + \left(1 + \rho/\sqrt{4+\rho^2}\right) \frac{\omega}{\omega_2} \sin \omega_2 t\right] \\ &= A_1 \sin \omega_1 t + A_2 \sin \omega_2 t \end{aligned} \tag{6.35}$$

With the same normalization Equation 6.34 becomes:

$$a_0 = \sin \omega t \tag{6.36}$$

For this simple model Question 10 may be rephrased as: Is the difference between Equation 6.35 and Equation 6.36 significant? We cannot give an absolute answer to this question since the difference of results depends on the problem at hand. We do, however, present numerical results showing how the differences depend on the masses and spring constant.

The numerical results are given in the form of tables. The first table, Table 6-2, shows how the frequency and period of a simple spring mass system (Equation 6.34) varies with the ratio of the spring constant to the weight. The formulas are:

Table 6-2

FREQUENCY AND PERIOD OF SIMPLE SPRING MASS SYSTEM

Spring Constant/Weight K/W (in.-1)	Freq (HZ)	Period (MS)
1.00D-01	0.99	1011.31
1.78D-01	1.32	758.38
3.16D-01	1.76	568.70
5.62D-01	2.34	426.47
1.00D+00	3.13	319.81
1.78D+00	4.17	239.82
3.16D+00	5.56	179.84
5.62D+00	7.42	134.86
1.00D+01	9.89	101.13
1.78D+01	13.19	75.84
3.16D+01	17.58	56.87
5.62D+01	23.45	42.65
1.00D+02	31.27	31.98
1.78D+02	41.70	23.98
3.16D+02	55.60	17.98
5.62D+02	74.15	13.49
1.00D+03	98.88	10.11
1.78D+03	131.86	7.58
3.16D+03	175.84	5.69
5.62D+03	234.48	4.26
1.00D+04	312.69	3.20
1.78D+04	416.98	2.40
3.16D+04	556.05	1.80
5.62D+04	741.50	1.35
1.00D+05	988.81	1.01

frequency $f = \frac{1}{2\pi}\ \omega = \frac{1}{2\pi}\ \sqrt{\frac{k}{w}\,g}$, *Hertz*

period $T = {}^{1000}/_{f}$, *milliseconds*

where $W = mg$, *pounds*

$k =$ *spring constant, pounds/inch*

$g =$ *acceleration of gravity, 386 inches/second*^{2}

From Table 6-2 we note that for $k/w = 10$ the period is about 100 milliseconds. The ratio of k/w must be 100000 to give a period of 1 millisecond.

The second table, Table 6-3, shows the effect when mass 2 of the 3-mass contact model is negligible $(\rho = 0)$ but mass 1 is not. The formulas are:

$V_1^*/V_1 = 1/(1 + r)$, *velocity ratio*

$A_1 = 1/(1 + r)^{3/2}$, *amplitude*

$T_1/T = \sqrt{1 + r}$, *period ratio*

$r = m_1/m$, *mass ratio*

The third table, Table 6-4, shows the response of the 3-mass system when mass 1 is negligible and ρ (the ratio of m_2 to m) is varied. The formulas are:

Table 6-3

EFFECT OF MASS RATIO ON RESPONSE OF 3-MASS CONTACT MODEL
WITH NEGLIGIBLE MASS 2

Mass Ratio M_1/M	Velocity Ratio V_1^*/V_1	Period Ratio T_1/T	Amplitude A_1
1.00D+01	0.0909	3.3166	0.0274
5.62D+00	0.1510	2.5736	0.0587
3.16D+00	0.2403	2.0402	0.1178
1.78D+00	0.3599	1.6668	0.2159
1.00D+00	0.5000	1.4142	0.3536
5.62D-01	0.6401	1.2499	0.5121
3.16D-01	0.7597	1.1473	0.6622
1.78D-01	0.8490	1.0853	0.7823
1.00D-01	0.9091	1.0488	0.8668
5.62D-02	0.9468	1.0277	0.9212
3.16D-02	0.9693	1.0157	0.9544
1.78D-02	0.9825	1.0089	0.9739
1.00D-02	0.9901	1.0050	0.9852
5.62D-03	0.9944	1.0028	0.9916
3.16D-03	0.9968	1.0016	0.9953
1.78D-03	0.9982	1.0009	0.9973
1.00D-03	0.9990	1.0005	0.9985
5.62D-04	0.9994	1.0003	0.9992
3.16D-04	0.9997	1.0002	0.9995
1.78D-04	0.9998	1.0001	0.9997
1.00D-04	0.9999	1.0000	0.9999
5.62D-05	0.9999	1.0000	0.9999
3.16D-05	1.0000	1.0000	1.0000
1.78D-05	1.0000	1.0000	1.0000
1.00D-05	1.0000	1.0000	1.0000

Table 6-4

EFFECT OF MASS RATIO ON RESPONSE OF 3-MASS CONTACT MODEL WITH NEGLIGIBLE MASS 1

Mass Ratio	Period Ratios			Amplitudes		Amplitude Ratio
M_2/M	T_1/T	T_2/T	T_1/T_2	A_1	A_2	A_2/A_1
1.00D+01	2.3557	0.6712	0.2849	0.0457	1.3293	29.0585
5.62D+00	1.8434	0.6432	0.3489	0.1066	1.2493	11.7219
3.16D+00	1.4920	0.5959	0.3994	0.2310	1.0996	4.7597
1.78D+00	1.2703	0.5249	0.4132	0.4262	0.8737	2.0498
1.00D+00	1.1441	0.4370	0.3820	0.6325	0.6325	1.0000
5.62D-01	1.0770	0.3481	0.3232	0.7855	0.4424	0.5632
3.16D-01	1.0418	0.2699	0.2591	0.8791	0.3121	0.3550
1.78D-01	1.0230	0.2061	0.2015	0.9324	0.2244	0.2407
1.00D-01	1.0127	0.1561	0.1542	0.9622	0.1639	0.1704
5.62D-02	1.0071	0.1177	0.1169	0.9788	0.1210	0.1237
3.16D-02	1.0040	0.0886	0.0882	0.9881	0.0900	0.0910
1.78D-02	1.0022	0.0665	0.0664	0.9933	0.0671	0.0676
1.00D-02	1.0013	0.0499	0.0499	0.9962	0.0502	0.0504
5.62D-03	1.0007	0.0375	0.0374	0.9979	0.0376	0.0377
3.16D-03	1.0004	0.0281	0.0281	0.9988	0.0282	0.0282
1.78D-03	1.0002	0.0211	0.0211	0.9993	0.0211	0.0211
1.00D-03	1.0001	0.0158	0.0158	0.9996	0.0158	0.0158
5.62D-04	1.0001	0.0119	0.0119	0.9998	0.0119	0.0119
3.16D-04	1.0000	0.0089	0.0089	0.9999	0.0089	0.0089
1.78D-04	1.0000	0.0067	0.0067	0.9999	0.0067	0.0067
1.00D-04	1.0000	0.0050	0.0050	1.0000	0.0050	0.0050
5.62D-05	1.0000	0.0037	0.0037	1.0000	0.0037	0.0037
3.16D-05	1.0000	0.0028	0.0028	1.0000	0.0028	0.0028
1.78D-05	1.0000	0.0021	0.0021	1.0000	0.0021	0.0021
1.00D-05	1.0000	0.0016	0.0016	1.0000	0.0016	0.0016

$$T_1/T = \sqrt{(2 + \rho + \sqrt{4+\rho^2})/4} \quad , \text{ period ratio}$$

$$T_2/T = \sqrt{\rho/(2 + \rho + \sqrt{4+\rho^2})} \quad , \text{ period ratio}$$

$$A_1 = (1 - \rho/\sqrt{4+\rho^2})\ \omega/\omega_1 \quad , \text{ amplitude}$$

$$A_2 = (1 + \rho/\sqrt{4+\rho^2})\ \omega/\omega_2 \quad , \text{ amplitude}$$

The ratios of T_2/T_1 and A_2/A_1 are also tabulated.

In conclusion the answer to the question as to whether or not it is necessary to include inertial effects for contacts is dependent on the situation. In this section we give numerical results for a simple contact model which should be helpful to the program user in making a decision as to whether or not inertial effects should be included. Table 6-2 which shows the periods of oscillation as a function of stiffness to weight is primarily of use in estimating the integrator step size or in reaching a decision on the use of an impulsive contact. The numerical integrator should have a maximum step size that is no greater than 1/10 of the period (this is relative to the accuracy desired); thus, Table 6-2 shows that if one wishes to use a maximum step size of 1 millisecond the stiffness to weight ratio should be no greater than 1000. Table 6-3 shows the effects of ignoring part of the system mass such as, for example, the mass of the material which is carried with the head on a windshield contact. For a mass ratio of 1/10 there is a 10% change in velocity, a 5% change in period and a 13% change in amplitude. Table 6-4 shows the effects of the first two modes of vibration of an elastic impact. In an actual physical problem, since we are dealing with continuous structures, there will be an infinite number of modes of vibration. In an impact problem the higher order modes will be of progressively less importance; that is, these amplitudes

will decrease as the frequency increases. Table 6-4 shows that if the effective mass of the impacted structure (M_2) is 1/10 of the effective impacting mass (M) the period of the principal resonance T_1 differs by about 1% from the period that would occur if mass 2 were ignored. The secondary resonance has a period that is 16% of the primary. The amplitude of the principal resonance differs by 4% and the secondary resonance has an amplitude of 17% of the primary. The principal effect of ignoring mass 2 would be the neglection of the 17% amplitude secondary frequency. It should be remembered that these values pertain to the acceleration response; the effects on position will be reduced by the square of the period ratio (T_1/T_2).

7.0 CONCLUDING REMARKS

Although this report may seem to the reader to be a collection of unrelated topics, the topics have one thing in common, i.e., they are all related to various aspects of the CVS program.

The user must remember that the CVS program is based on rigid body dynamics and, hence, when used to simulate real-life conditions can only approximate the true dynamics of the system. When the program is used to simulate a dummy, the skeletal structure of the dummy can be modelled quite accurately but the presence of the 'skin,' and the rubber neck and spine preclude the precise modelling with a program based on rigid body dynamics. The work on the shoulder model reported in Section 3.2 of this report demonstrates the flexibility of the program in allowing the user to define a more precise model of a dummy. The various topics discussed in Section 6 of this report point out some of the limitations of the model and attempt to give some insight to the effects of using impulsive forces instead of force-deflection relationships for "hard" type contacts, the use of point contact algorithms instead of deformable contact algorithms, and the use of simplified models of belt and air bag restraint systems instead of more precise models of these restraint systems.

The Response Measure Approximating Function Generator described in Section 4 should prove to be a useful tool for the user who wishes to perform parametric studies and have a means of interpolating the response measures as a function of several parameters.

The dynamically equivalent system algorithm described in Section 5 of this report has no direct bearing on the CVS program but points out a little known fact about a system of interconnected rigid bodies. In particular, it shows that the mass distribution to produce a particular system response is not unique. This implies that the exact internal structure of an interconnected rigid body system cannot be determined from the observation of external dynamic and kinematic responses. The theorem may prove useful in defining "canonical

models' of systems, i.e., a "canonical model' may be defined as one where all of the segments have the same mass.

Finally, the CVS program is a useful tool, but the success of its application to a particular problem requires a full understanding of its capabilities and limitations by the user. There is much work yet that could be done to improve the program, particularly the development of new contact algorithms to better model the interaction of deformable bodies which is the real world situation.

8.0 REFERENCES

1. Fleck, J. T. & Butler, F. E., "Validation of the Crash Victim Simulator," Calspan Report No. ZS-5881-V-1 to V-4.

   Volume 1: Engineering Manual-Part I: Analytical Formulation, December 1981.

   Volume 2: Engineering Manual-Part II: Validation Effort, August 1982.

   Volume 3: User's Manual, February 1982.

   Volume 4: Programmer's Manual, March 1982.

2. DeLeys, N. J., "Data for Validation of Crash Victim Simulator," Calspan Report No. 6107-V-1, August 1981.

3. Warburton, G. B., "The Dynamic Behaviour of Structures," The Macmillan Company, New York, 1964.

4. Brand, Louis, "Vector and Tensor Analysis," John Wiley and Sons, 1947.

APPENDIX A

PLOTS OF RESPONSE MEASURES FROM SHOULDER MODEL SIMULATION STUDY

This appendix contains plots of selected response measures for the six CVS runs performed as part of the study of dummy shoulder models that are described in Section 3.2 of this report. For each run the plots are presented in the following order:

(a) Right lower arm resultant acceleration versus time
(b) Right lower arm Z displacement versus X displacement
(c) Right lower arm Y displacement versus X displacement
(d) Shoulder yoke-clavicle pivot flexure angle versus time
(e) Precession and nutation angles of the shoulder Euler joint versus time
(f) Precession and nutation angles of the elbow Euler joint versus time
(g) Upper torso resultant acceleration versus time
(h) Upper torso pitch angle versus time.

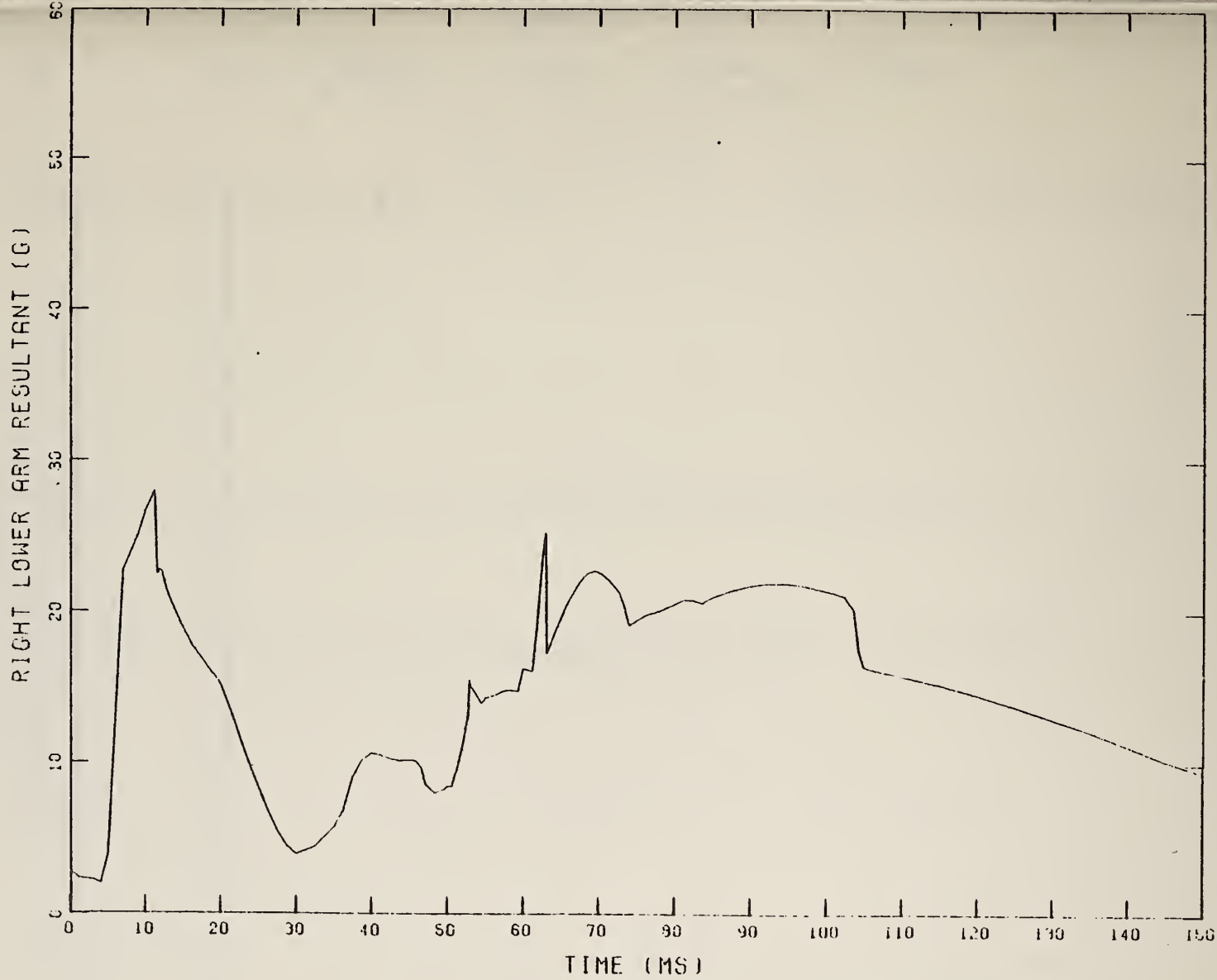

(a) RLA RESULTANT ACCELERATION VS. TIME

X,Y,Z = UNLOCK, P = LOCK, N = UNLOCK, S = LOCK

Figure A-1 RUN NO. 1 RESPONSE MEASURE PLOTS

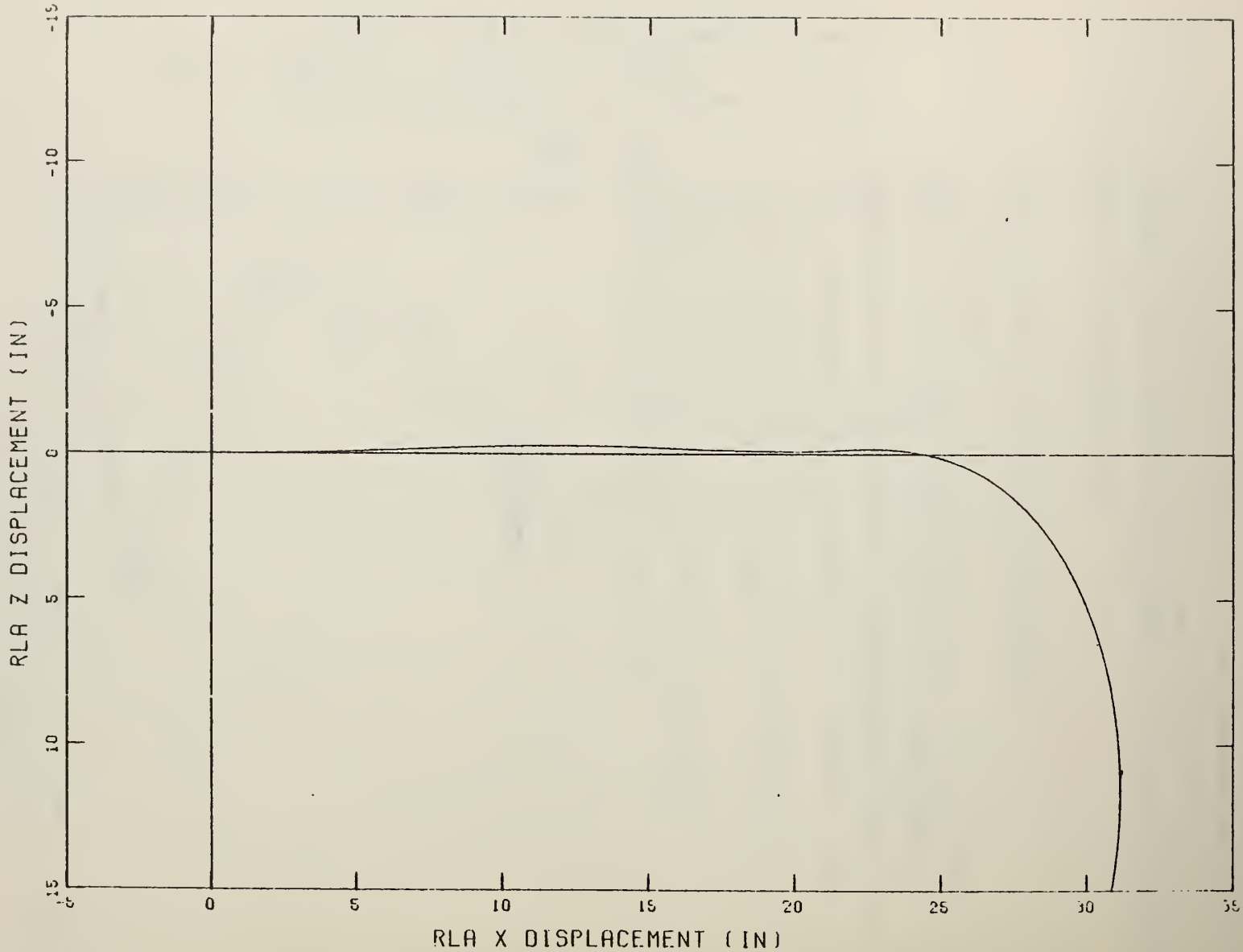

(b) RLA Z VS. RLA X DISPLACEMENT
X,Y,Z = UNLOCK, P = LOCK, N = UNLOCK, S = LOCK

Figure A-1 (Cont'd.)

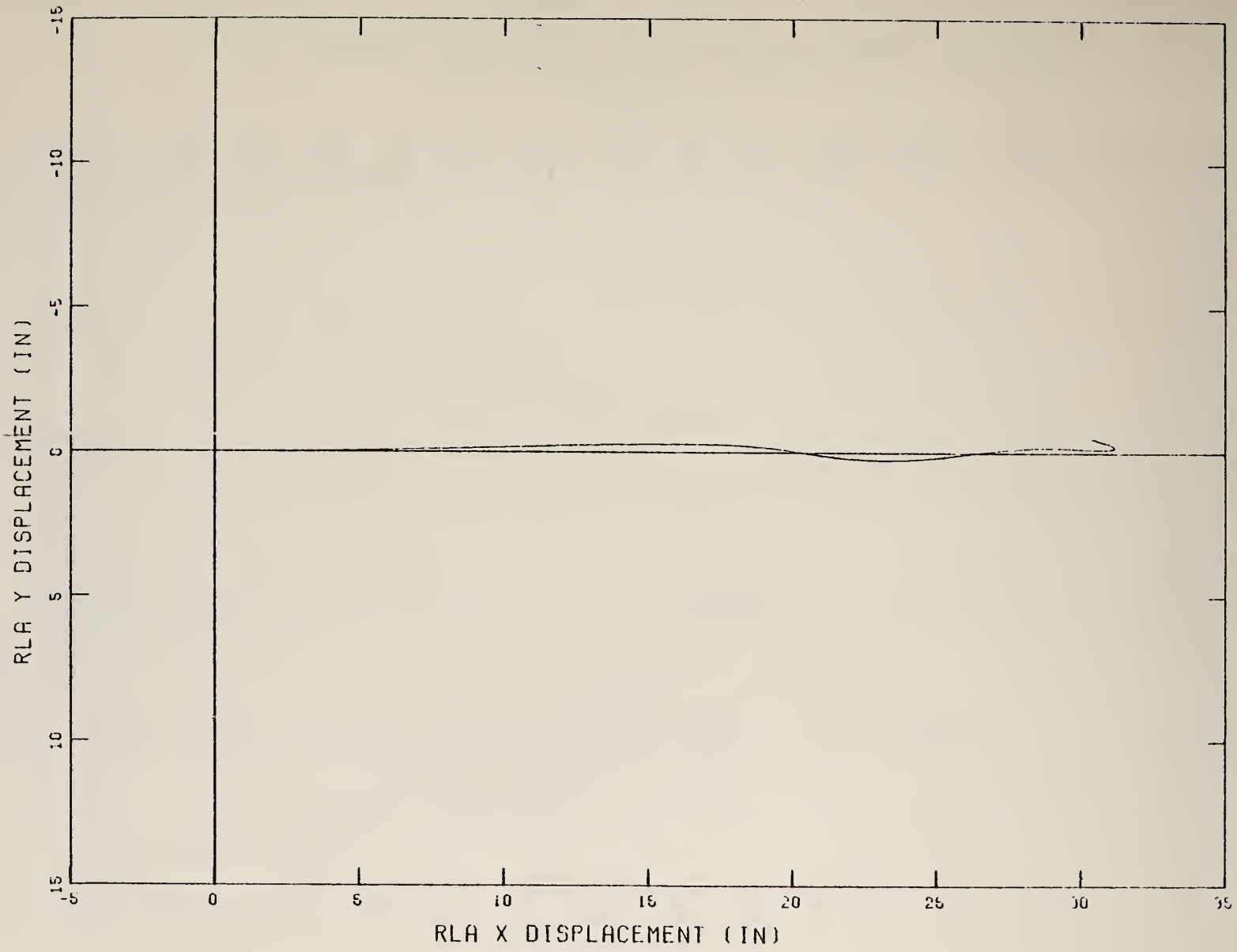

(c) RLA Y VS. RLA X DISPLACEMENT
X,Y,Z = UNLOCK, P = LOCK, N = UNLOCK, S = LOCK

Figure A-1 (Cont'd.)

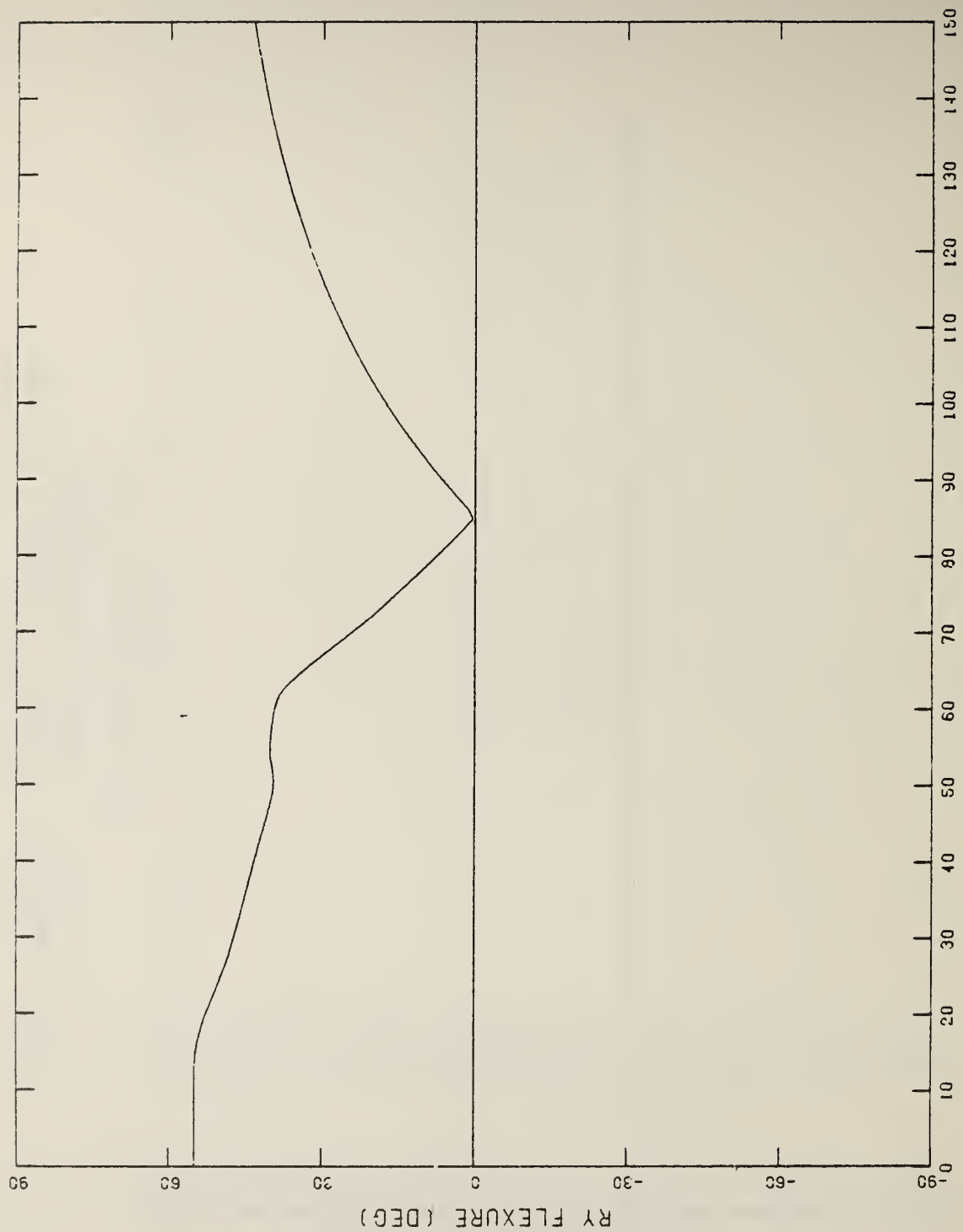

(d) RY FLEXURE VS. TIME

X,Y,Z = UNLOCK, P = LOCK, N = UNLOCK, S = LOCK

Figure A-1 (Cont'd.)

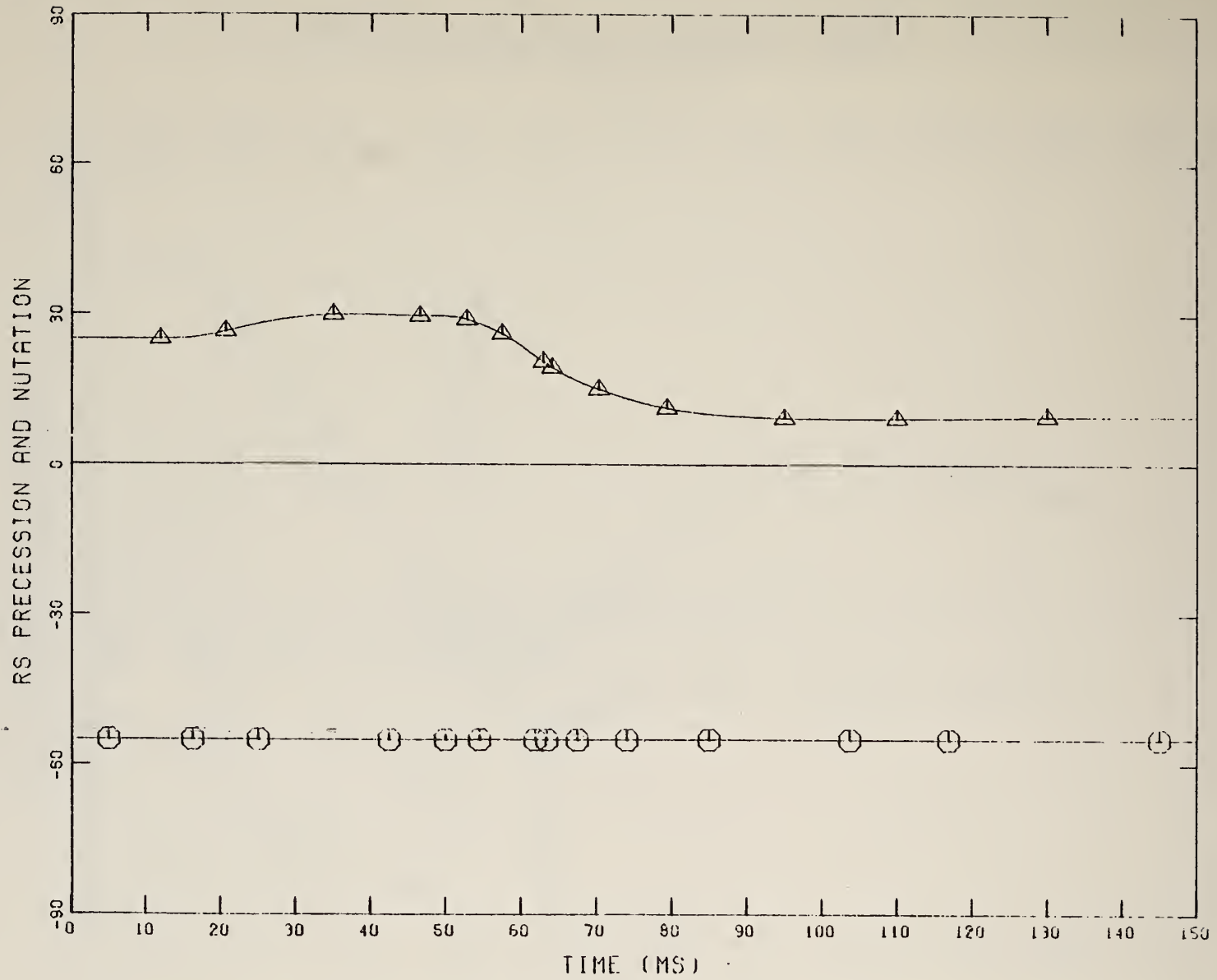

(e) RS PRECESSION AND NUTATION VS. TIME
X,Y,Z = UNLOCK, P = LOCK, N = UNLOCK, S = LOCK

Figure A-1 (Cont'd.)

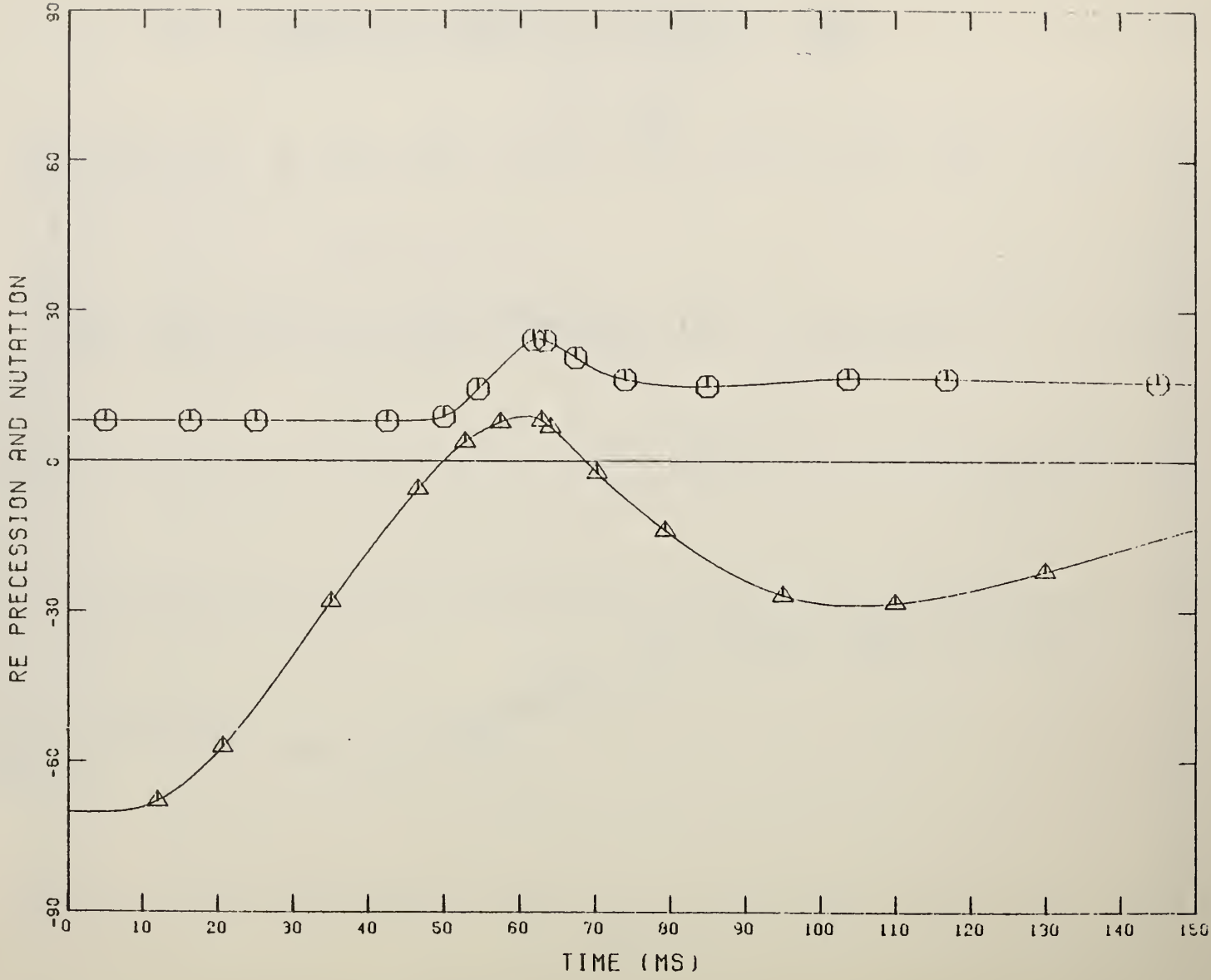

(f) RE PRECESSION AND NUTATION VS. TIME
X.Y.Z = UNLOCK. P = LOCK. N = UNLOCK. S = LOCK

Figure A-1 (Cont'd.)

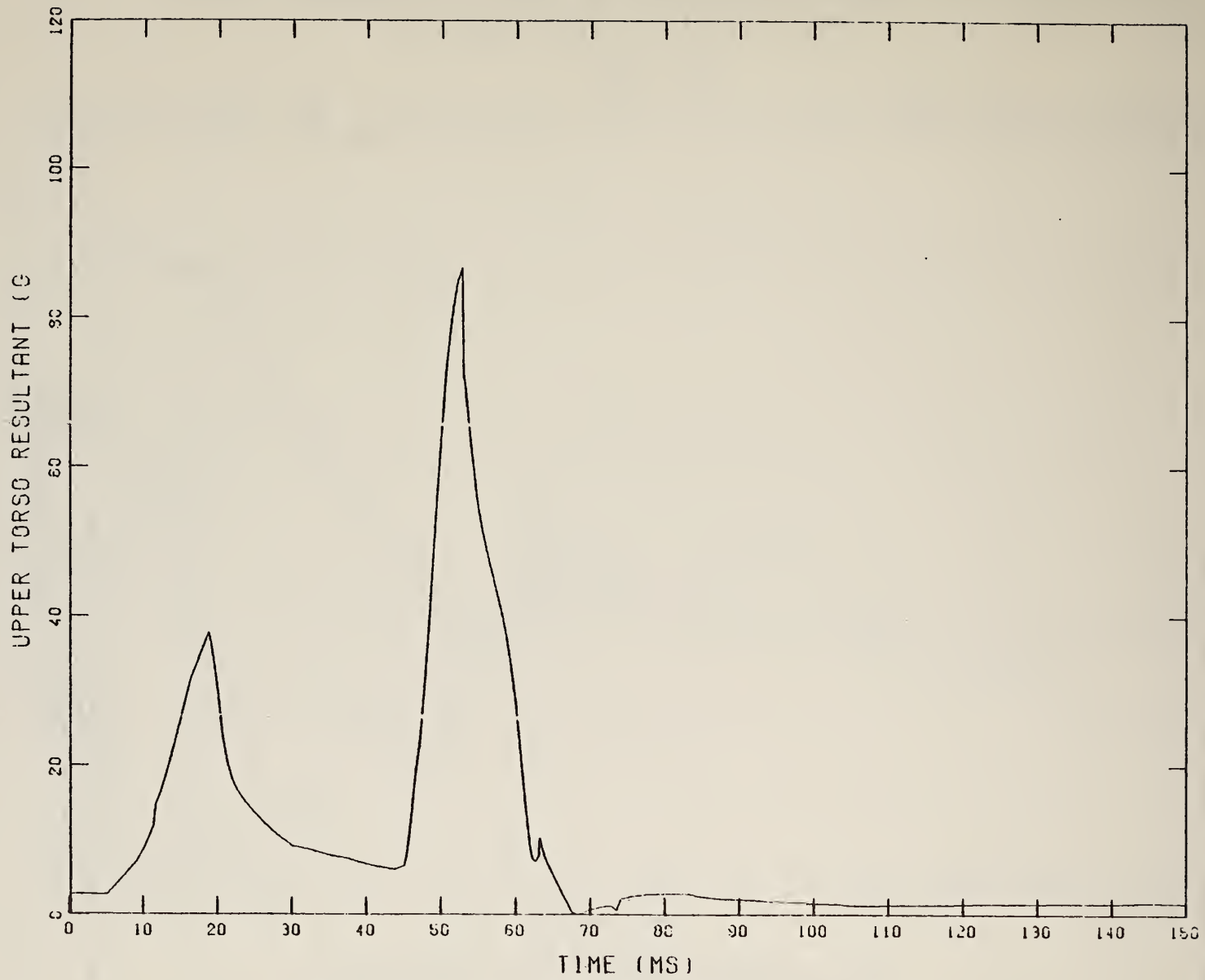

(g) UPPER TORSO RESULTANT ACCELERATION VS. TIME
X,Y,Z = UNLOCK, P = LOCK, N = UNLOCK, S = LOCK

Figure A-1 (Cont'd.)

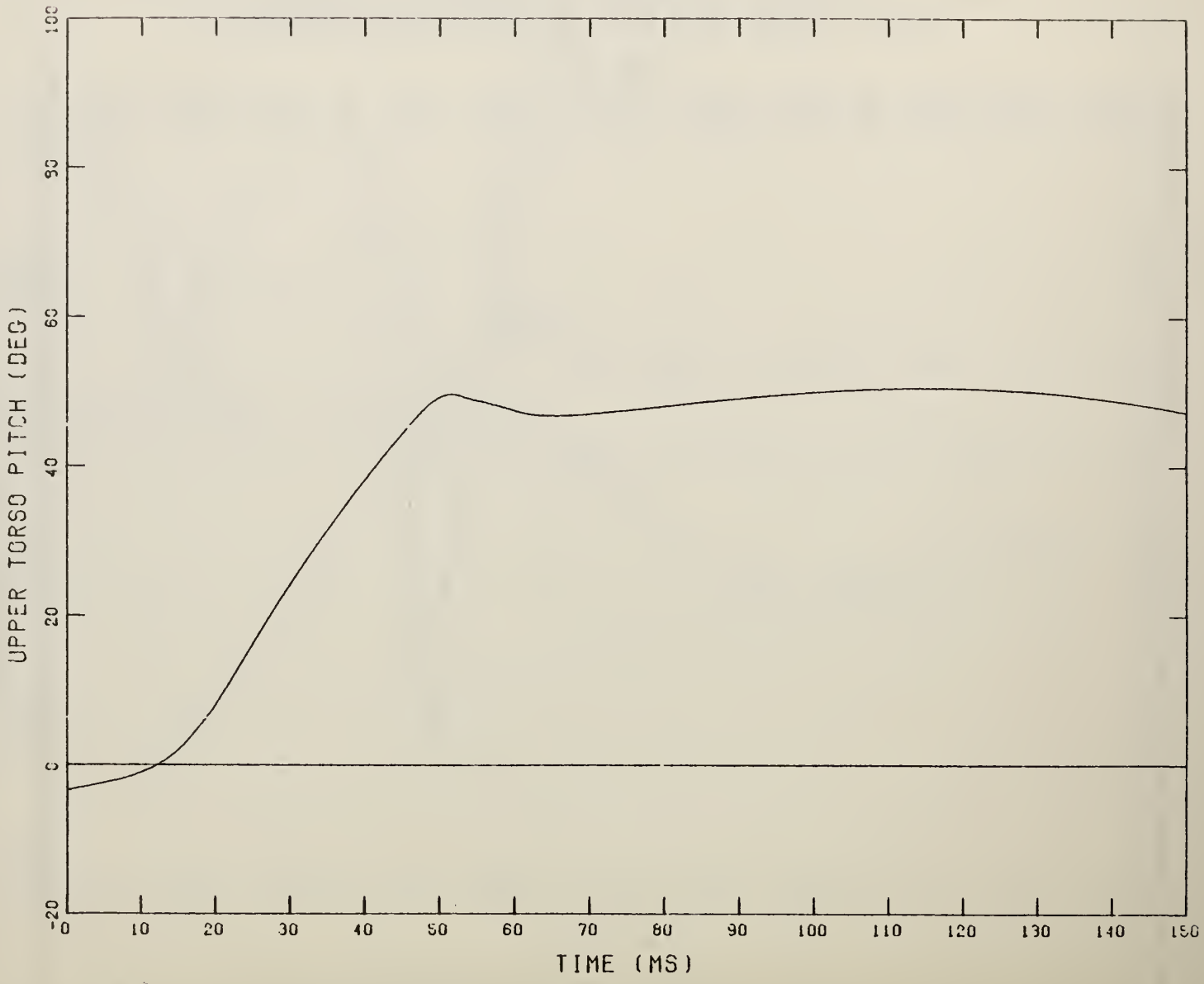

(h) UPPER TORSO PITCH VS. TIME
X,Y,Z = UNLOCK, P = LOCK, N = UNLOCK, S = LOCK

Figure A-1 (Cont'd.)

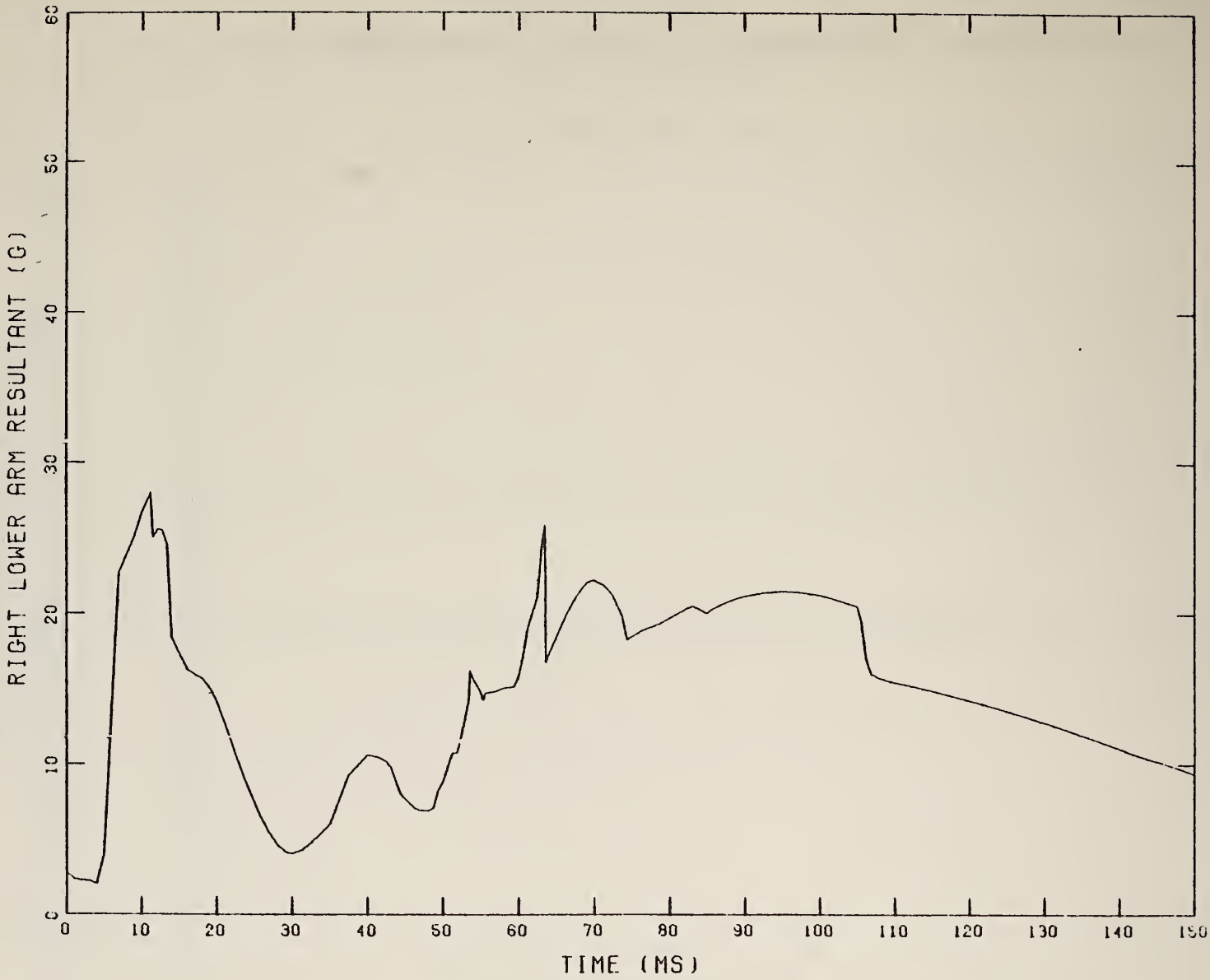

(a) RLA RESULTANT ACCELERATION VS.TIME
X,Z = UNLOCKED,Y = LOCKED,P,N = UNLOCKED,S = LOCKED

Figure A-2 RUN NO. 2 RESPONSE MEASURE PLOTS

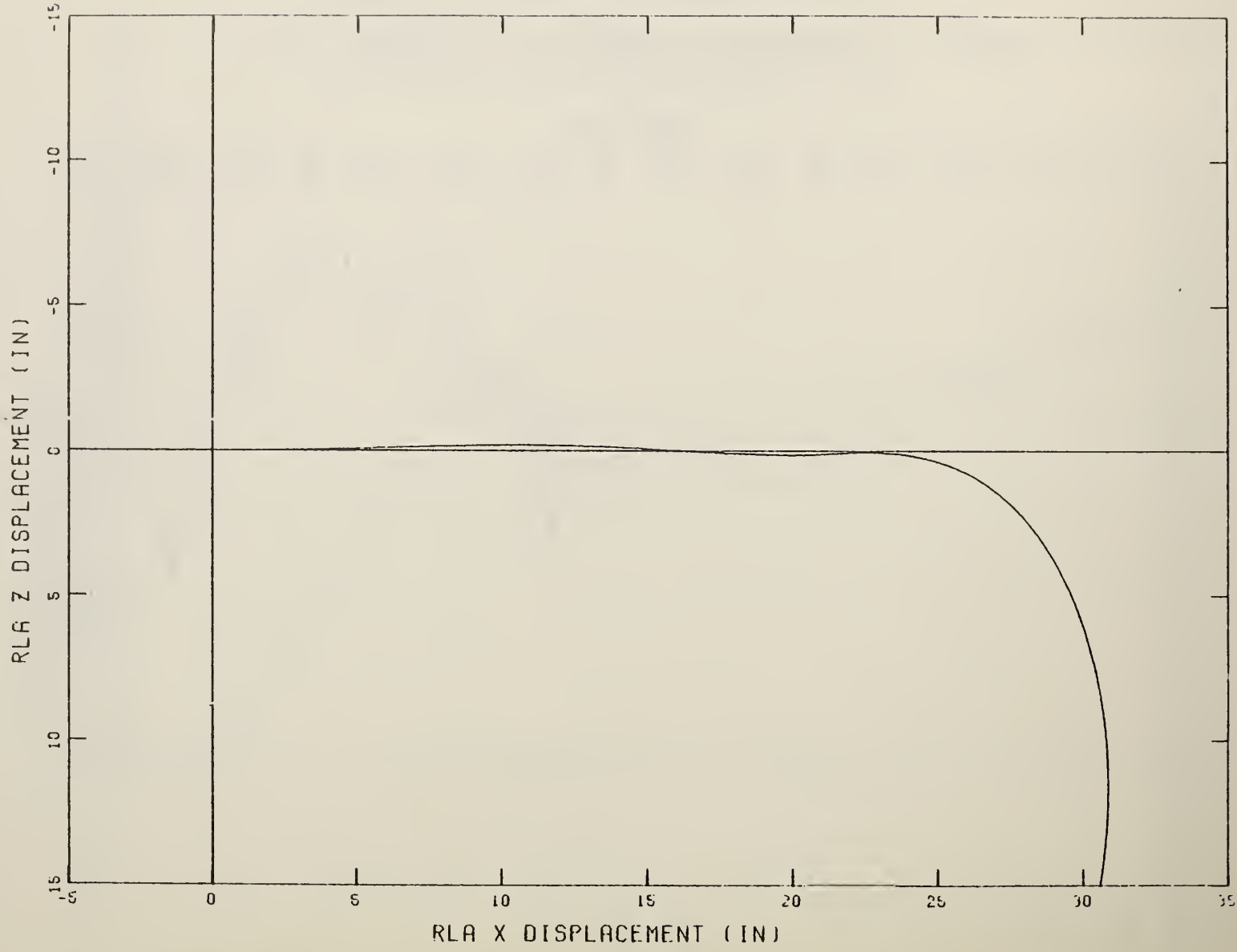

(b) RLA Z VS. RLA X DISPLACEMENT
X,Z = UNLOCKED,Y = LOCKED,P,N = UNLOCKED,S = LOCKED

Figure A-2 (Cont'd.)

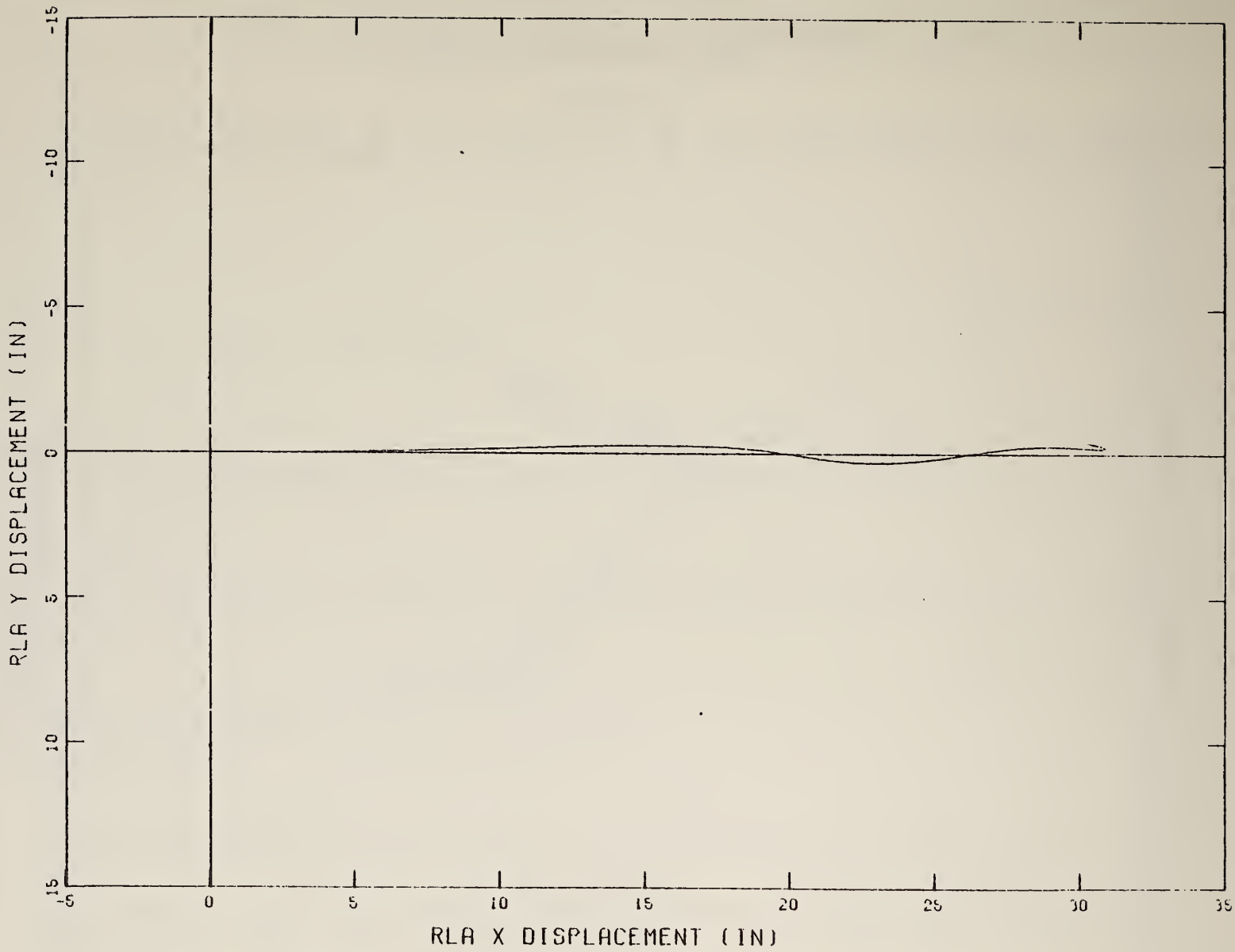

(c) RLA Y VS. RLA X DISPLACEMENT
X,Z = UNLOCKED,Y = LOCKED,P,N = UNLOCKED,S = LOCKED

Figure A-2 (Cont'd.)

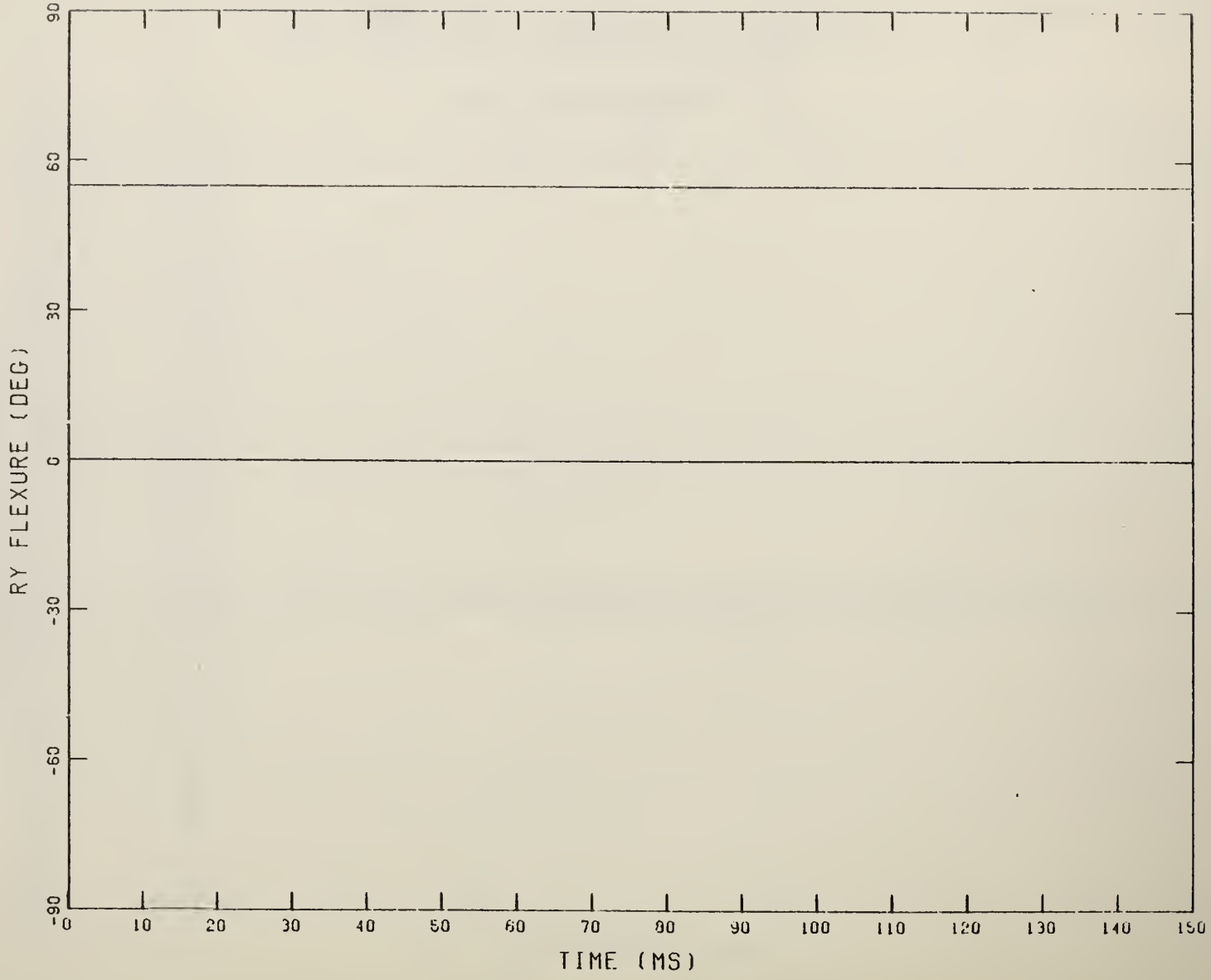

(d) RY FLEXURE VS. TIME
X,Z = UNLOCKED,Y = LOCKED,P,N = UNLOCKED,S = LOCKED

Figure A-2 (Cont'd.)

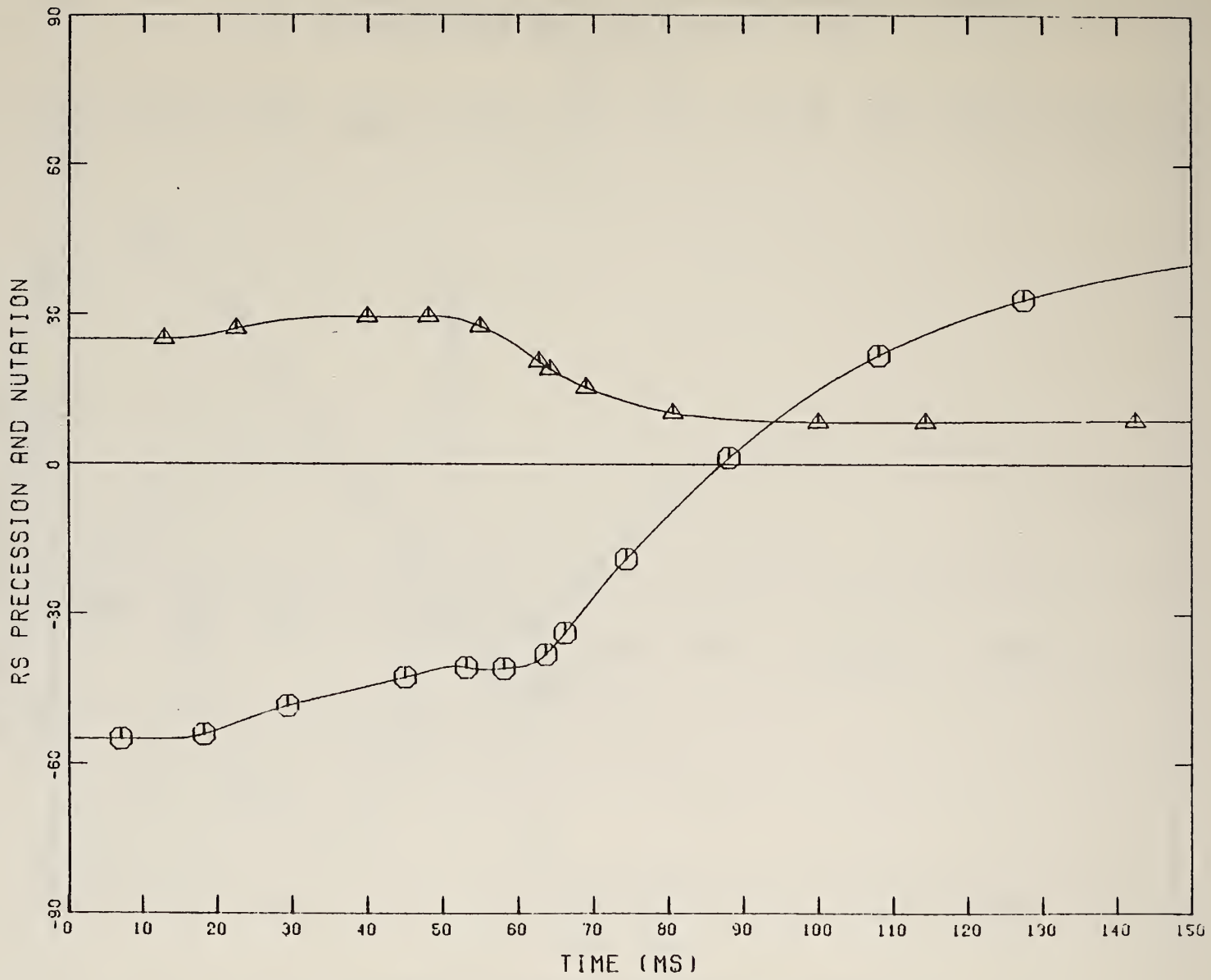

(e) RS PRECESSION AND NUTATION VS. TIME
X,Z = UNLOCKED,Y = LOCKED,P,N = UNLOCKED,S = LOCKED

Figure A-2 (Cont'd.)

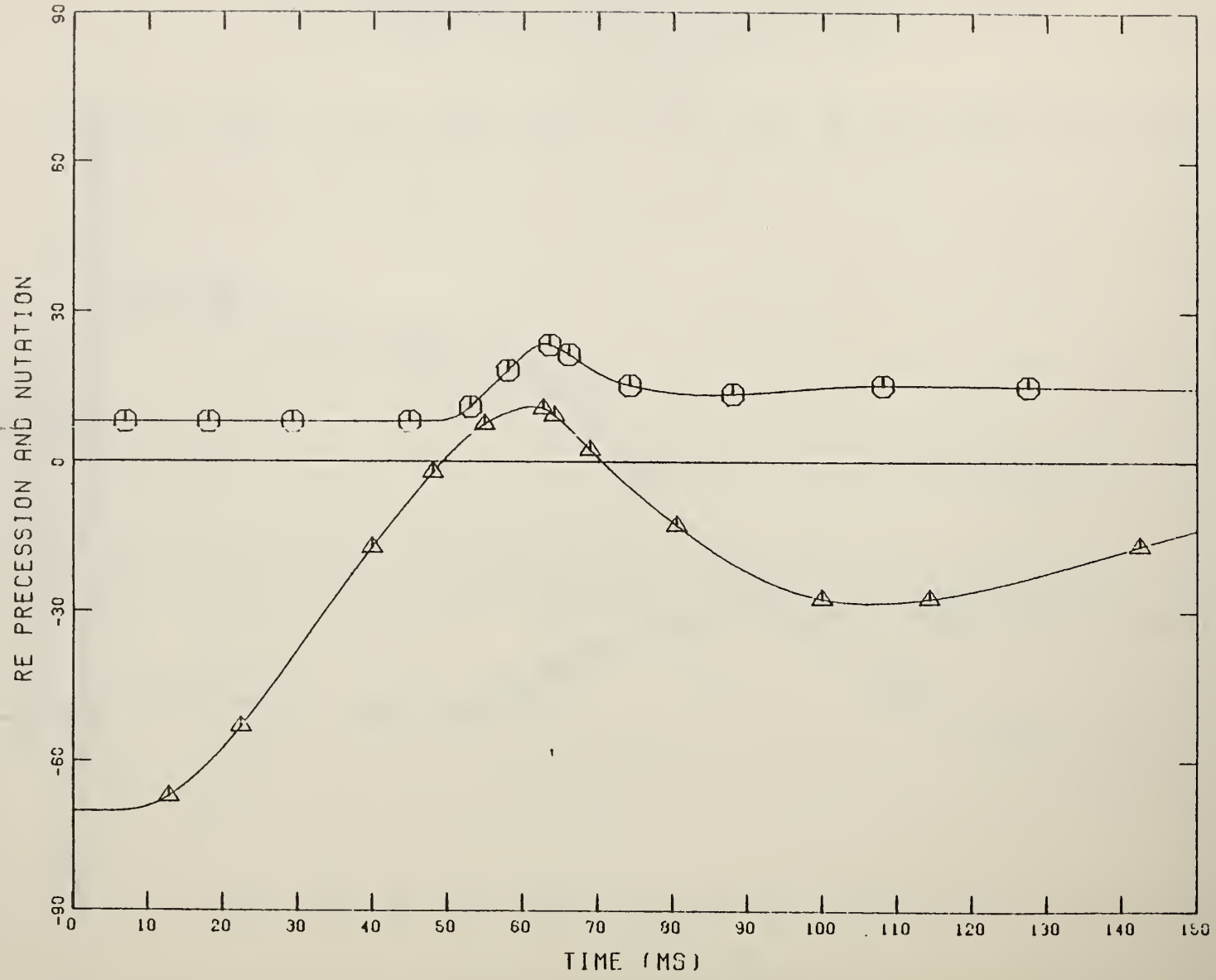

(f) RE PRECESSION AND NUTATION VS. TIME
X,Z = UNLOCKED,Y = LOCKED,P,N = UNLOCKED,S = LOCKED

Figure A-2 (Cont'd.)

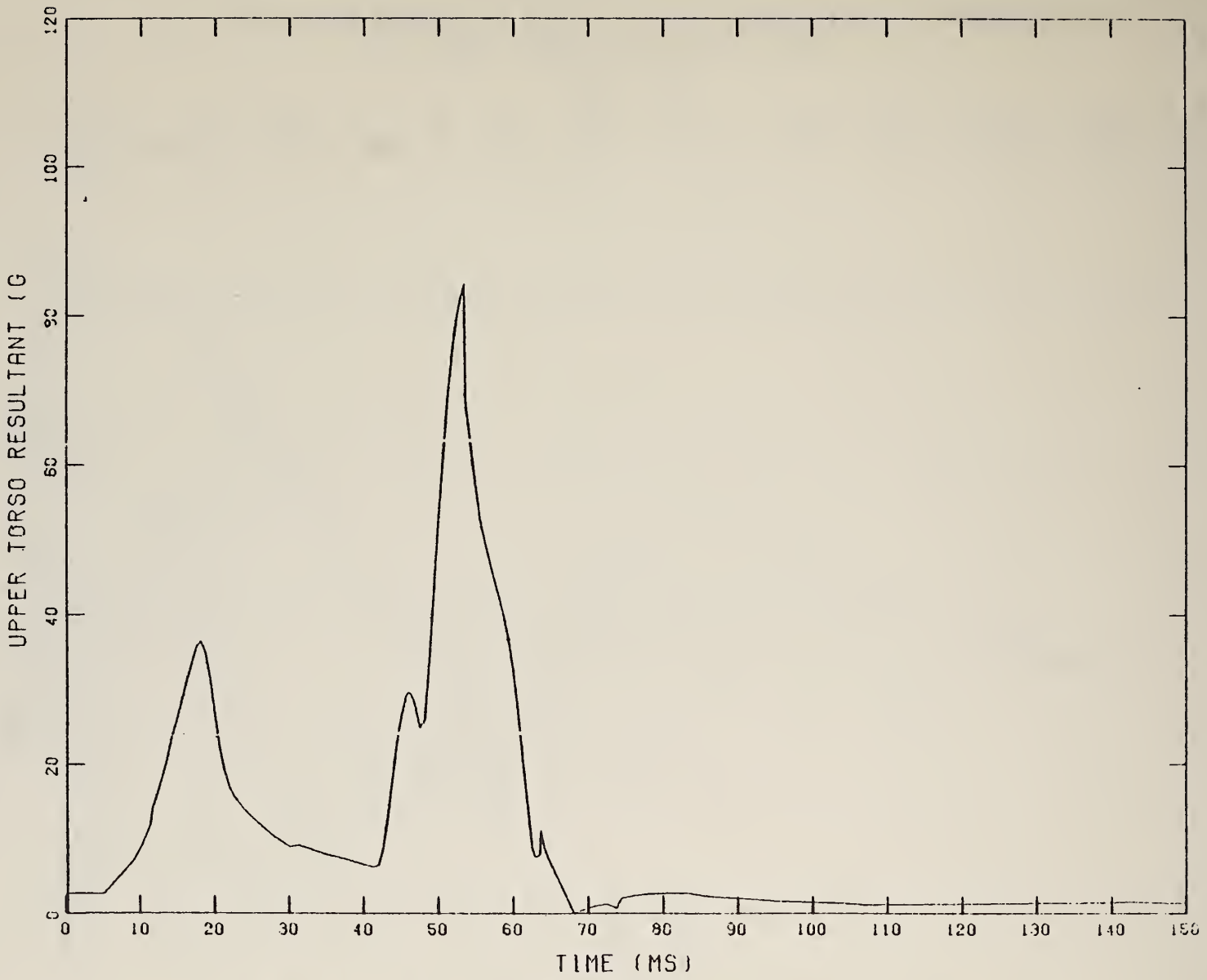

(g) UPPER TORSO RESULTANT ACCELERATION VS. TIME
X,Z = UNLOCKED,Y = LOCKED,P,N = UNLOCKED,S = LOCKED

Figure A-2 (Cont'd.)

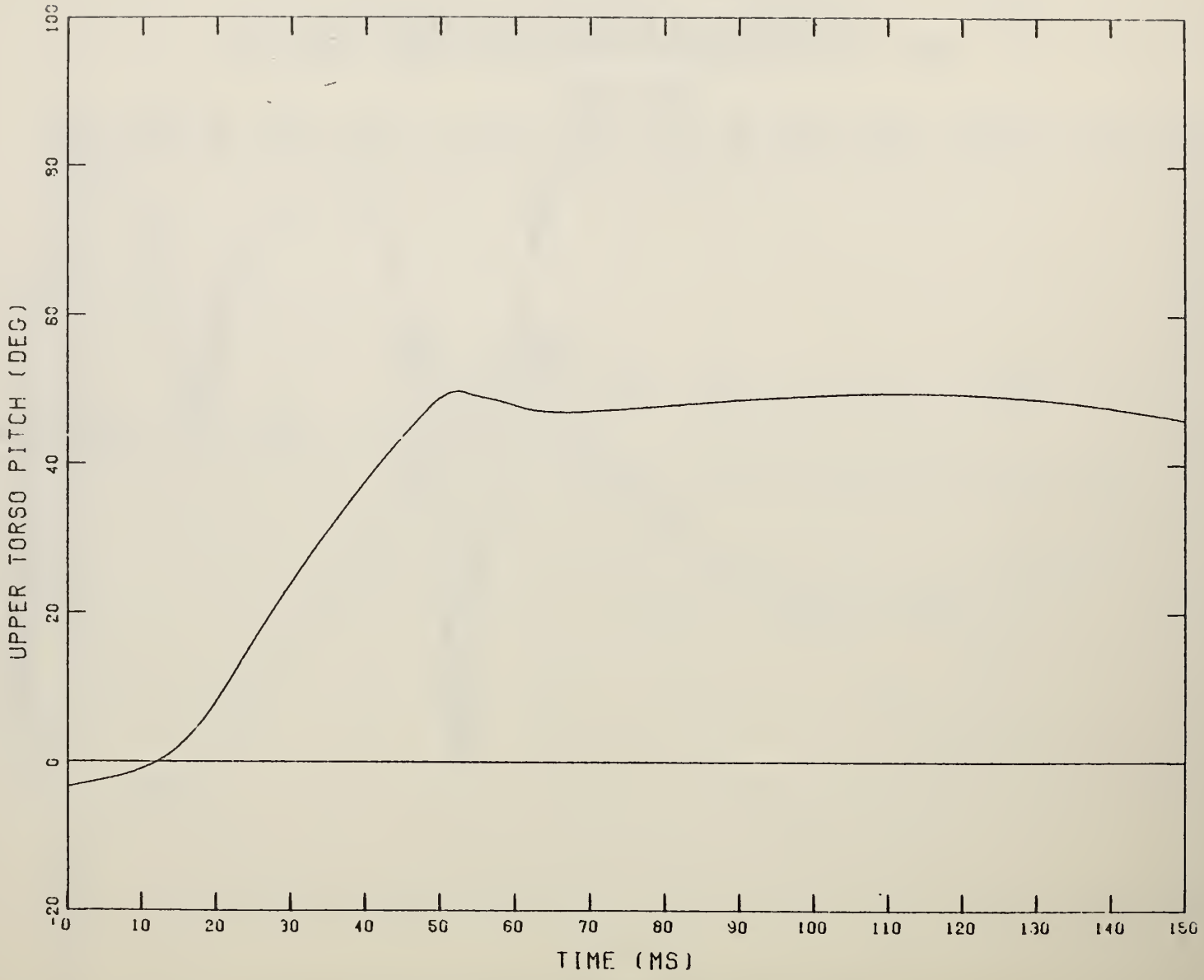

(h) UPPER TORSO PITCH VS. TIME
X,Z = UNLOCKED,Y = LOCKED,P,N = UNLOCKED,S = LOCKED

Figure A-2 (Cont'd.)

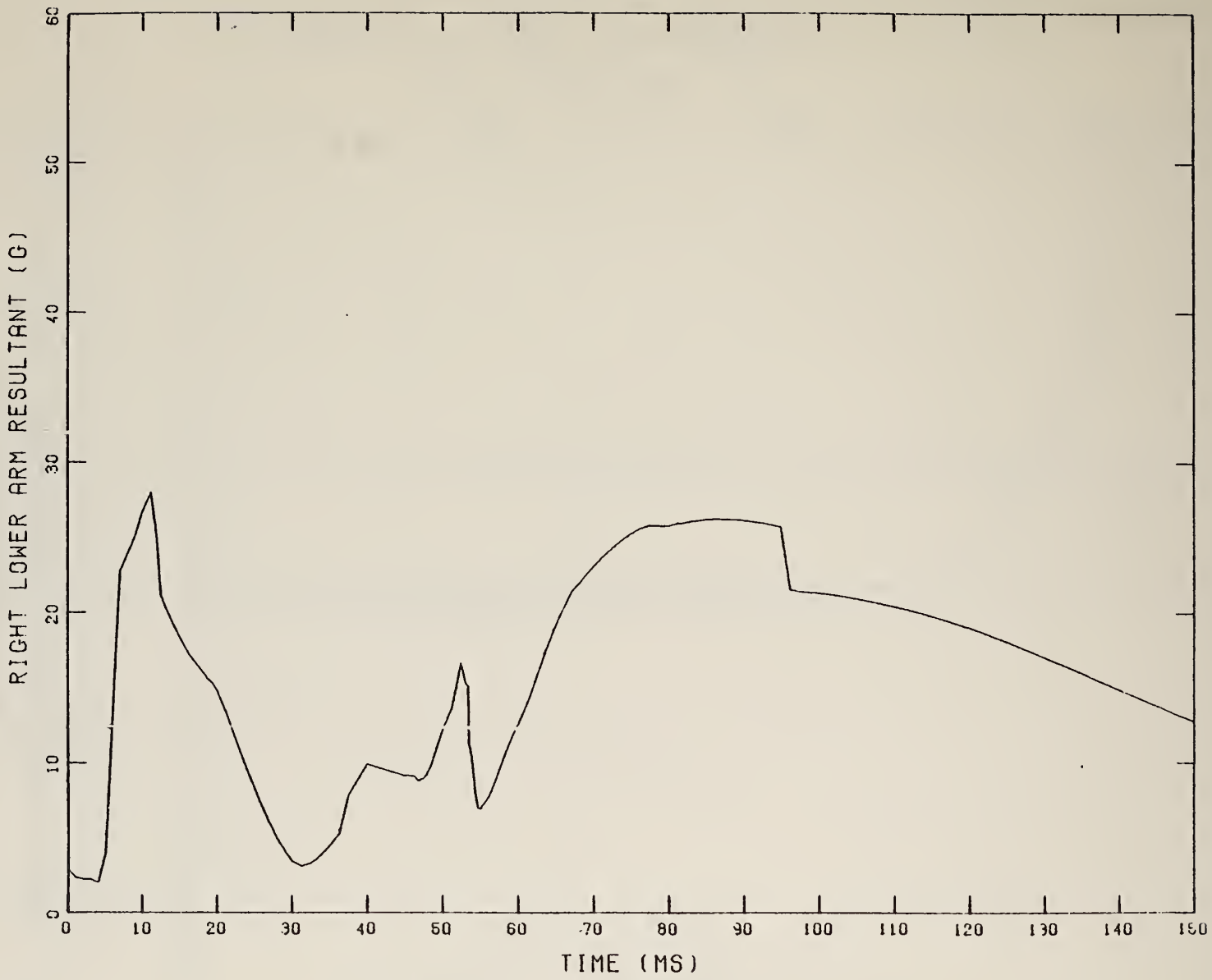

(a) RLA RESULTANT ACCELERATION VS.TIME
X = UNLOCKED, Z,Y = LOCKED, P,N = UNLOCKED, S = LOCKED

Figure A-3 RUN NO. 3 RESPONSE MEASURE PLOTS

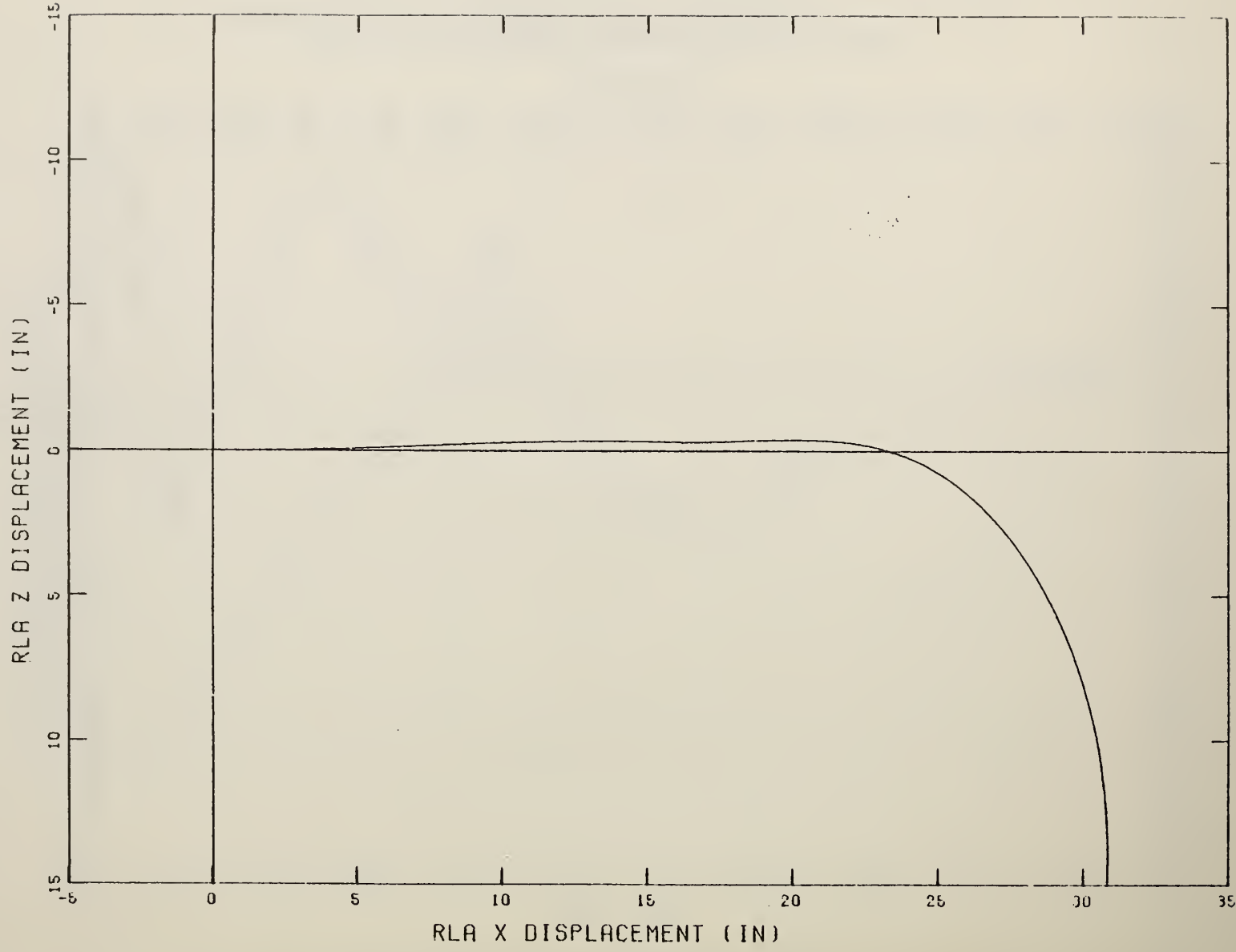

(b) RLA Z VS. RLA X DISPLACEMENT
X = UNLOCKED, Z,Y = LOCKED, P,N = UNLOCKED, S = LOCKED

Figure A-3 (Cont'd.)

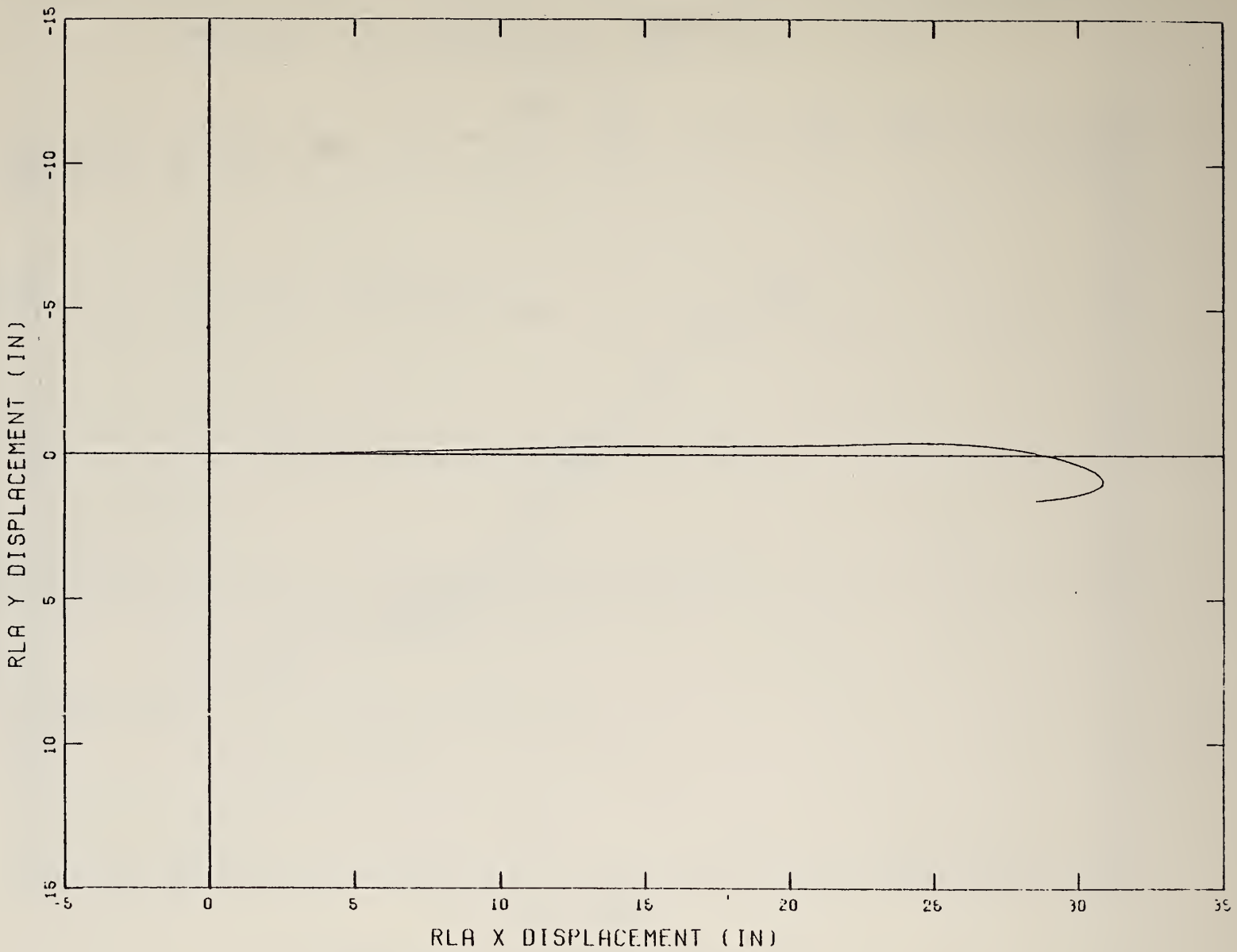

(c) RLA Y VS. RLA X DISPLACEMENT
X = UNLOCKED, Z,Y = LOCKED, P,N = UNLOCKED, S = LOCKED

Figure A-3 (Cont'd.)

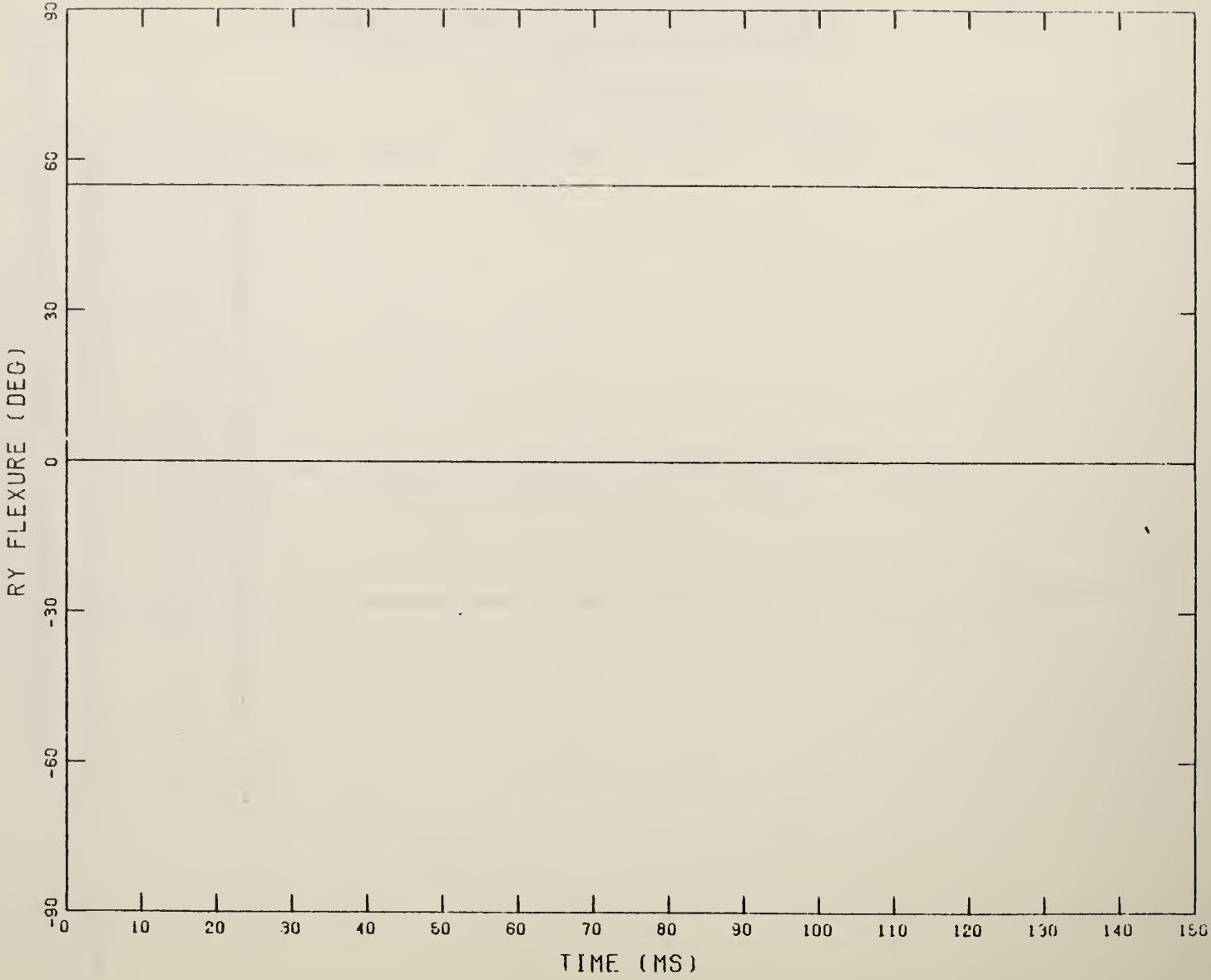

(d) RY FLEXURE VS. TIME
X = UNLOCKED. Z.Y = LOCKED. P.N = UNLOCKED. S = LOCKED

Figure A-3 (Cont'd.)

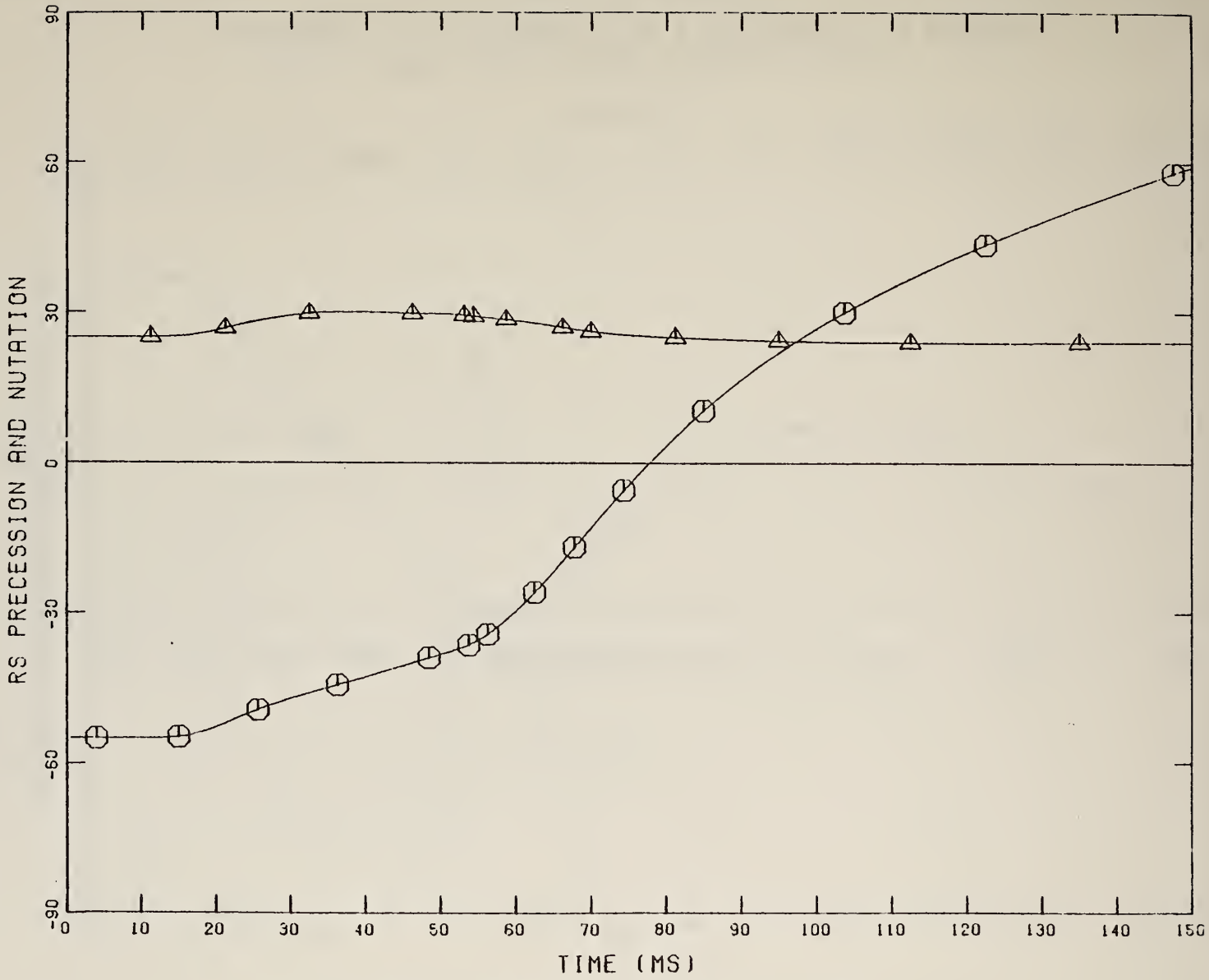

(e) RS PRECESSION AND NUTATION VS. TIME
X = UNLOCKED, Z,Y = LOCKED, P,N = UNLOCKED, S = LOCKED

Figure A-3 (Cont'd.)

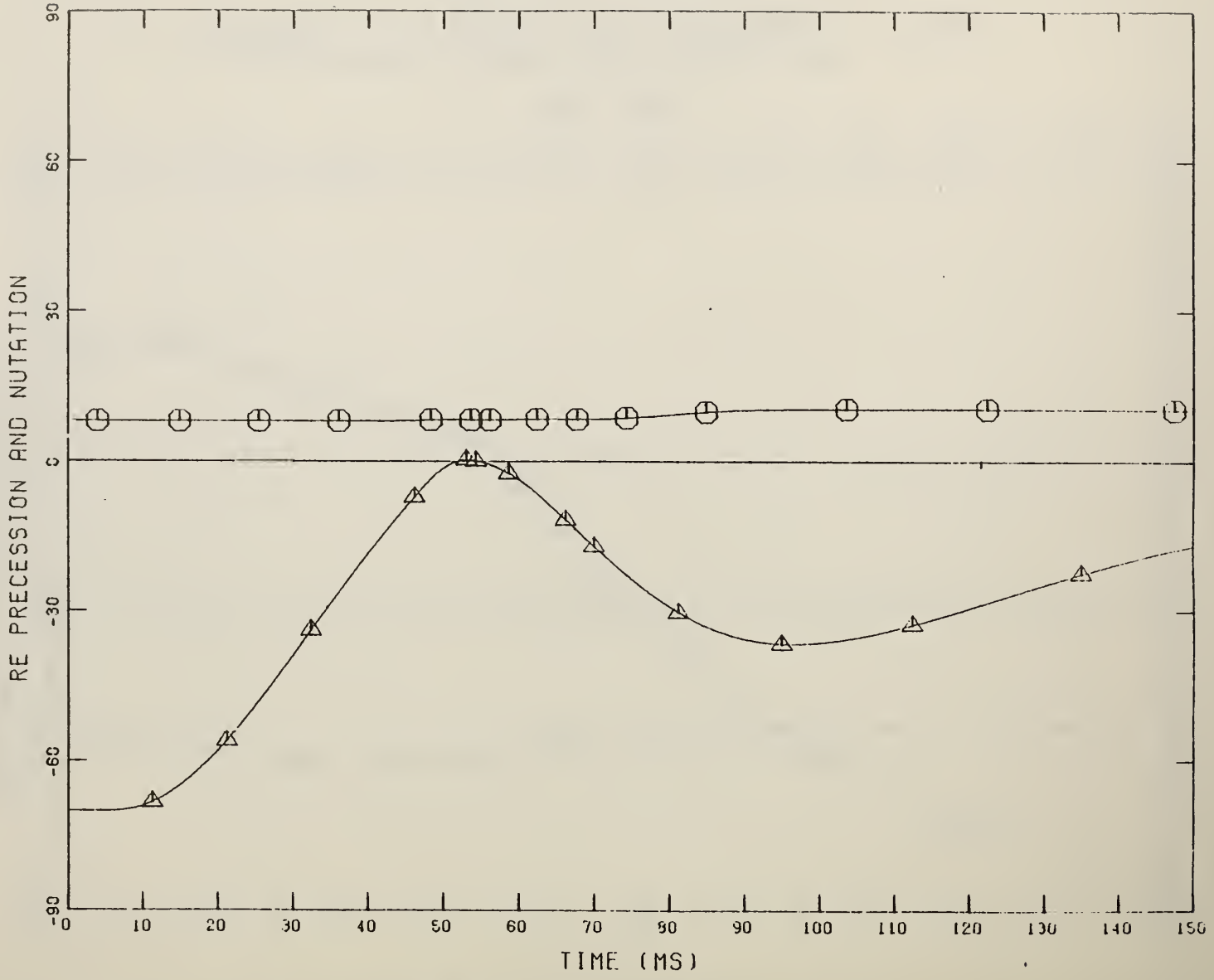

(f) RE PRECESSION AND NUTATION VS. TIME
X = UNLOCKED, Z,Y = LOCKED, P,N = UNLOCKED, S = LOCKED

Figure A-3 (Cont'd.)

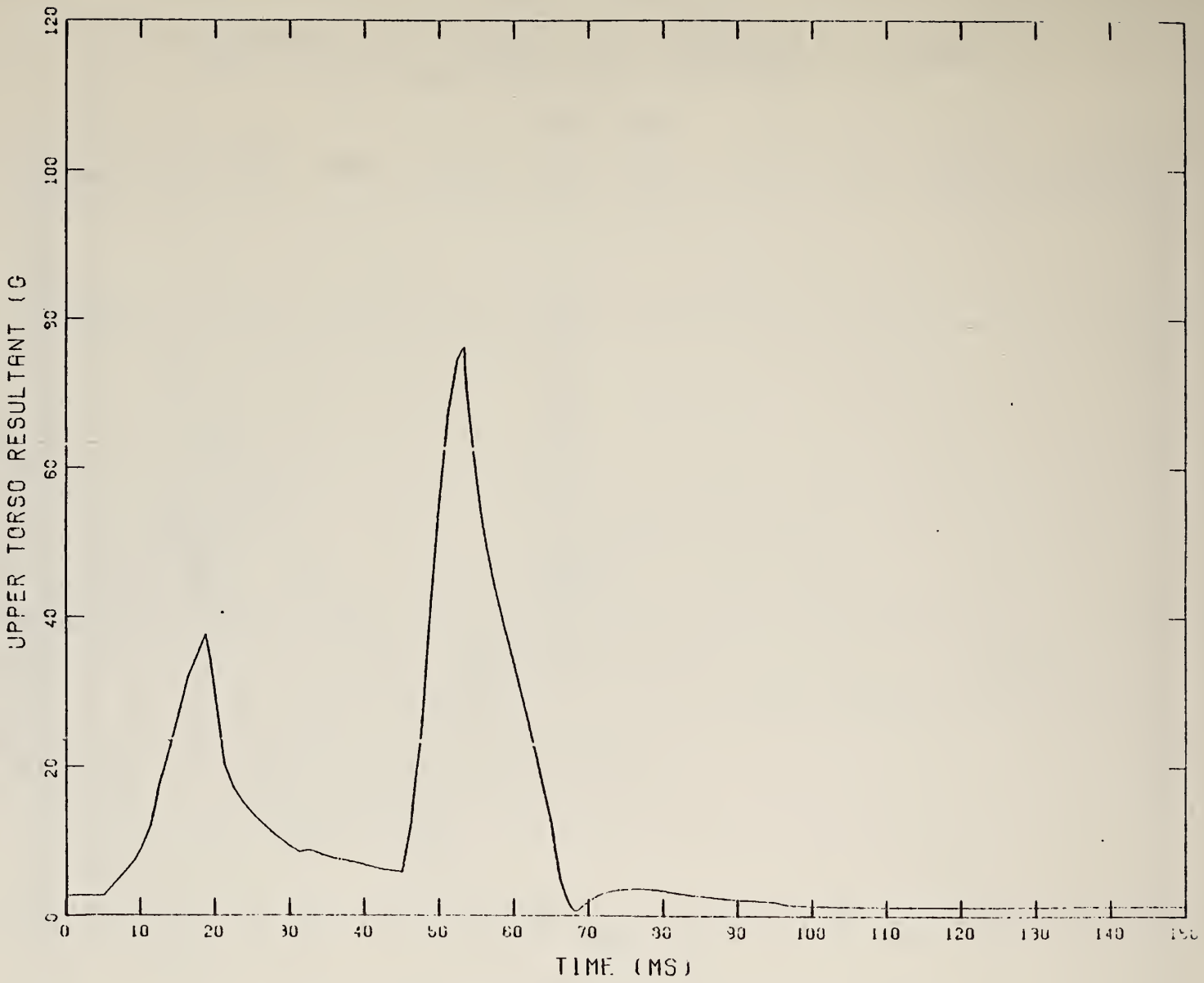

(g) UPPER TORSO RESULTANT ACCELERATION VS. TIME
X = UNLOCKED, Z,Y = LOCKED, P,N = UNLOCKED, S = LOCKED

Figure A-3 (Cont'd.)

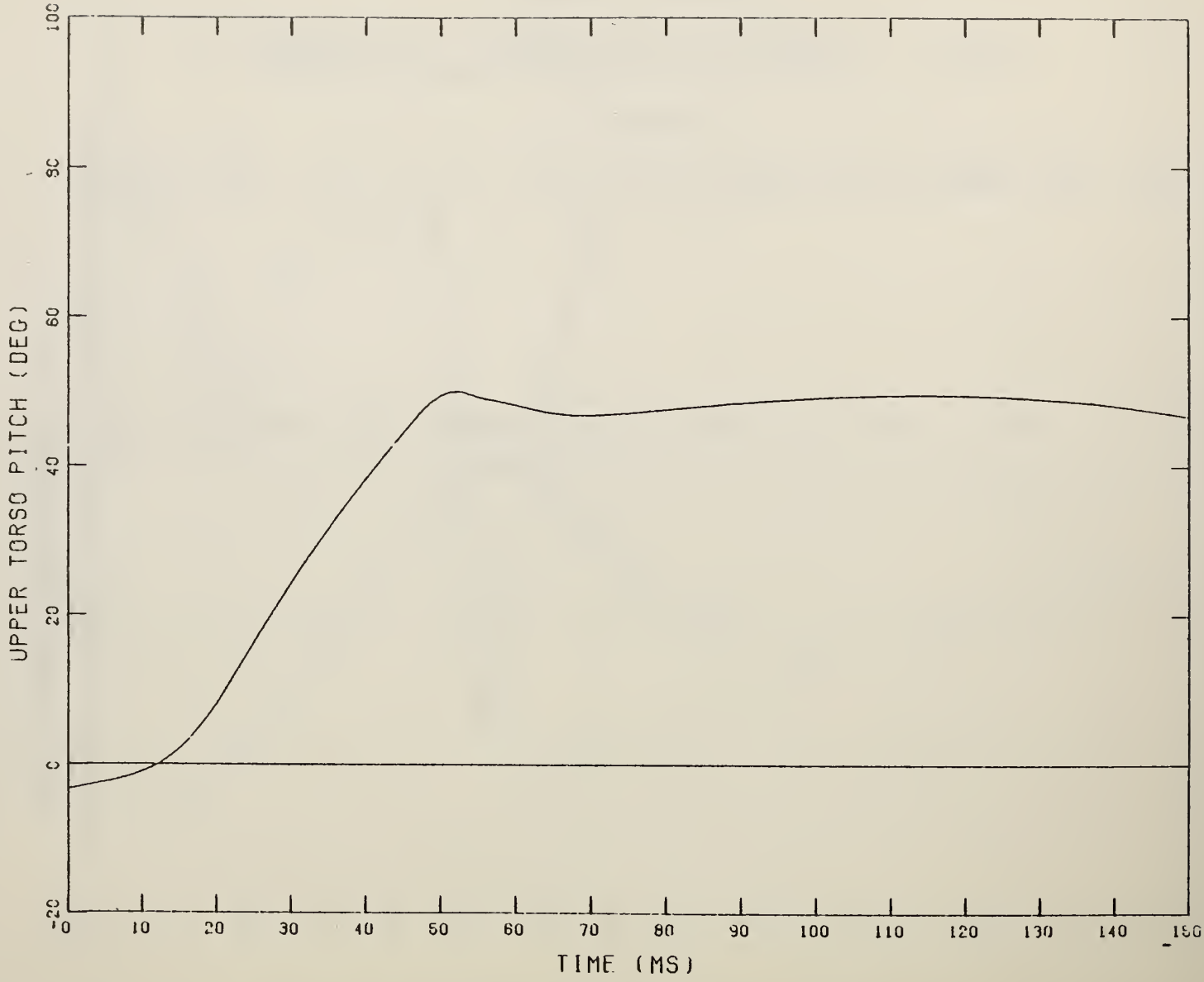

(h) UPPER TORSO PITCH VS. TIME
X = UNLOCKED, Z,Y = LOCKED, P,N = UNLOCKED, S = LOCKED

Figure A-3 (Cont'd.)

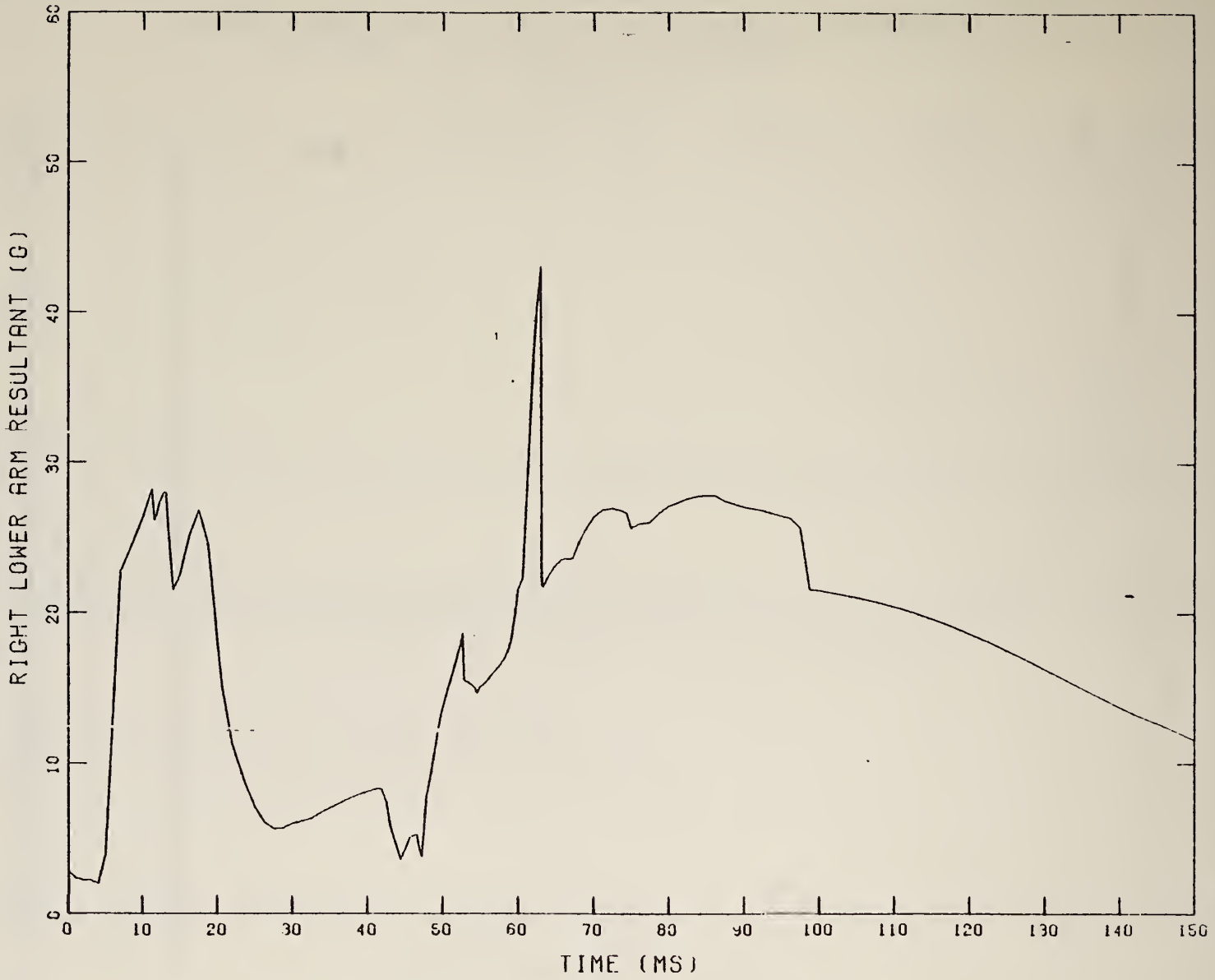

(a) RLA RESULTANT ACCELERATION VS.TIME
X=LOCKED.Z=UNLOCKED.Y=LOCKED.P.N=UNLOCKED.S=LOCKED

Figure A-4 RUN NO. 4 RESPONSE MEASURE PLOTS

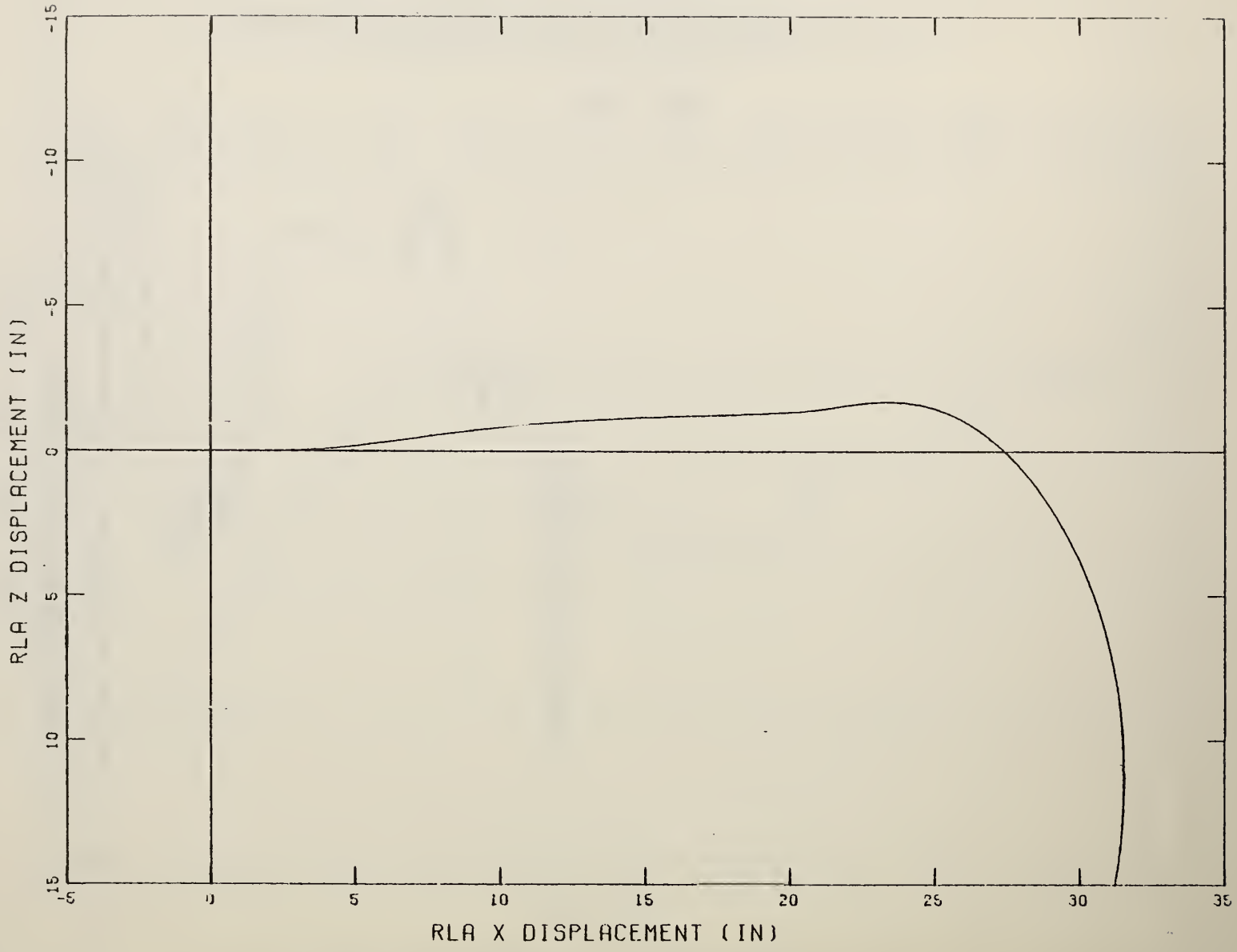

(b) RLA Z VS. RLA X DISPLACEMENT
X=LOCKED, Z=UNLOCKED, Y=LOCKED, P, N=UNLOCKED, S=LOCKED

Figure A-4 (Cont'd.)

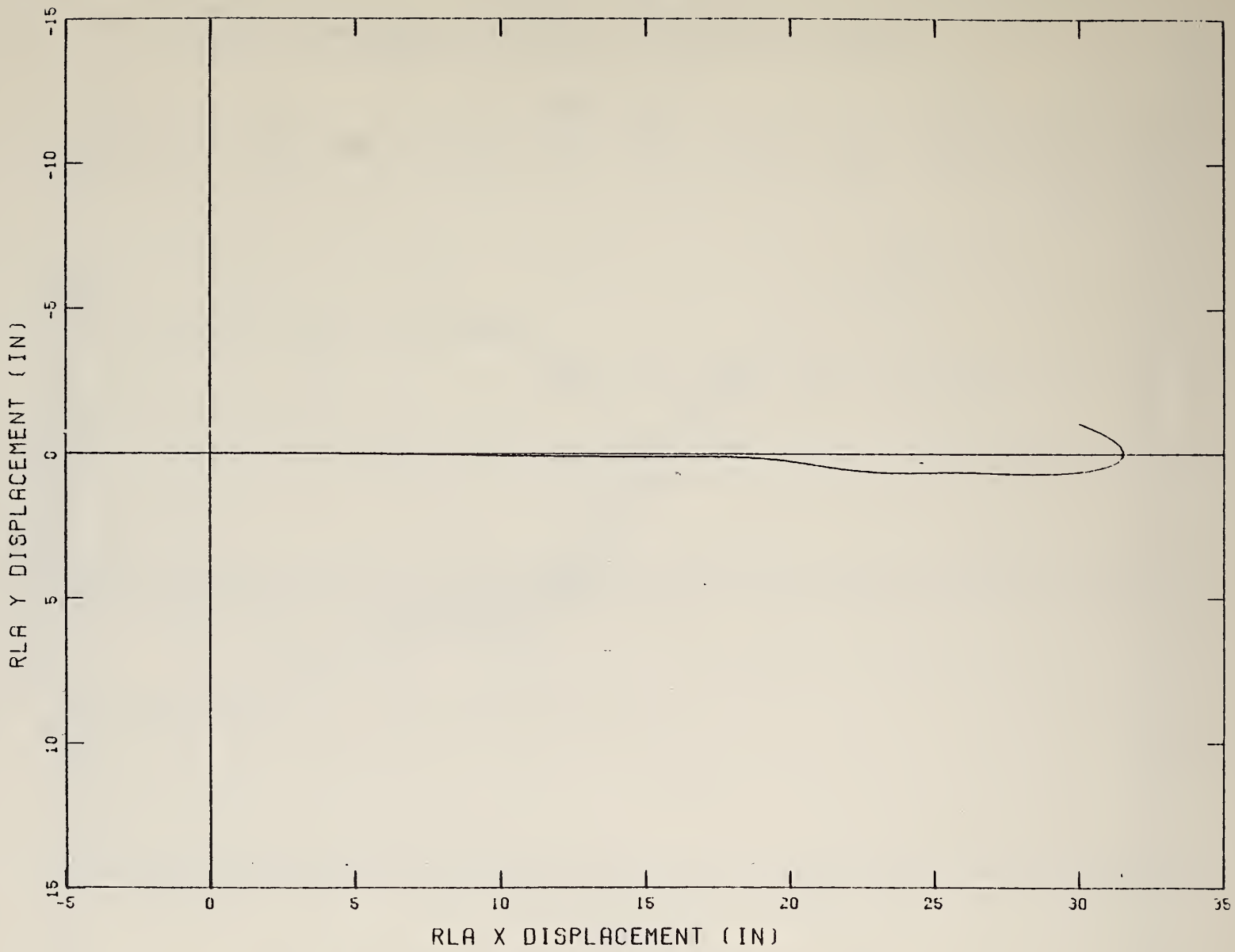

(c) RLA Y VS. RLA X DISPLACEMENT
X=LOCKED, Z=UNLOCKED, Y=LOCKED, P, N=UNLOCKED, S=LOCKED

Figure A-4 (Cont'd.)

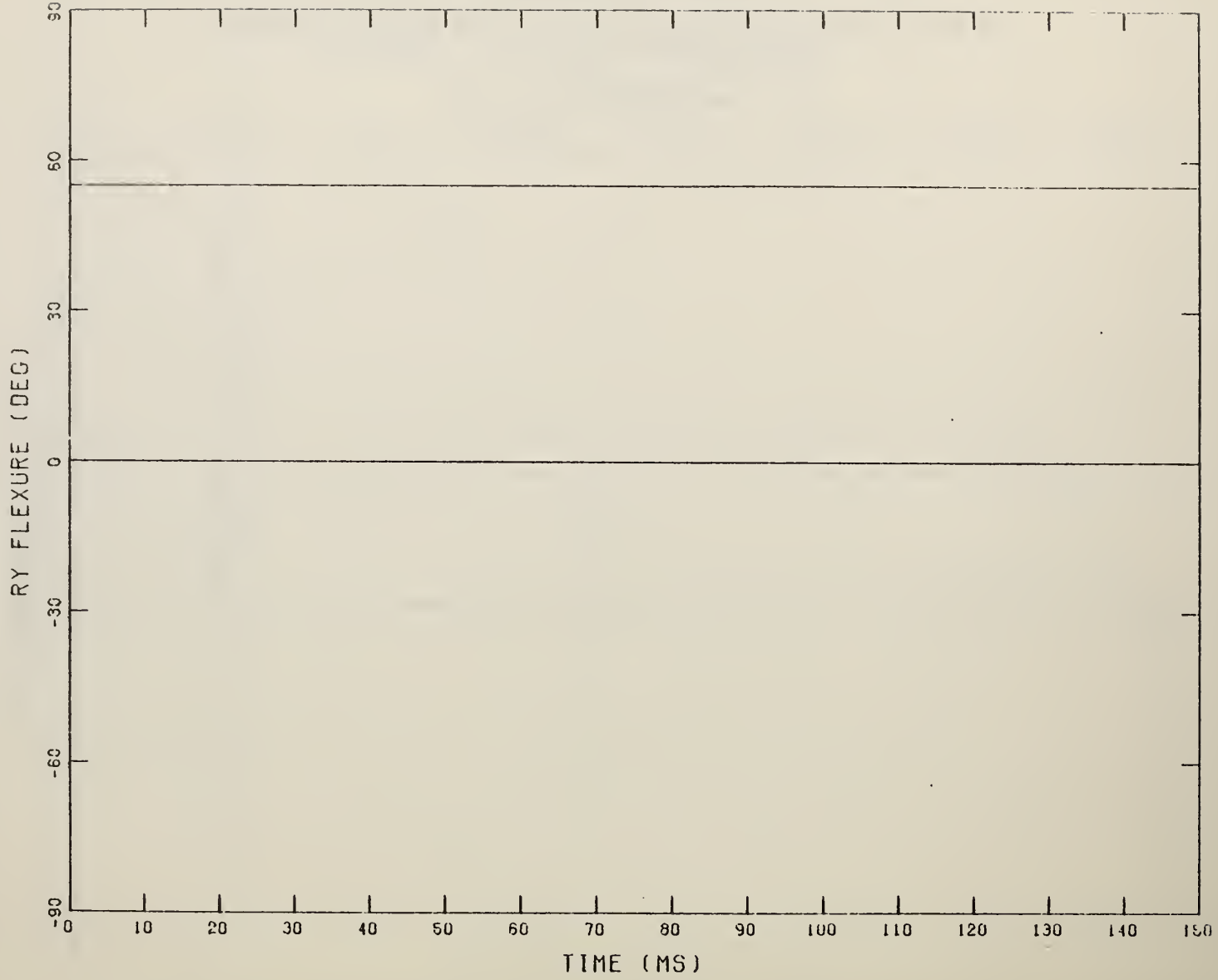

(d) RY FLEXURE VS. TIME
X=LOCKED, Z=UNLOCKED, Y=LOCKED, P, N=UNLOCKED, S=LOCKED

Figure A-4 (Cont'd.)

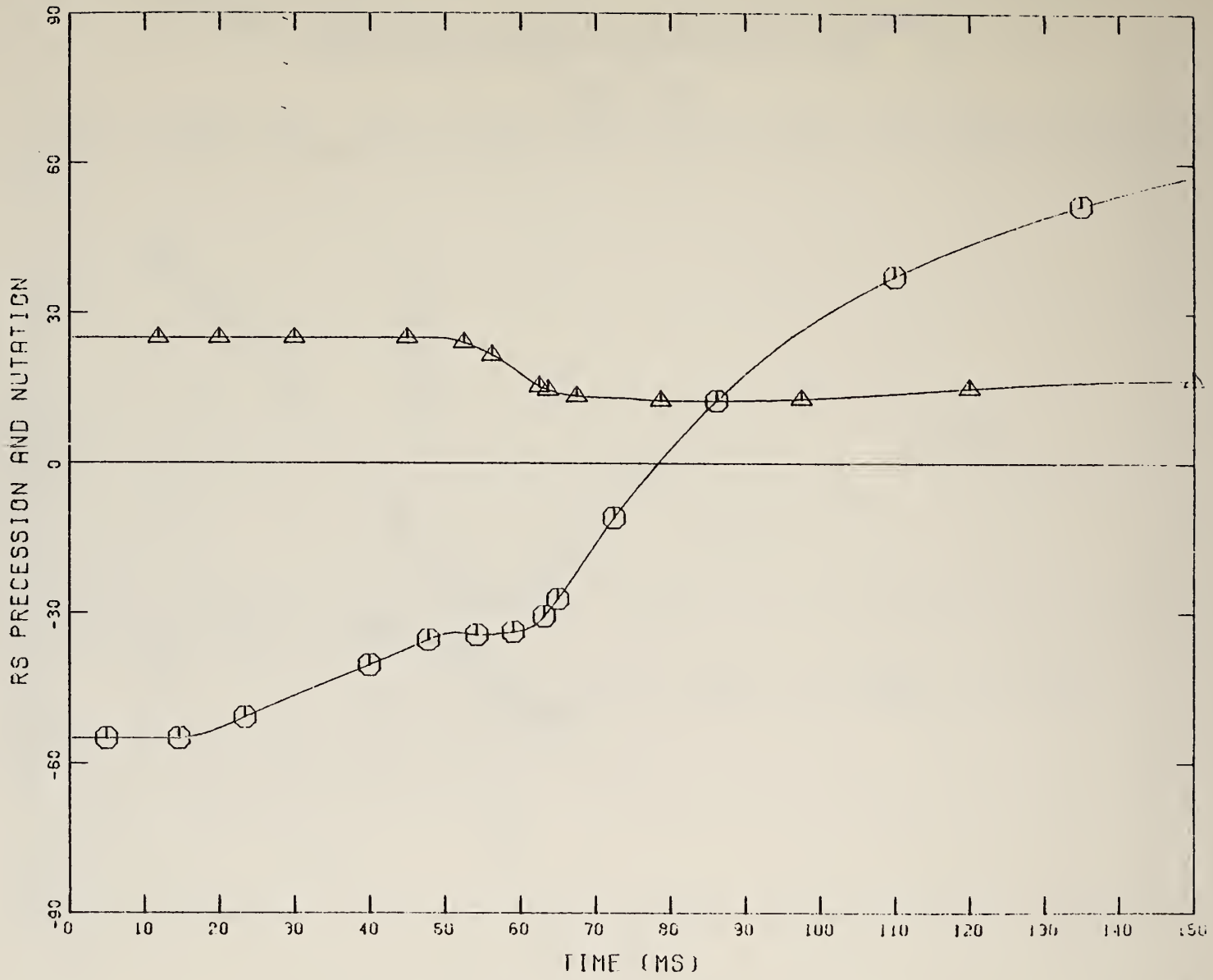

(e) RS PRECESSION AND NUTATION VS. TIME
X=LOCKED.Z=UNLOCKED.Y=LOCKED.P.N=UNLOCKED.S=LOCKED

Figure A-4 (Cont'd.)

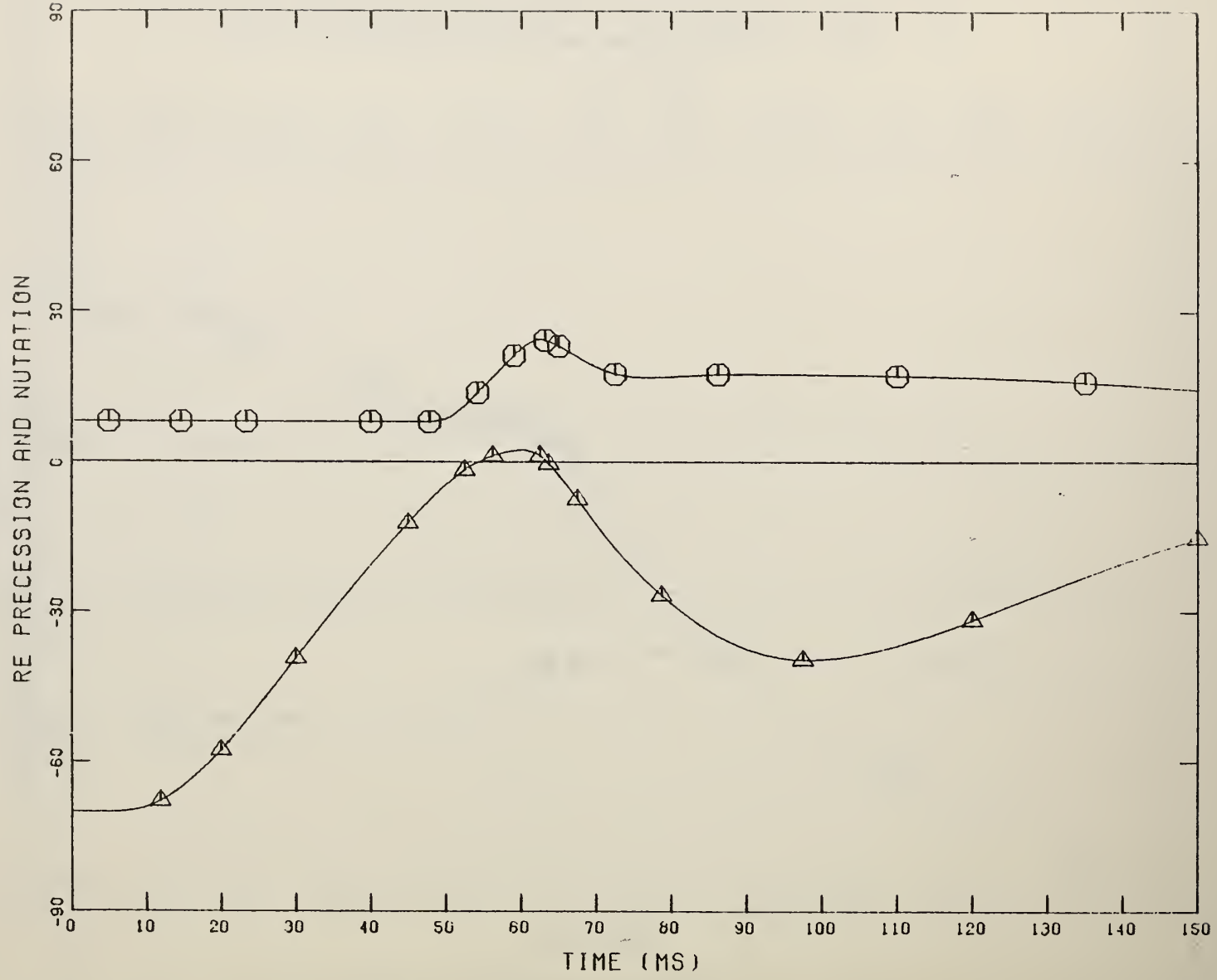

(f) RE PRECESSION AND NUTATION VS. TIME
X=LOCKED, Z=UNLOCKED, Y=LOCKED, P, N=UNLOCKED, S=LOCKED

Figure A-4 (Cont'd.)

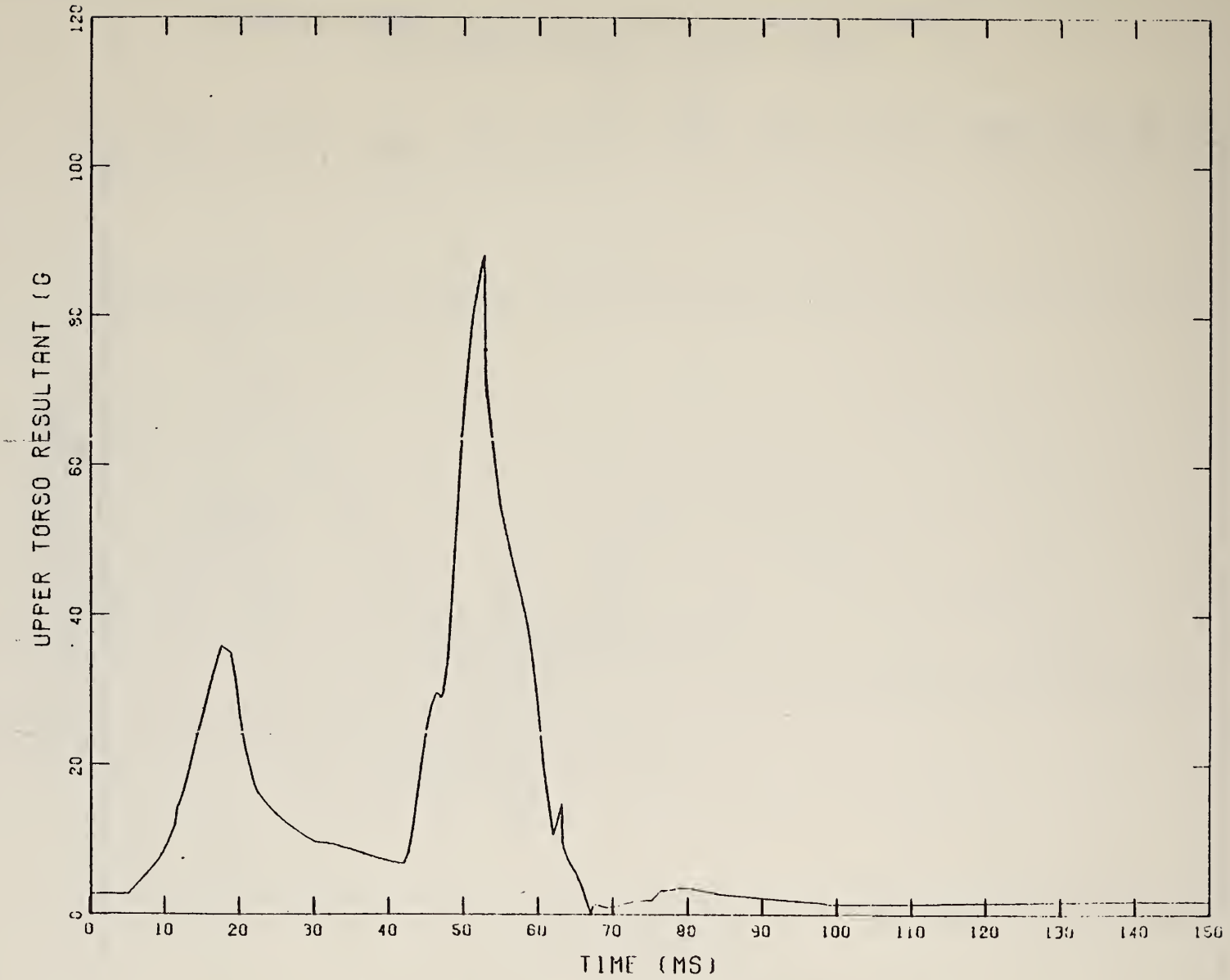

(g) UPPER TORSO RESULTANT ACCELERATION VS. TIME
X=LOCKED, Z=UNLOCKED, Y=LOCKED, P, N=UNLOCKED, S=LOCKED

Figure A-4 (Cont'd.)

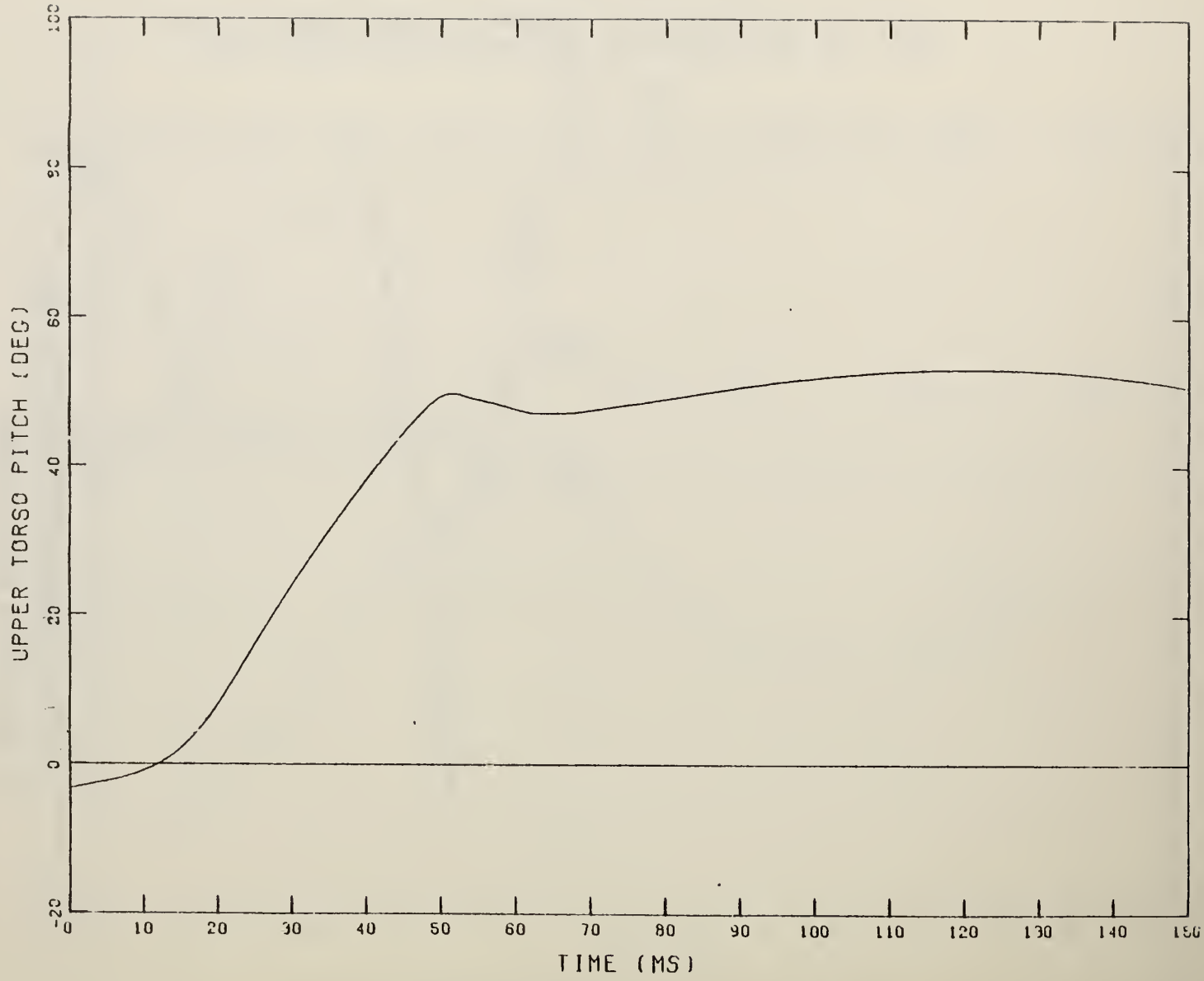

(h) UPPER TORSO PITCH VS. TIME
X=LOCKED, Z=UNLOCKED, Y=LOCKED, P, N=UNLOCKED, S=LOCKED

Figure A-4 (Cont'd.)

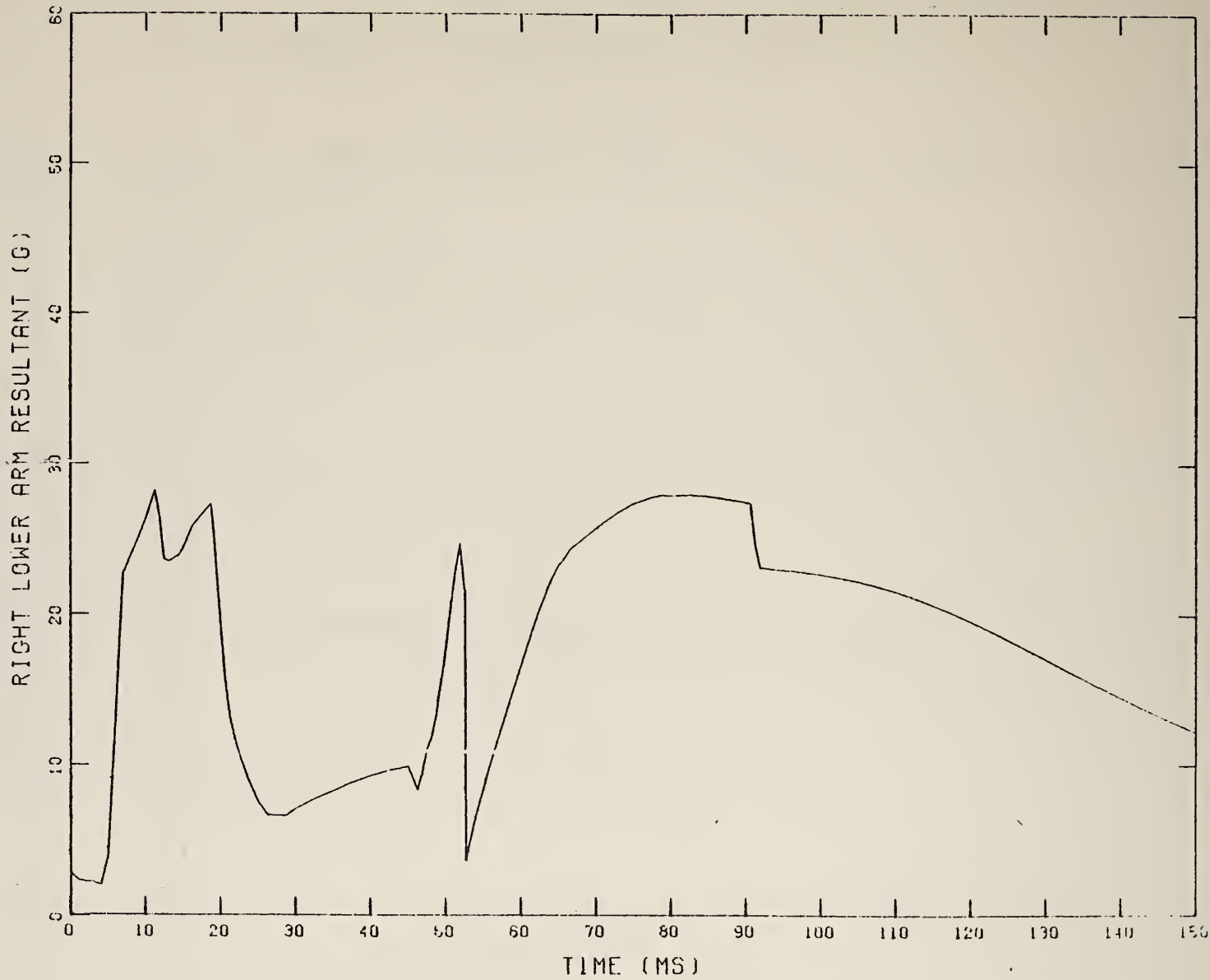

(a) RLA RESULTANT ACCELERATION VS.TIME
X,Z,Y = LOCKED, P,N = UNLOCKED, S = LOCKED

Figure A-5 RUN NO. 5 RESPONSE MEASURE PLOTS

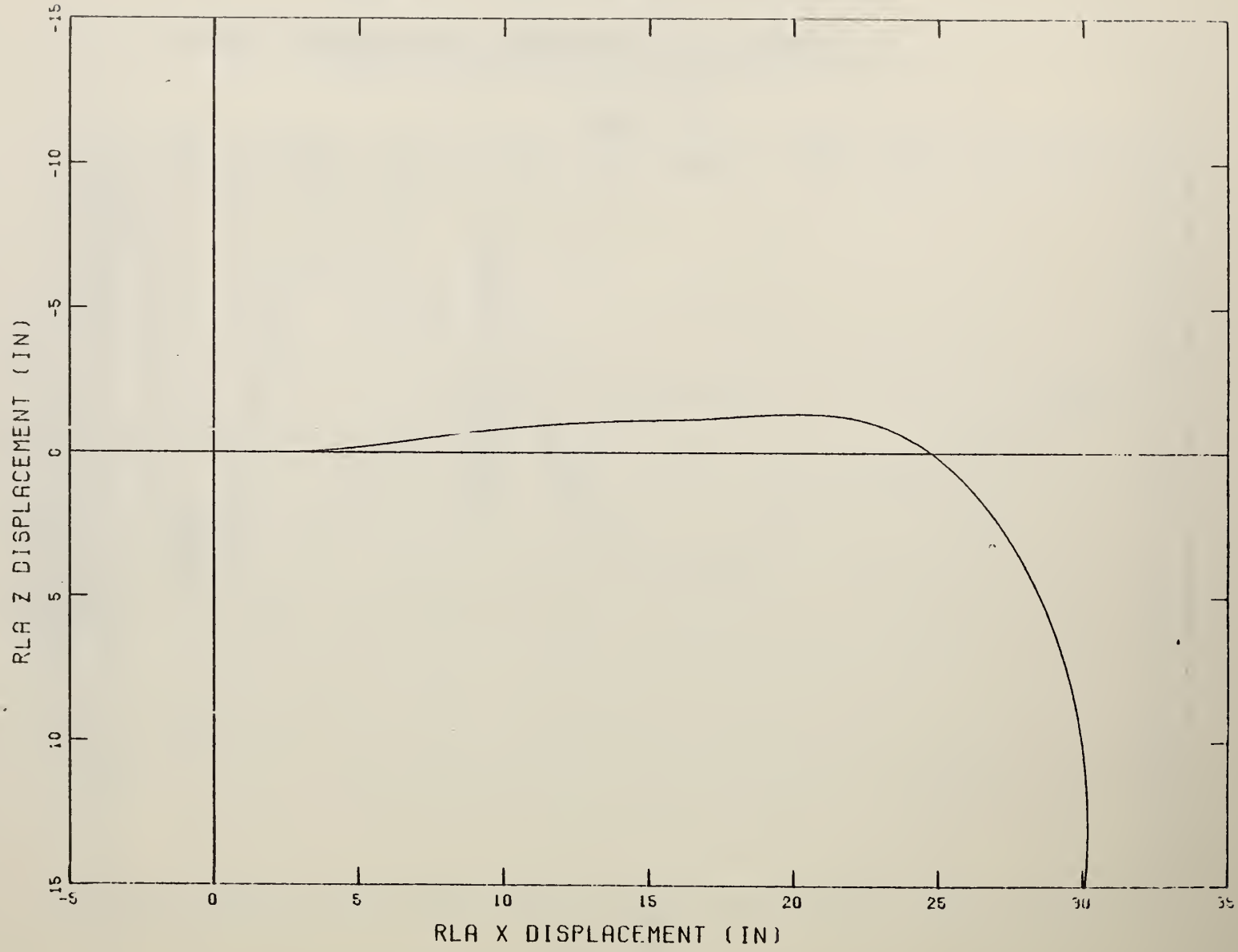

(b) RLA Z VS. RLA X DISPLACEMENT
X,Z,Y = LOCKED, P,N = UNLOCKED, S = LOCKED

Figure A-5 (Cont'd.)

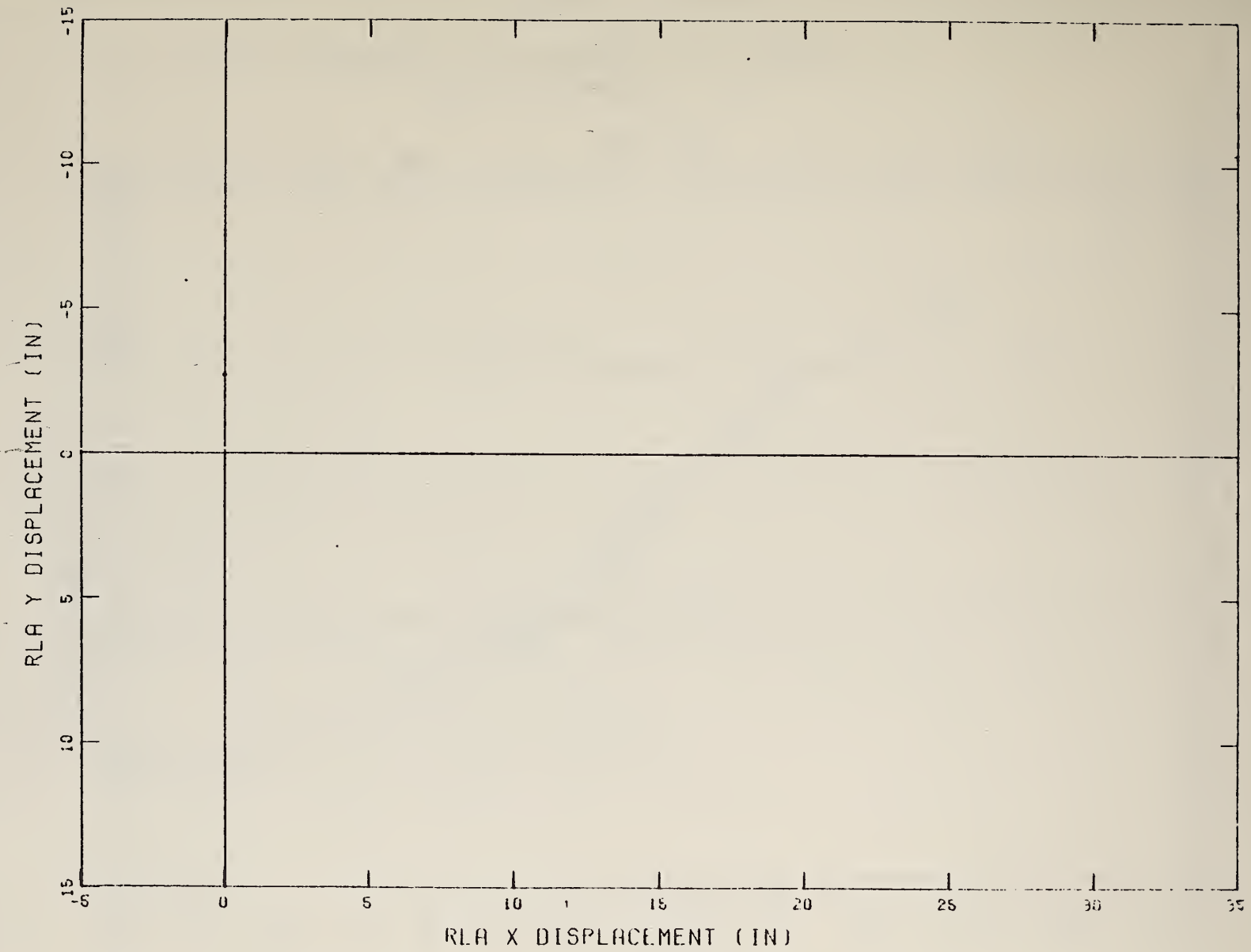

(c) RLA Y VS. RLA X DISPLACEMENT
X,Z,Y = LOCKED, P,N = UNLOCKED, S = LOCKED

Figure A-5 (Cont'd.)

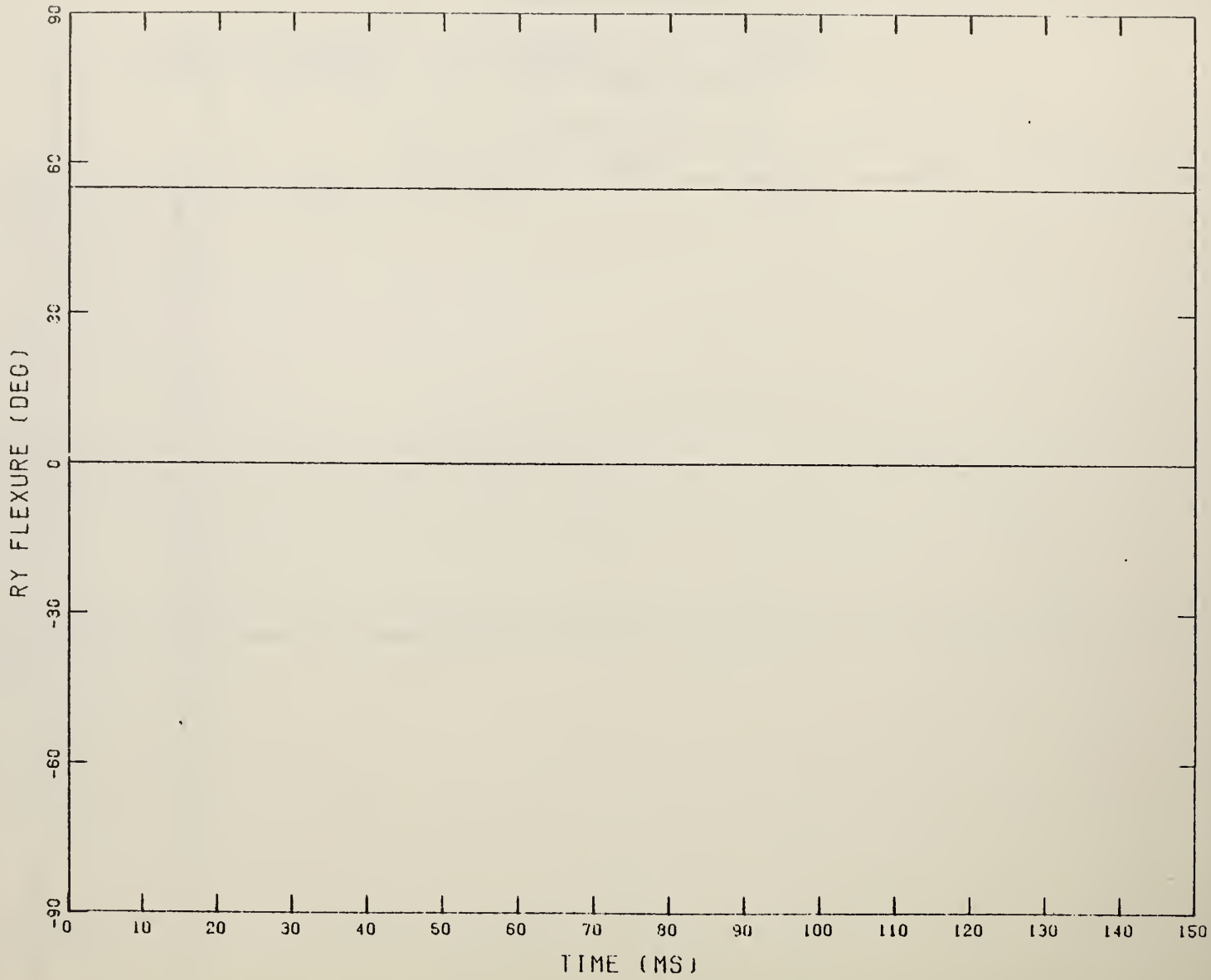

(d) RY FLEXURE VS. TIME
X.Z.Y = LOCKED. P.N = UNLOCKED. S = LOCKED

Figure A-5 (Cont'd.)

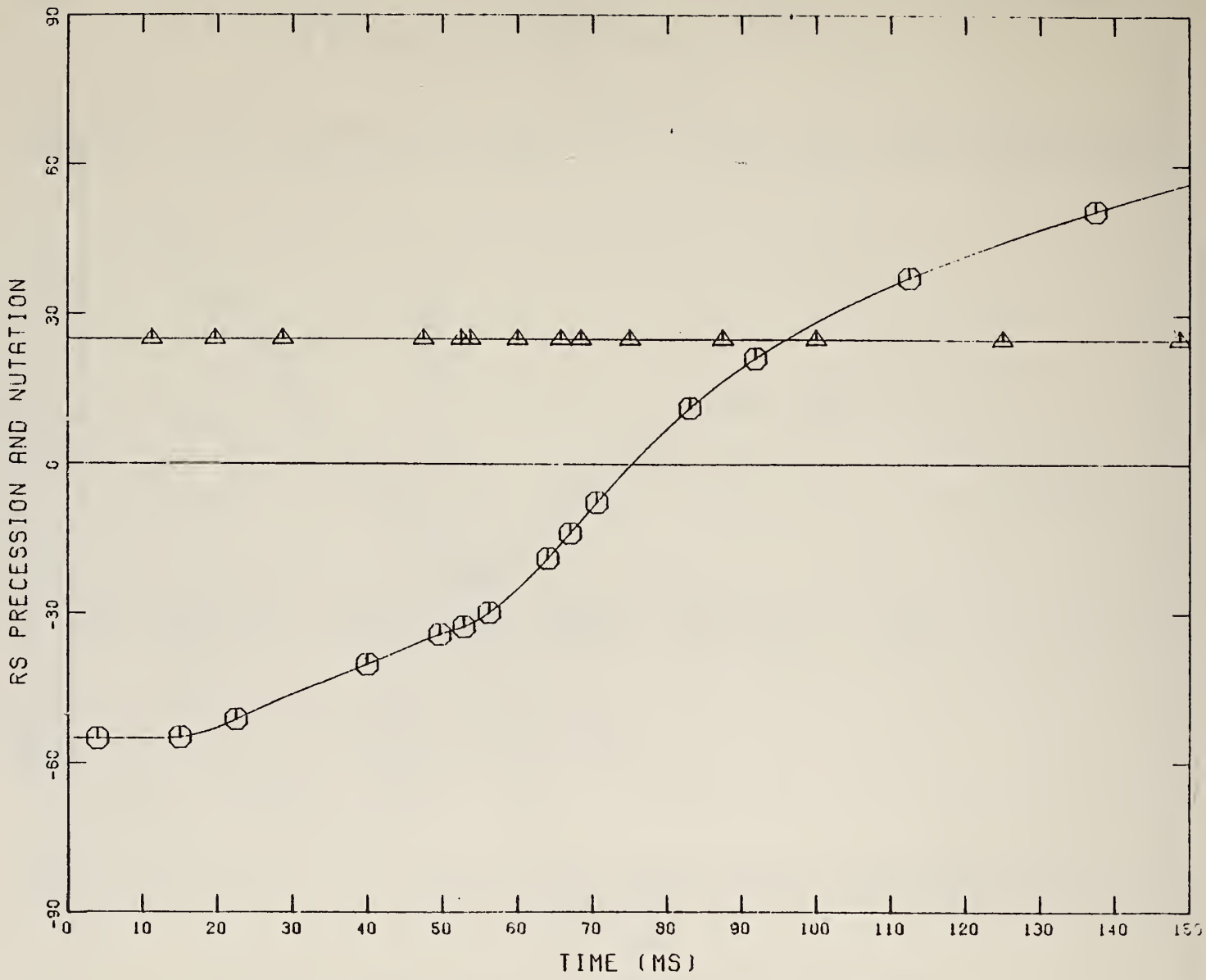

(e) RS PRECESSION AND NUTATION VS. TIME
X,Z,Y = LOCKED, P,N = UNLOCKED, S = LOCKED

Figure A-5 (Cont'd.)

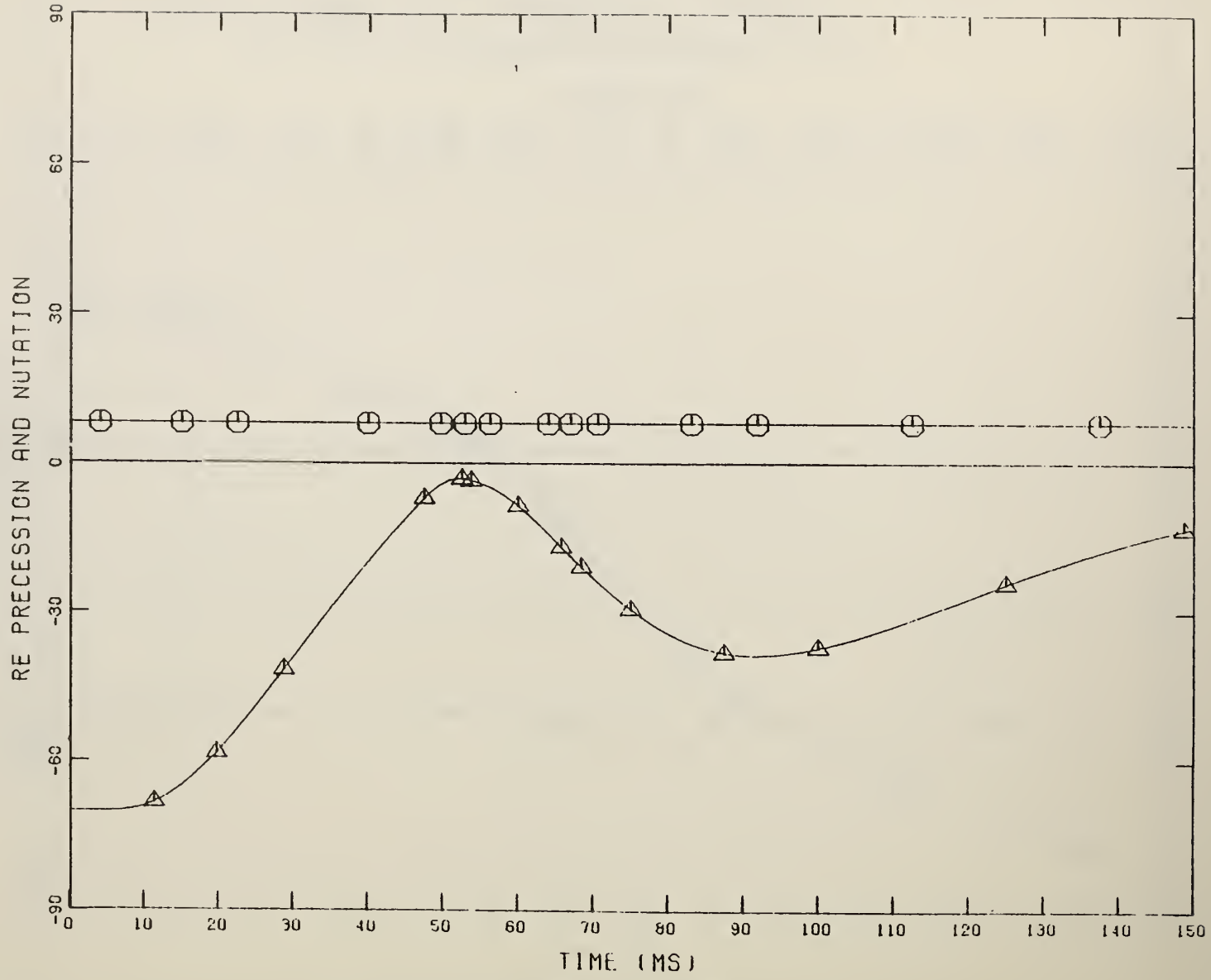

(f) RE PRECESSION AND NUTATION VS. TIME
X.Z.Y = LOCKED. P.N = UNLOCKED. S = LOCKED

Figure A-5 (Cont'd.)

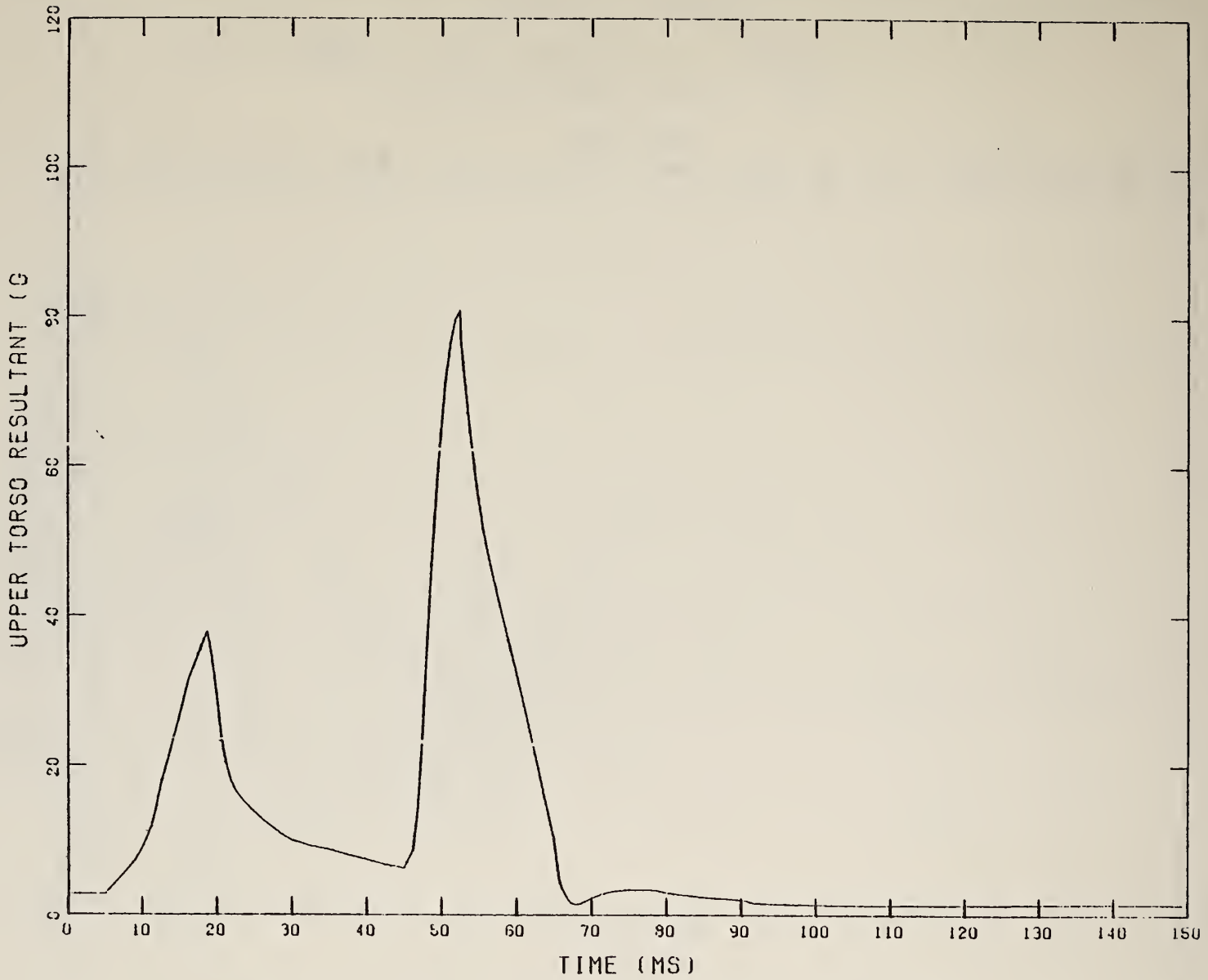

(g) UPPER TORSO RESULTANT ACCELERATION VS. TIME
X,Z,Y = LOCKED, P,N = UNLOCKED, S = LOCKED

Figure A-5 (Cont'd.)

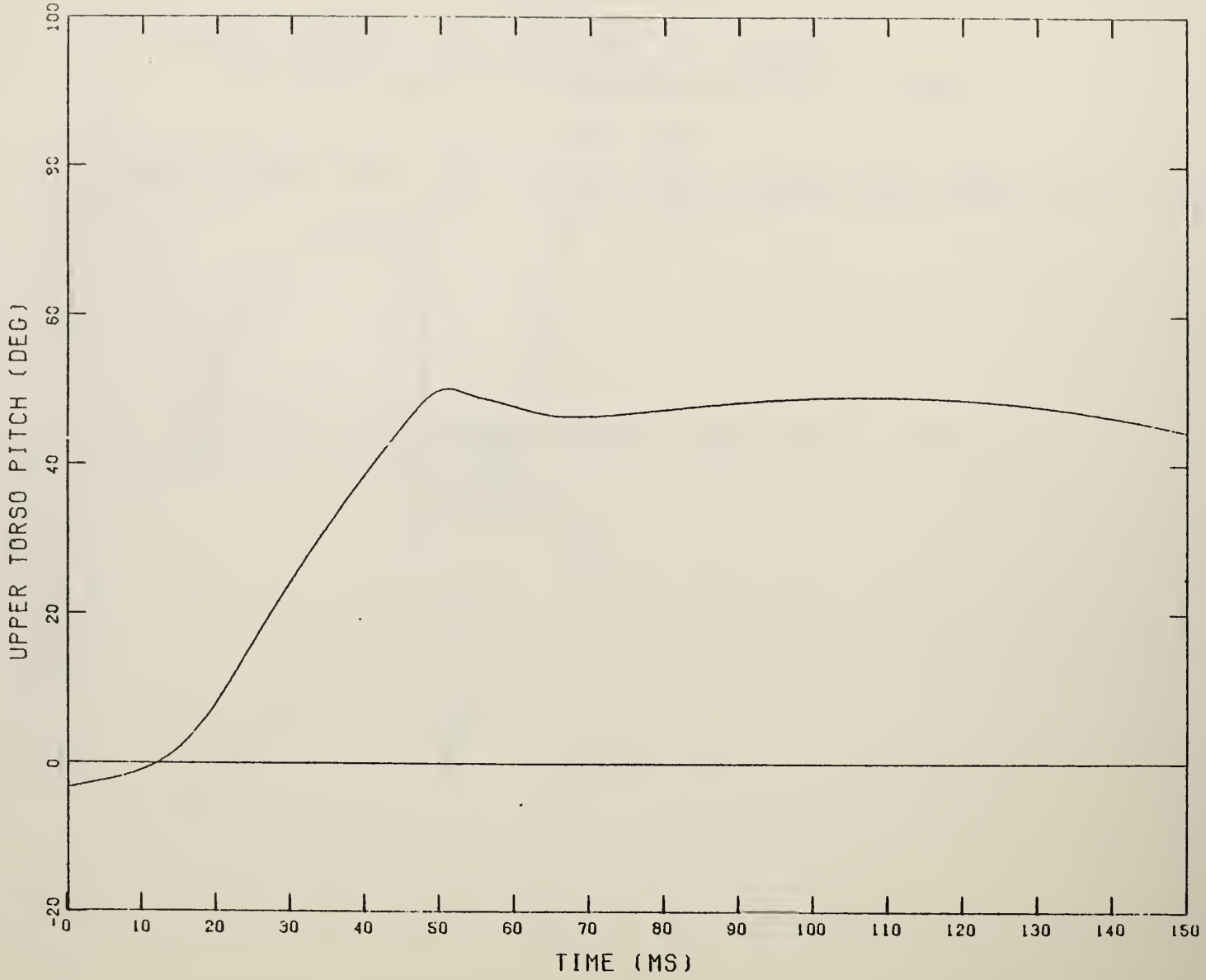

(h) UPPER TORSO PITCH VS. TIME
X.Z.Y = LOCKED. P.N = UNLOCKED. S = LOCKED

Figure A-5 (Cont'd.)

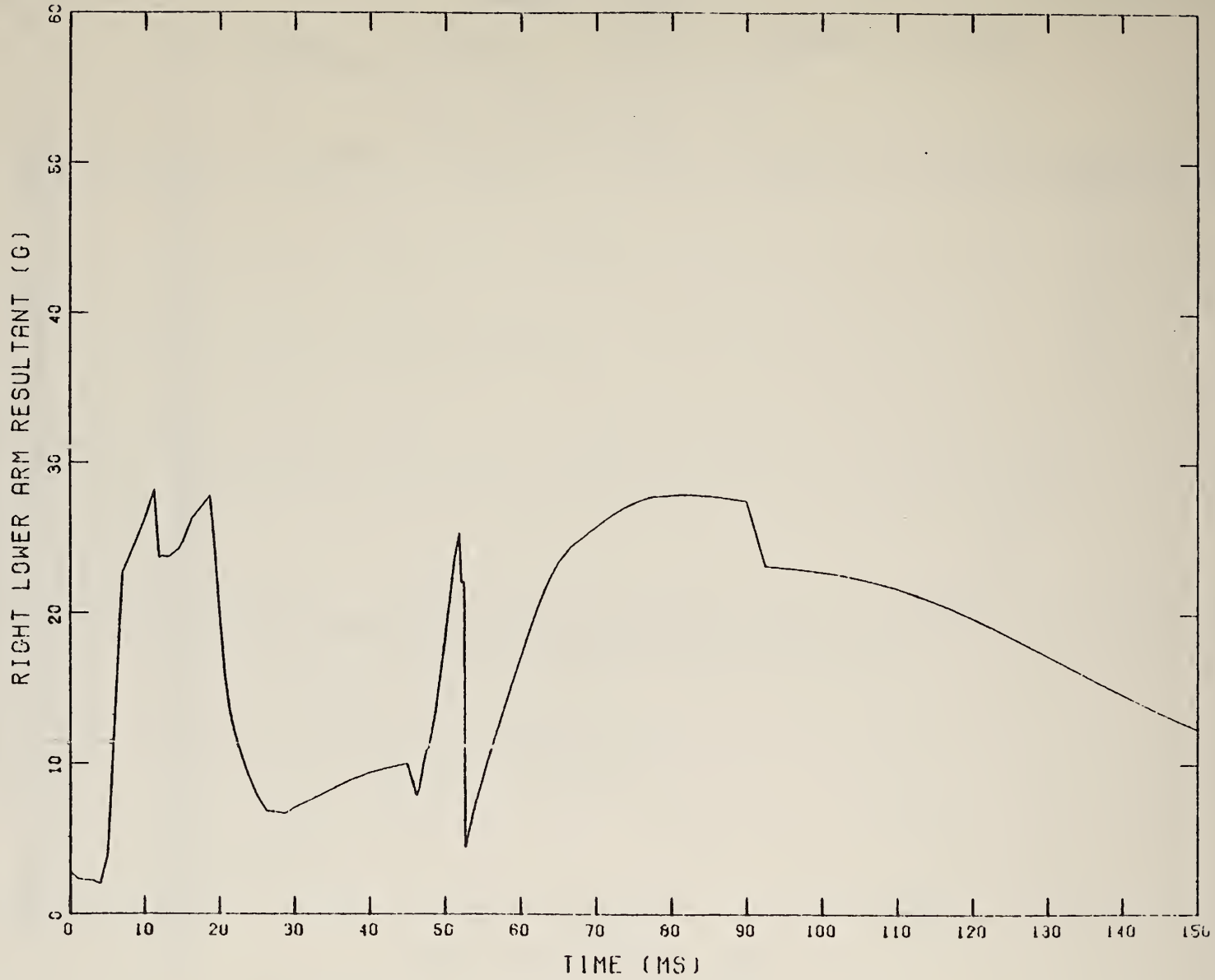

(a) RLA RESULTANT ACCELERATION VS.TIME
X,Z = LOCK, Y = UNLOCK, P = LOCK, N = UNLOCK, S = LOCK

Figure A-6 RUN NO. 6 RESPONSE MEASURE PLOTS

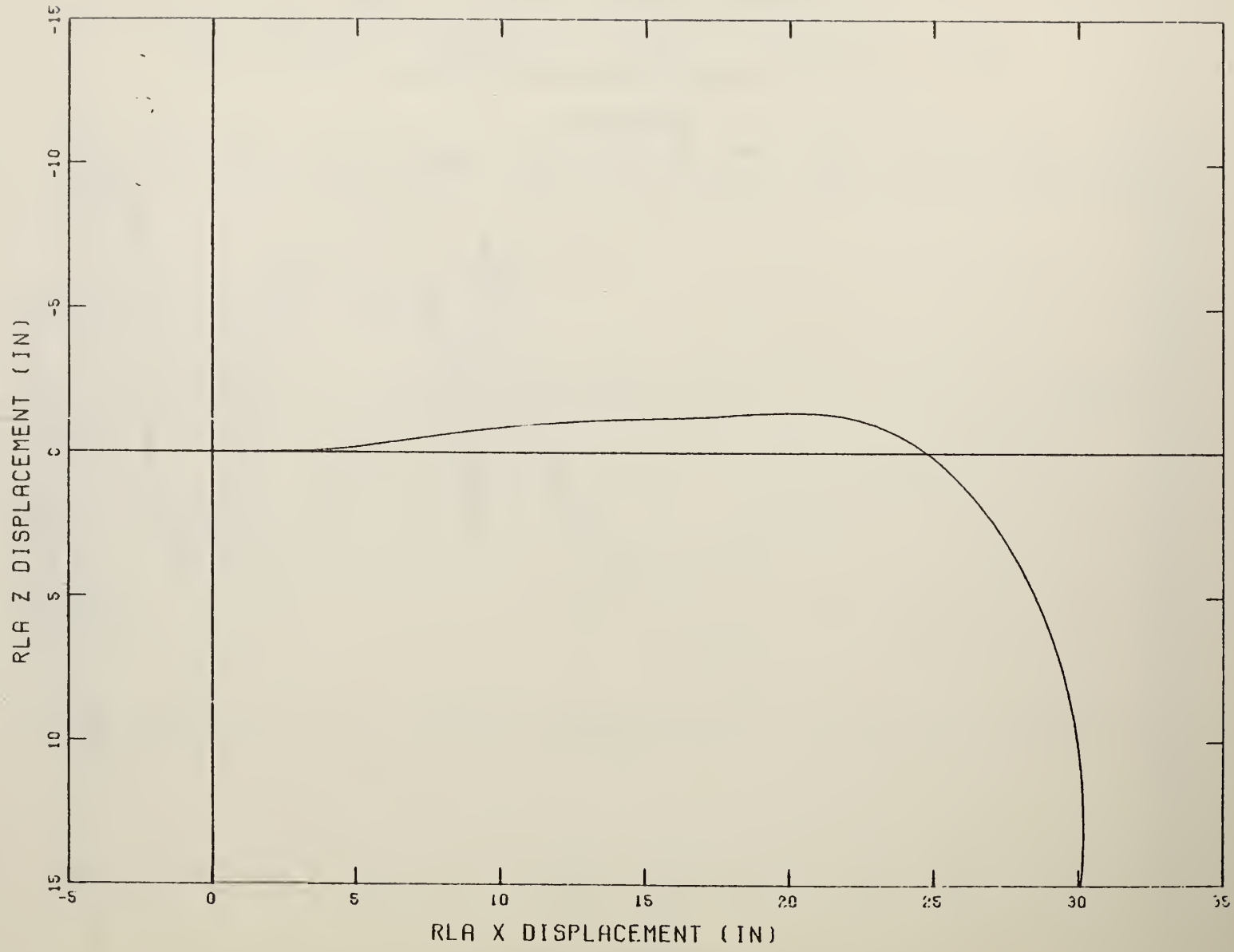

(b) RLA Z VS. RLA X DISPLACEMENT

X,Z = LOCK, Y = UNLOCK, P = LOCK, N = UNLOCK, S = LOCK

Figure A-6 (Cont'd.)

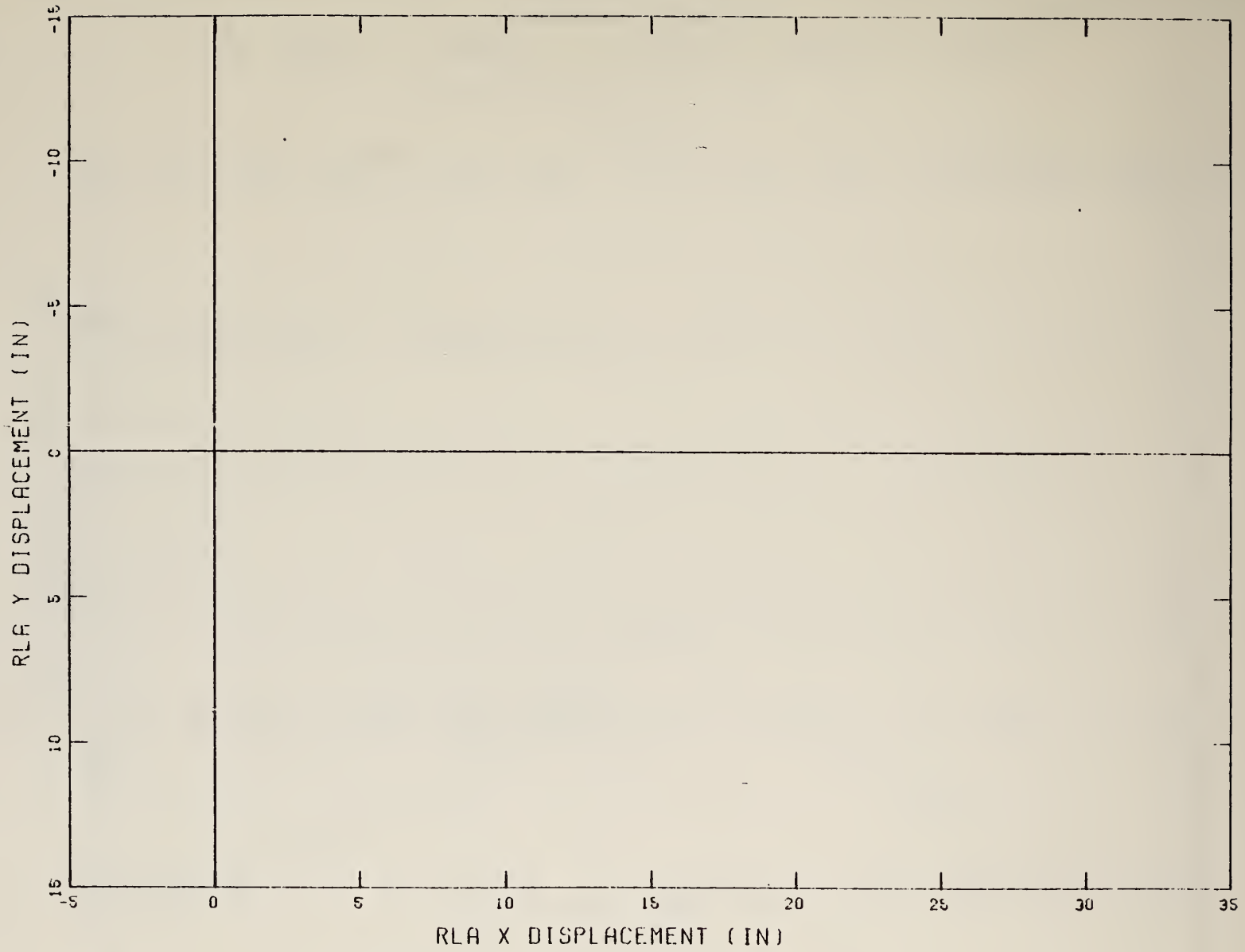

(c) RLA Y VS. RLA X DISPLACEMENT
X,Z = LOCK, Y = UNLOCK, P = LOCK, N = UNLOCK, S = LOCK

Figure A-6 (Cont'd.)

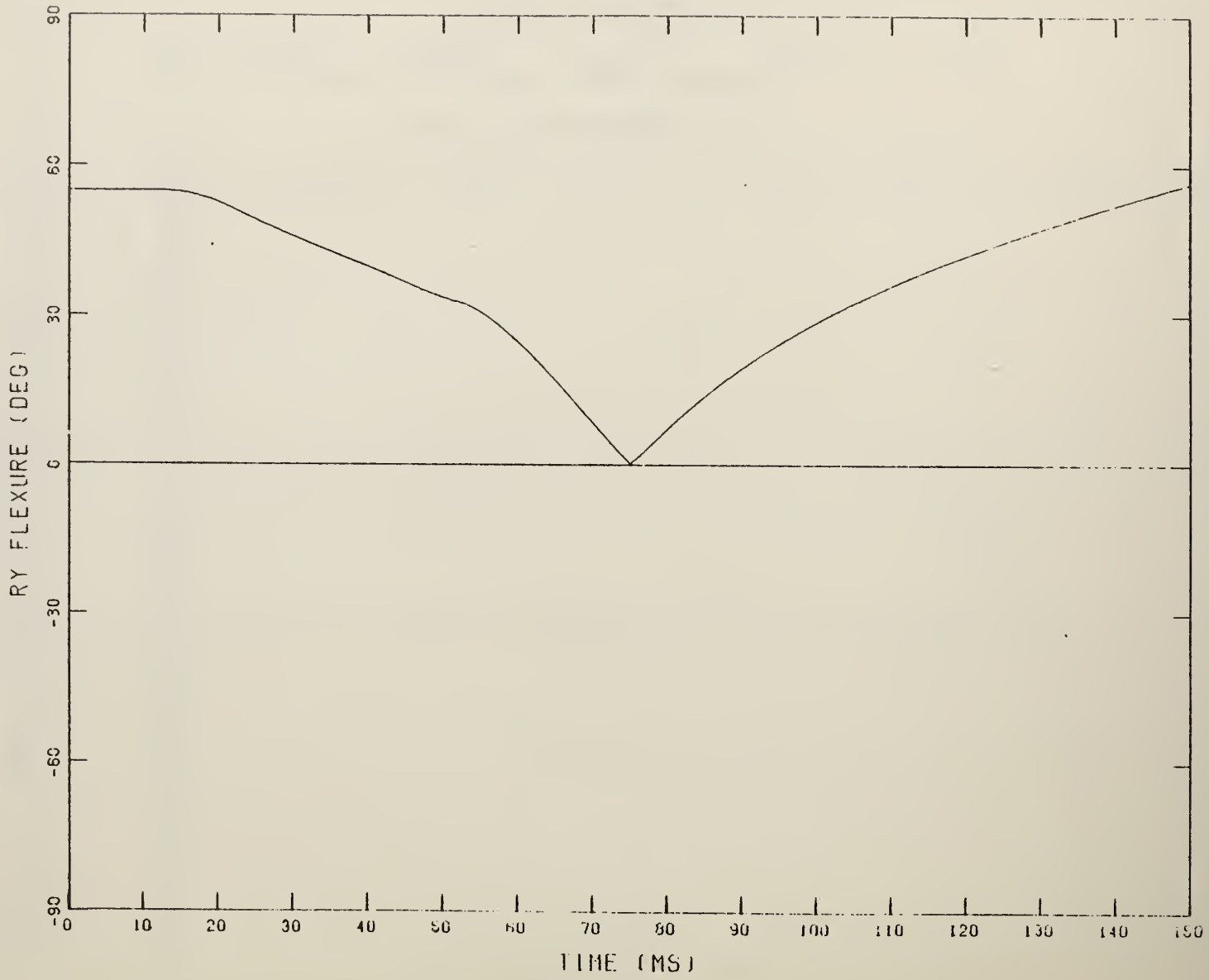

(d) RY FLEXURE VS. TIME

X,Z = LOCK, Y = UNLOCK, P = LOCK, N = UNLOCK, S = LOCK

Figure A-6 (Cont'd.)

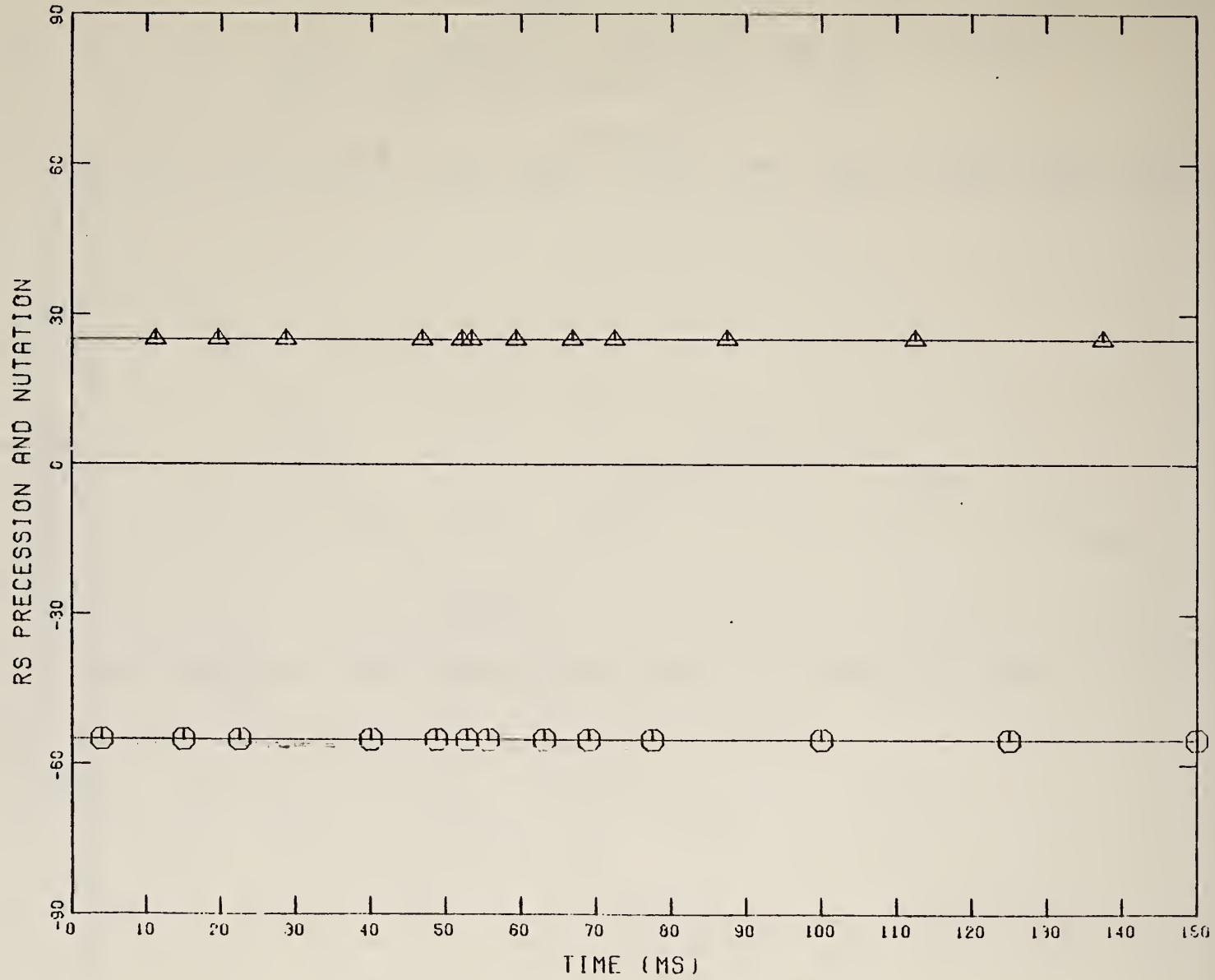

(e) RS PRECESSION AND NUTATION VS. TIME
X,Z = LOCK, Y = UNLOCK, P = LOCK, N = UNLOCK, S = LOCK

Figure A-6 (Cont'd.)

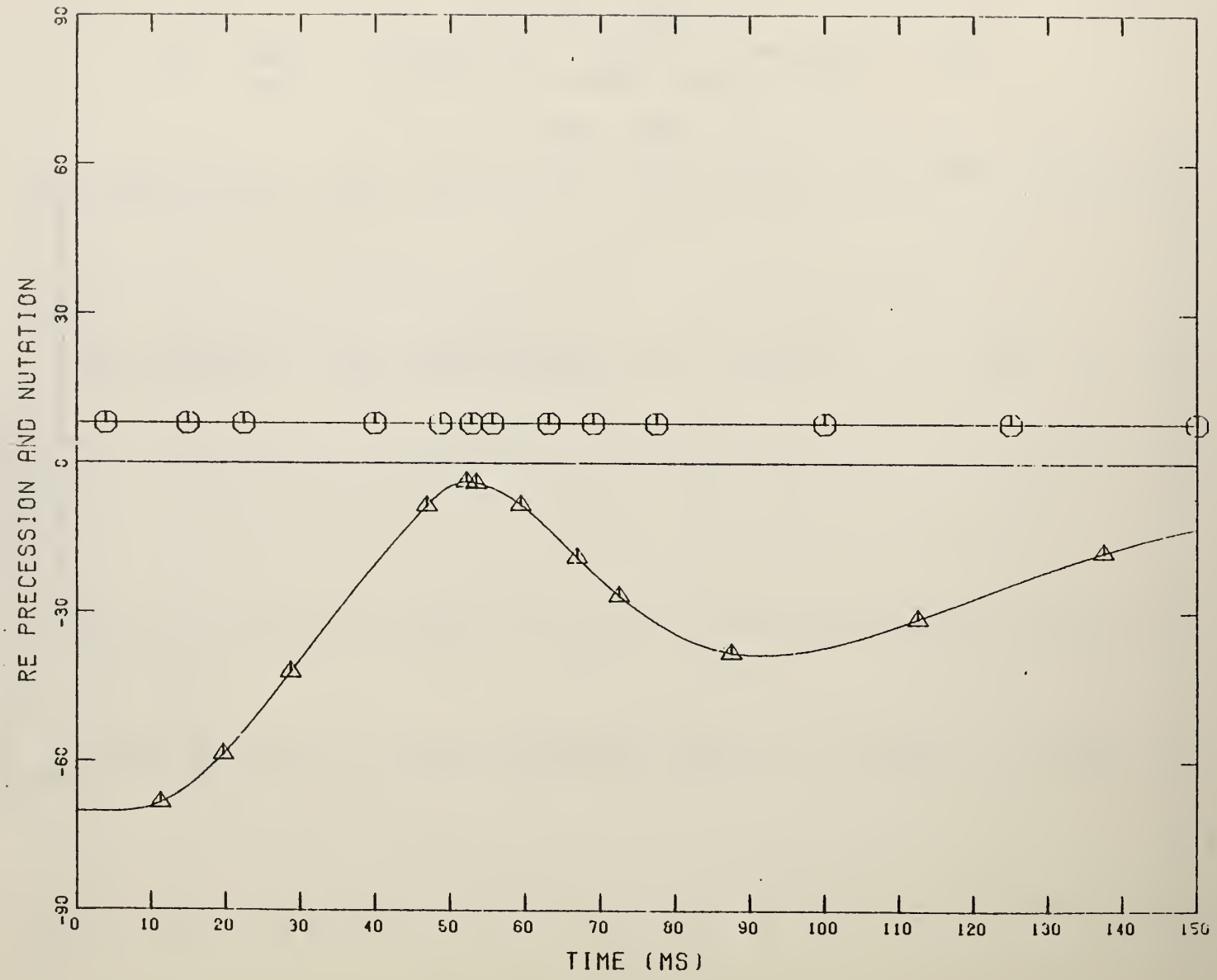

(f) RE PRECESSION AND NUTATION VS. TIME
X,Z = LOCK, Y = UNLOCK, P = LOCK, N = UNLOCK, S = LOCK

Figure A-6 (Cont'd.)

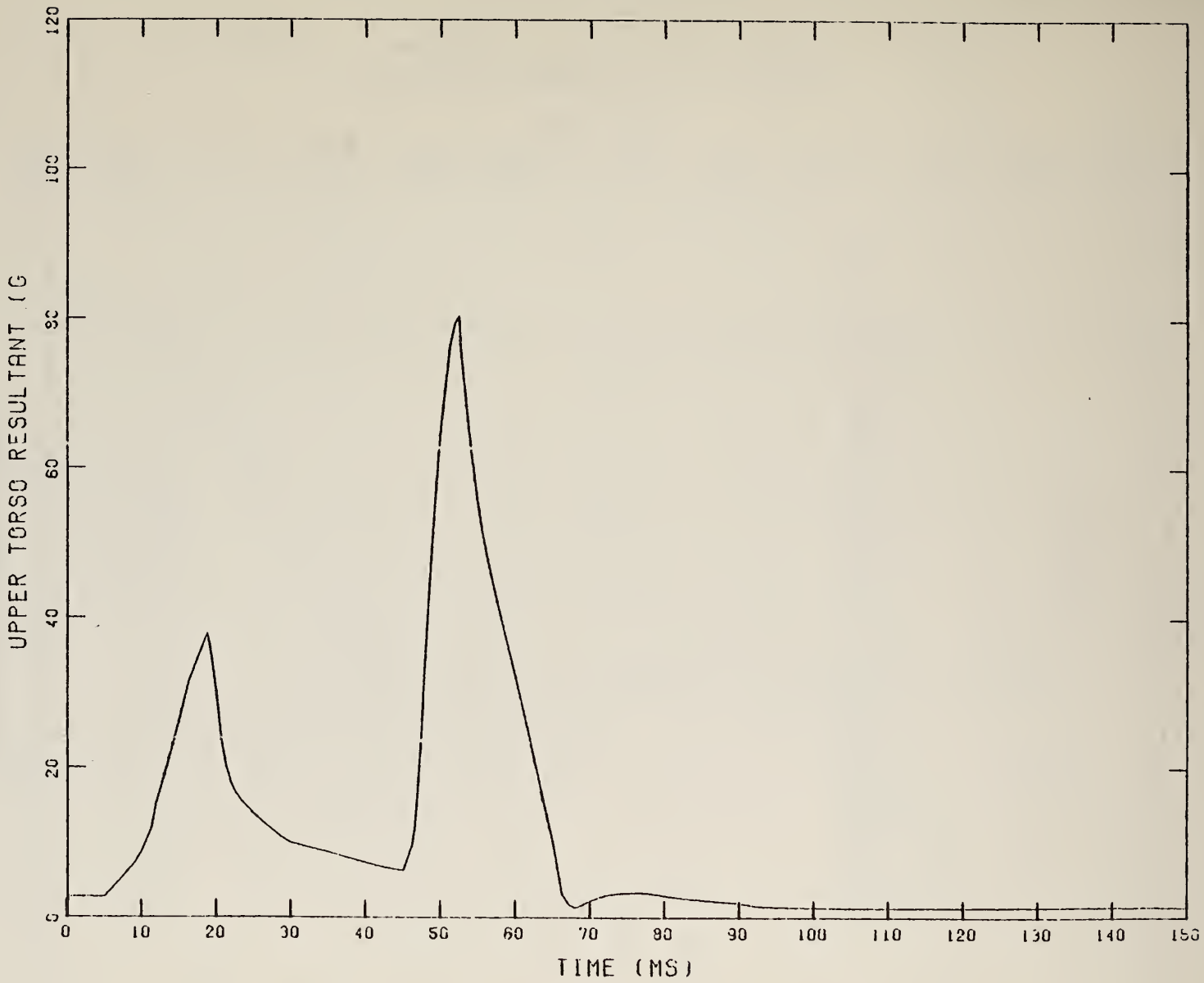

(g) UPPER TORSO RESULTANT ACCELERATION VS. TIME
X,Z = LOCK, Y = UNLOCK, P = LOCK, N = UNLOCK, S = LOCK

Figure A-6 (Cont'd.)

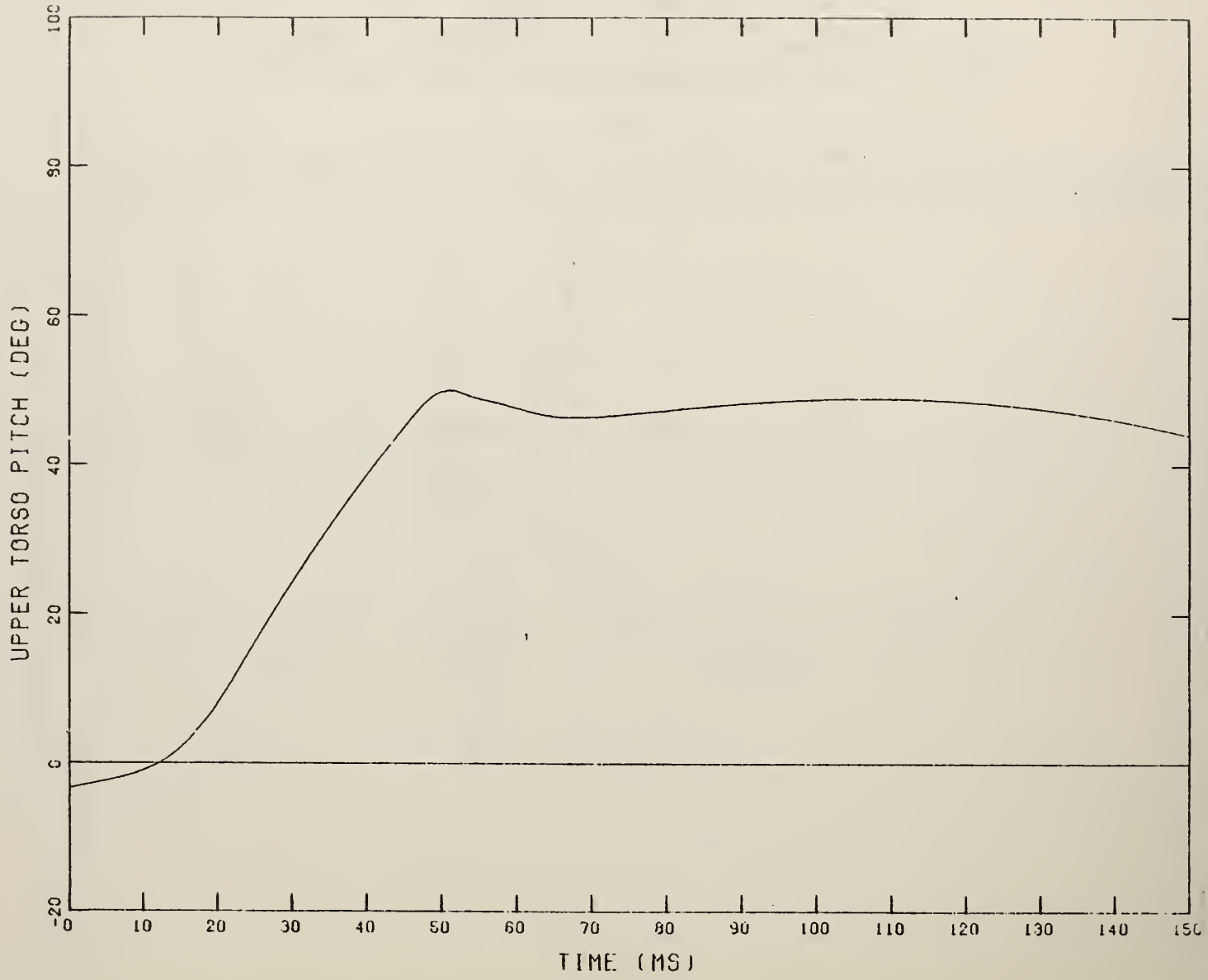

(h) UPPER TORSO PITCH VS. TIME
X,Z = LOCK, Y = UNLOCK, P = LOCK, N = UNLOCK, S = LOCK

Figure A-6 (Cont'd.)

APPENDIX B

LISTING OF THE FORTRAN PROGRAM FOR THE RESPONSE MEASURE APPROXIMATING FUNCTION GENERATOR

```
C RMAFG         LINK WITH SETZ, SETU, SIGM, SOLVE
C THIS VERSION OF THE RMAFG IS FOR TERMINAL OPERATION
C       CHANGE READ AND WRITE STATEMENTS TO CONVERT TO BATCH OPERATION
C INPUT (CARDS REFER TO LINES OF DATA SET)
CARD 1  FORMAT(20A4) INPUT DESCRIPTION
CARD 2  FORMAT(20A4) INPUT DESCRIPTION,CONTINUED
CARD 3
C       FORMAT(20I4)
C       NY,N,NDG(J),J=1,N
C       NY        NUMBER OF DEPENDENT VARIABLES
C       N         NUMBER OF INDEPENDENT VARIABLES
C         IF N=0 PROGRAM TERMINATES
C       NDG(J)    MAXIMUM DEGREE OF VARIABLE J
C                 NDG(J-1).LE.NDG(J)
C
CARD 4  FORMAT(20I4)
C       NDATA,MODE,IVAL
C       NDATA     NUMBER OF SETS OF DATA POINTS
C       MODE      0  NORMAL
C                 1  REMOVE MEAN FROM INDEPENDENT VARIABLES
C                 2  REMOVE MEAN AND DIVIDE BY STANDARD DEVIATION
C       IVAL      0  COMPUTE FIT ONLY AT POINT X( ) USED TO EVALUATE C
C                 1  READ ADDITIONAL POINTS X( ) TO COMPUTE FIT AND EVALUATE
C
CARDS 5-NDATA+2   FORMAT(10F8.0)
C      (X(J,K),J=1,N),(Y(K,L),L=1,NY)
C       X(J,K),J=1,N    VALUES OF INDEPENDENT VARIABLES AT K
C       Y(K,L),L=1,NY   VALUES OF DEPENDENT VARIABLES (FUNCTION) AT K
C
CARD NDATA+3      FORMAT(20I4)
C       IF IVAL = 0 THIS IS THE SAME AS CARD 1
C       IF IVAL < 0 OR > 0  PROGRAM READS VALUE OF NV
C       NV        NUMBER OF POINTS TO BE EVALUATED USING COMPUTED FIT
C
CARDS NDATA+4-NDATA+3+NV  FORMAT(10F8.0)
C      (X(J,M),J=1,N),(Y(M,L),L=1,NY)
C       X(J,M),J=1,N    ADDITIONAL VALUES OF INDEPENDENT VARIABLES
C       Y(M,L),L=1,NY   VALUES OF DEPENDENT VARIABLES (IF KNOWN) AT M
C                       PROGRAM WILL COMPUTE YP(M) FOR EACH L
C
C       PROGRAM STOPS
C
C******
C
C       PROGRAM COMPUTES THE BEST LEAST SQUARE FIT FOR EACH DEGREE
C       FROM 0 TO MAXIMUM AS SPECIFIED ON CARD 3
C
C******
C
C       OUTPUT
C       KM,ERR,(Z(L),C(L,I+1),L=1,KM)
C       KM        NUMBER OF TERMS(COEFFICIENTS) IN FIT
C       ERR       RMS ERROR OF FIT
C       Z(L)      SUBSCRIPT OF L'TH COEFFICIENT
C       C(L,I+1)VALUE OF COEFFICIENT Z(L)
C
```

```
C       PROGRAM PROVIDES A PRINTER PLOT OF THE HISTOGRAM OF
C       ERRORS AND THE FIRST TEN POINTS WITHIN THE SPECIFIED ERROR RANGE
C
C       PROGRAM PRINTS THE FUNCTION VALUE COMPUTED FROM THE FIT
C
        IMPLICIT REAL*8(A-H,O-Z)
        REAL*4    STAR,CNT,B,CNTM,CCS,BLANK,HY
        DIMENSION HY(20,2)
C DIMENSION PROGRAM FOR 3 INDEPENDENT VARIABLES, 7 DEPENDENT VARIABLES
C AND 90 DATA SETS
        DIMENSION Y(90,7),X(3,90),YP(90),XX(3,90),XM(3),XS(3)
        DIMENSION NDG(3),NIW(3),LIW(3)
C DIMENSION PROGRAM FOR A MAXIMUM OF 20 COEFFICIENTS
        DIMENSION U(20),Z(20),C(20,22)
C DIMENSION PROGRAM FOR A MAXIMUM OF 10 POINTS ON HISTOGRAM
        DIMENSION CNT(11),NM(11),JH(11),JHP(10,11)
        DATA      NMAX/3/,MMAX/ 90/,KMAX/20/
        DATA      STAR/'*'/,BLANK/'    '/
C
C       NY        NUMBER OF DEPENDENT VARIABLES
C       N         NUMBER OF INDEPENDENT VARIABLES
C       MDEG      MAXIMUM DEGREE
C       NDG       MAXIMUM DEGREE OF INDEPENDENT VARIABLE J
C       NMAX      STORAGE LIMIT ON INDEPENDENT VARIABLES
C       MMAX      STORAGE LIMIT ON DATA POINTS
C       KMAX      STORAGE LIMIT ON COEFFICIENTS
C
C       Y(K,L)    VALUE OF FUNCTION L AT POINT K
C       X(J,K)    VARIABLE J POINT K
C
C OPEN INPUT FILE
        CALL OPEN(9,'RMAFG.DAT ')
    2   READ(9,4)HY
    4   FORMAT(20A4)
        READ(9,6,END=12)NY,N,(NDG(J),J=1,N)
    6   FORMAT(20I4)
        IF(N.EQ.0)STOP 100
        MDEG=NDG(N)
        CALL SETZ(N,MDEG,NDG,NIW,LIW,NM,Z,NMAX,KMAX)
        READ(9,6)NDATA,MODE,IVAL
        WRITE(1,6)NY,N,(NDG(J),J=1,N),NDATA,MODE,IVAL
        IF(NDATA.LE.MMAX)GO TO  10
        WRITE(1,8)NDATA,MMAX
    8   FORMAT(' THE NUMBER OF DATA POINTS',I5,/'EXCEEDS THE
     X ALLOWED STORAGE',I5,' PROGRAM TERMINATED')
        STOP
   10   IF(NDATA.GE.NM(MDEG+1))GO TO  14
        WRITE(1,22)NDATA,NM(MDEG+1)
   12   STOP
   14   DO  16 K=1,NDATA
        READ(9,18,END=12)(XX(J,K),J=1,N),(Y(K,J),J=1,NY)
   16   WRITE(1,20)(XX(J,K),J=1,N),(Y(K,J),J=1,NY)
   18   FORMAT(10F8.0)
   20   FORMAT(1X,F7.2,9F8.3)
   22   FORMAT(' THE NUMBER OF DATA POINTS',I5/' IS LESS THAN THE
     X NUMBER OF COEFFICIENTS',I5,' PROGRAM TERMINATED')
```

```
24    WRITE(1,26)
26    FORMAT(' ENTER LP,L1,L2'/
     X  ' LP = 2 FOR LINE PRINTER,'/
     X  ' L1,L2 SELECTS DEPENDENT VARIABLES, L = L1,L2 ')
      READ(1,6)LP,L1,L2
      IF(LP.NE.2)LP = 1
      DO  92 L = L1,L2
      DO  28 K = 1,NDATA
      DO  28 J = 1,N
28    X(J,K) = XX(J,K)
      CALL SIGM(N,NDATA,NMAX,MODE,YM,YS,XM,XS,Y(1,L),X)
      M=KMAX+2
      DO  30 K=1,KMAX
      DO  30 J=1,M
30    C(K,J)=0.
      FER=0.
      I=NM(MDEG+1)
      DO  36 ND=1,NDATA
      WRITE(1,32)ND
      CALL SETU(N,MDEG,NIW,LIW,NDG,U,X(1,ND))
32    FORMAT(' ND ',I4)
      DO  34 J=1,I
      C(J,I+1)=C(J,I+1)+U(J)*Y(ND,L)
      DO  34 K=J,I
34    C(J,K)=C(J,K)+U(J)*U(K)
36    FER=FER+Y(ND,L)**2
      DO  38 J=1,I
38    C(J,I+2)=C(J,I+1)
      WRITE(LP,40)HY
40    FORMAT(1X,20A4/20A4/)
      WRITE(LP,42)YM,YS
42    FORMAT('    Mean ',F20.5,'  Sigma ',F20.5,'  for Function Y'//
     X  '   J   Degree ',5X,'  Mean',5X,'  Sigma:  for Parameters X( )')
      WRITE(LP,44)(J,NDG(J),XM(J),XS(J),J=1,N)
44    FORMAT(1X,I3,I5,2F15.5)
      IF(MODE.EQ.1)WRITE(LP,46)
      IF(MODE.EQ.2)WRITE(LP,48)
46    FORMAT(/' MEAN removed from Parameters X( ).')
48    FORMAT(/' MEAN removed from Parameters X( ), X normalized.')
      I2=I+2
      A=NDATA
      M=1
      DO  54 J=1,I
      CALL SOLVE(J,C,I,KMAX)
      IF(J.LT.NM(M))GO TO  54
      KM=NM(M)
      M=M+1
      ERR=FER
      DO  50 K=1,KM
50    ERR=ERR-C(K,I+1)*C(K,I+2)
      IF(ERR.GT.0.)ERR=DSQRT(ERR/A)
      WRITE(LP,52)KM,ERR,(Z(K),C(K,I+1),K=1,KM)
52    FORMAT(/' The error using',I5,' coefficients is',F15.5/
     X        ' Coefficients',10X,'  Value'//25(1X,F10.0,F20.6/))
54    CONTINUE
      DO  56 J=1,11
```

```
      JH(J)=0
   56 CNT(J)=0.
      CNTM=0.
      DO  60 ND=1,NDATA
      CALL SETU(N,MDEG,NIW,LIW,NDG,U,X(1,ND))
      FCN=0.
      DO  58 K=1,I
   58 FCN=FCN+U(K)*C(K,I+1)
C SET UP HISTOGRAM
      J=2.*(FCN-Y(ND,L))/ERR+6.5
      YP(ND)=FCN
      IF(J.LT.1)J=1
      IF(J.GT.11)J=11
      CNT(J)=CNT(J)+1.
      IF(JH(J).GE.10)GO TO  60
      JH(J)=JH(J)+1
      M=JH(J)
      JHP(M,J)=ND
   60 IF(CNT(J).GT.CNTM)CNTM=CNT(J)
      WRITE(LP,62)
   62 FORMAT(' Error Distribution - Histogram'/
     X ' Sigma       # Points',20x,'Point IndeX')
      CCS=1.
      IF(CNTM.GT.20)CCS=20./CNTM
      B=-2.5
      DO  64 J=1,11
      M=CNT(J)*CCS
      IF(M.EQ.0.AND.CNT(J).NE.0.)M=1
      M2=JH(J)
      M1=21-M
      IF(M.EQ.0)WRITE(LP,66)B,CNT(J)
      IF(M.GT.0.AND.M2.EQ.0)WRITE(LP,66)B,CNT(J),(STAR,K=1,M)
      IF(M.GT.0.AND.M2.GT.0)WRITE(LP,66)B,CNT(J),(STAR,K=1,M),
     X                          (BLANK,K=1,M1),(JHP(K,J),K=1,M2)
   64 B=B+.5
   66 FORMAT(1X,F6.2,F10.0,1X,21A1,10I4)
C PRINT FUNCTION Y AT VALUES OF X( ) USED TO DETERMINE FIT
      WRITE(LP,68)L
   68 FORMAT('1 Function',I2,' Evaluations at Given Input Points,'/
     X ' Point   Y(Input)     Y(Fit)        Parameters X( )')
      DO  72 M=1,NDATA
      IF(MODE.EQ.0)GO TO  72
      DO  70 K=1,N
      IF(MODE.EQ.2)X(K,M)=XS(K)*X(K,M)
   70 X(K,M)=X(K,M)+XM(K)
   72 WRITE(LP,74)M,Y(M,L),YP(M),(X(J,M),J=1,N)
   74 FORMAT(1X,I3,5F12.3)
      IF(IVAL.EQ.0)GO TO  92
C
COMPUTE AND PRINT EVALUATED VALUES AT SPECIFIED INPUT POINTS
C
      READ(9,6)NV
      IF(NV.EQ.0)GO TO  92
      WRITE(LP,76)L
   76 FORMAT(/' Function',I2,' Evaluations at Specified Input Points.'
     X /' Point   Y(Input)     Y(Fit)        Parameters X( )')
```

```
      DO  78 M=1,NV
   78 READ(9,80,END=92)(X(J,M),J=1,N),(Y(M,K),K=1,NY)
   80 FORMAT(10F8.0)
      DO  90 M=1,NV
      IF(MODE.EQ.0)GO TO  84
      DO  82 K=1,N
      X(K,M)=X(K,M)-XM(K)
   82 IF(MODE.EQ.2)X(K,M)=X(K,M)/XS(K)
   84 CALL SETU(N,MDEG,NIW,LIW,NDG,U,X(1,M))
      YP(M)=0.
      DO  86 K=1,I
   86 YP(M) = YP(M)+U(K)*C(K,I+1)
      IF(MODE.EQ.0)GO TO  90
      DO  88 K=1,N
      IF(MODE.EQ.2)X(K,M)=X(K,M)*XS(K)
   88 X(K,M)=X(K,M)+XM(K)
   90 WRITE(LP,74)M,Y(M,L),YP(M),(X(J,M),J=1,N)
C RETURN FOR OTHER DATA SETS
   92 IF(L.LT.L2)WRITE(LP,94)
   94 FORMAT(1H1)
      STOP
      END
```

```
COMPUTATION OF SUBSCRIPTS Z
C INITIAL COEFFICIENT CHECK; MODIFIED DEC 3 1981 FOR WP
      SUBROUTINE SETZ(N,MDEG,NDG,NIW,LIW,NM,Z,NMAX,KMAX)
      IMPLICIT REAL*8(A-H,O-Z)
      DIMENSION NIW(1),LIW(1),NDG(1),NM(1),Z(1)
      IF(N.LE.NMAX)GO TO  10
      WRITE(1,5)N,NMAX
    5 FORMAT(' THE NUMBER OF VARIABLES',I4,'EXCEEDS THE STORAGE LIMIT
     X OF',I4,' N HAS BEEN SET TO NMAX')
   10 Z(1)=0.
      IF(N.EQ.1)GO TO  25
      DO  20 J=2,N
      IF(NDG(J).GE.NDG(J-1))GO TO  20
      WRITE(1,15)(NDG(K),K=1,N)
   15 FORMAT(' THE VARIABLES ARE NOT ORDERED ON DEGREE-PROGRAM HAS
     X BEEN TERMINATED'/(1X,10I3))
      STOP
   20 CONTINUE
   25 I=1
      DO  30 J=1,N
   30 NIW(J) = I
      DO  55 M=1,MDEG
      NM(M)=I
      LU   =I
      DO  50 J=1,N
      LL = NIW(J)
      NIW(J) = I + 1
      IF(NDG(J).LT.M)LL = LL + 1
      DO  45 L=LL,LU
      IF(I.LT.KMAX)GO TO  40
      WRITE(1,35)KMAX
   35 FORMAT(' THE NUMBER OF COEFFICIENTS EXCEEDS THE STORAGE
     X LIMITS',I4,' PROGRAM HAS BEEN TERMINATED')
      STOP
   40 I=I+1
      Z(I)=10.*Z(L)+J
   45 CONTINUE
   50 CONTINUE
   55 CONTINUE
      NM(MDEG+1)=I
      RETURN
      END
```

```
C RMSUB.FOR
COMPUTATION OF U VECTOR; MODIFIED DEC 3 1981 FOR WP
      SUBROUTINE SETU(N,MDEG,NIW,LIW,NDG,U,X)
      IMPLICIT REAL*8(A-H,O-Z)
      DIMENSION NIW(1),LIW(1),NDG(1),U(1),X(1)
      U(1)=1.
      I   =1
      DO   5 J=1,N
    5 NIW(J)=I
      DO  20 M=1,MDEG
      LU=I
      DO  15 J=1,N
      LL = NIW(J)
      NIW(J) = I + 1
      IF(NDG(J).LT.M)LL = LL + 1
      DO  10 L=LL,LU
      I=I+1
      U(I)=X(J)*U(L)
   10 CONTINUE
   15 CONTINUE
   20 CONTINUE
      RETURN
      END
```

```
CALCULATION OF MEANS AND SIGMAS, DATA NORMALIZATION
      SUBROUTINE SIGM(N,NDATA,NMAX,MODE,YM,YS,XM,XS,Y,X)
      IMPLICIT REAL*8(A-H,O-Z)
      DIMENSION XM(1),XS(1),Y(1),X(3,1)
      YM=0.
      YS=0.
      DO   5 I=1,NMAX
      XM(I)=0.
    5 XS(I)=0.
      DO  10 ND=1,NDATA
      YM=YM+Y(ND)
      YS=YS+Y(ND)**2
      DO  10 J=1,N
      XM(J)=XM(J)+X(J,ND)
   10 XS(J)=XS(J)+X(J,ND)**2
      A=NDATA
      YM=YM/A
      DO  15 J=1,N
      XM(J)=XM(J)/A
   15 XS(J)=DSQRT(XS(J)/A-XM(J)**2)
      YS=DSQRT(YS/A-YM**2)
      IF(MODE.EQ.0)GO TO  25
      DO  20 ND=1,NDATA
      DO  20 J=1,N
      X(J,ND)=X(J,ND)-XM(J)
   20 IF(MODE.EQ.2)X(J,ND)=X(J,ND)/XS(J)
   25 RETURN
      END
```

```
C SOLUTION OF SYSTEM EQUATIONS, SINGLE ROW AT EACH CALL
      SUBROUTINE SOLVE(I,A,N,M)
      IMPLICIT REAL*8(A-H,O-Z)
      DIMENSION A(20,1)
      IF(I.EQ.1)GO TO  15
      IM=I-1
      DO  10 J=1,IM
      A(I,J)=0.
      DO   5 K=1,IM
    5 A(I,J)  = A(I,J)+A(J,K)*A(K,I)
      A(I,N+1)= A(I,N+1)-A(J,I)*A(J,N+1)
   10 A(I,I)  = A(I,I)-A(I,J)*A(J,I)
   15 IF(A(I,I).NE.0.)A(I,I)=1./A(I,I)
      A(I,N+1)= A(I,N+1)*A(I,I)
      IF(I.EQ.1)GO TO  30
      DO  25 J=1,IM
      A(J,I)  =-A(I,J)*A(I,I)
      DO  20 K=J,IM
      A(J,K)  = A(J,K)-A(I,K)*A(J,I)
   20 A(K,J)  = A(J,K)
      A(J,N+1)= A(J,N+1)-A(I,N+1)*A(I,J)
   25 A(I,J)  = A(J,I)
   30 RETURN
      END
```

APPENDIX C

LISTING OF DELTA ALGORITHM FORTRAN PROGRAM FOR COMPUTATION OF DYNAMICALLY EQUIVALENT SYSTEM

```
COMPUTATION OF DYNAMICALLY EQUIVALENT SYSTEM USING DELTA ALGORITHM
C        NJNT=NSEG-1 ONLY
       IMPLICIT REAL*8(A-H,O-Z)
        BYTE TITLE(80,6)
        DIMENSION SEG(22),CGS(22),PHI(3,3,22),CK(3,22)
        DIMENSION W(22),RW(22),DM(22),PH(3,22),BD(6,22)
        DIMENSION SR(3,42),YPR1(3,21),YPR2(3,21)
        DIMENSION JOINT(21),JS(21),JNT(21),IPIN(21)
        DIMENSION D(3,3,22),ANG(3,22),PHS(3,3,22)
C TEMP**********************   DATA FOR SAMPLE CASE
        DATA LP/2/
        DATA DM/-1.25, 0.00, 0.50,-1.00, 0.50,-0.25, 0.25, 0.50,
     X          -0.25, 0.25, 0.50,-0.25, 0.50,-0.25, 0.50,7*0.0/
C TEMP**********************  END DATA FOR SAMPLE CASE
        DASIN(Z) = DTAN2(Z,DSQRT(1.0D0 - Z*Z))
        PI = DTAN2(0.0D0,-1.0D0)
        RADIAN = 180.0/PI
C OPEN INPUT FILE, USES STANDARD CVS FORMAT FOR MODEL DESCRIPTION
        CALL OPEN(6,'CVSKANE.DAT ')
    1   READ(6,2,END=110,ERR=110)TITLE
    2   FORMAT(80A1)
        READ(6,5) NSEG,NJNT,G
    5   FORMAT(2I6,F10.0)
        DO 10 I = 1,NSEG
   10   READ(6,15)  SEG(I),CGS(I),W(I),(PH(J,I) ,J=1,3),(BD(J,I),J=1,6)
   15   FORMAT(A4,1X,A1,10F6.0)
        DO 20 J = 1,NJNT
   20   READ(6,25) JOINT(J),JS(J),JNT(J),IPIN(J),(SR(I,2*J-1),I=1,3),
     *             (SR(I,2*J),I=1,3),(YPR1(I,J),I=1,3),(YPR2(I,J),I=1,3)
   25   FORMAT(A4,1X,A1,2I4,6F6.0/14X,6F6.0)
C
C ENTER WEIGHT PERTURBATIONS:  (FROM TERMINAL)
C TEMPORARILY USE DATA STATEMENT **INSERT DESIRED INPUT STATEMENTS
C       WRITE(1,26)
C  26   FORMAT(' ENTER LP,DM(I); LP = 2 FOR PRINTER, SUM DM`S = 0'/
C    X  ' PROGRAM WILL COMPUTE DM(1) TO PRODUCE A ZERO SUM'/)
C       READ(1,27)LP,(DM(I),I=1,NSEG)
C  27   FORMAT(I3,15F5.0)
C TEMPORARILY USE DATA STATEMENT ******************************
C END OF INPUT FROM TERMINAL
        IF(LP.NE.2) LP = 1
        SUM = 0.0D0
        DO 28 I = 2,NSEG
   28   SUM = SUM + DM(I)
        DM(1) = - SUM
C
   30   FORMAT(10F6.0)
        WRITE(LP,31)TITLE
   31   FORMAT(' DYNAMICALLY EQUIVALENT SYSTEM'/6(1X,80A1/))
        WRITE(LP,35) NSEG,NJNT
```

```
35   FORMAT(1X,'SEGMENTS',I5,'  JOINTS',I5//
  *  32X,'SEGMENT MOMENT OF INERTIA',19X,'SEGMENT CONTACT ELLIPSOID'/
  *   '   SEGMENT',7X,'WEIGHT',45X,'SEMIAXES',19X,'CENTER'/)
     DO 40 I = 1,NSEG
40   WRITE(LP,45)I,SEG(I),CGS(I),W(I),(PH(J,I),J=1,3),(BD(J,I),J=1,6)
45   FORMAT(I3,1X,A4,2X,A1,5X,F7.3,3X,3F11.5,2(5X,3F7.2))
     WRITE(LP,50)
50   FORMAT(///
  *  3X,'JOINT',15X,'LOCATION',8X,'SEG(JNT)',
  *              3X,'LOCATION',8X,'SEG(J+1)',
  *              2X, 'PRIN. AXIS(DEG) - SEG(JNT)',
  *              2X, 'PRIN. AXIS(DEG) - SEG(J+1)'/
  *   '  J SYM PLOT JNT PIN',2(6X,'X',8X,'Y',8X,'Z',3X),
  *               2(5X,'YAW',5X,'PITCH',5X,'ROLL',1X)/)
     DO 55 J = 1,NJNT
55   WRITE(LP,60)J,JOINT(J),JS(J),JNT(J),IPIN(J),(SR(I,2*J-1),I=1,3),
  *            (SR(I,2*J),I=1,3),(YPR1(I,J),I=1,3),(YPR2(I,J),I=1,3)
60   FORMAT(1X,I2,1X,A4,2X,A1,2I4,4(1X,3F9.2))
     WRITE(LP,65)(DM(I),I=1,NSEG)
65   FORMAT(//' WEIGHT PERTURBATIONS'//2(4X,15F8.4/))
     WRITE(LP,66)
66   FORMAT(1H1)
     DO 75 N = 1,NSEG
     DO 75 I = 1,3
       DO 70 J = 1,3
70     PHI(I,J,N)=0.
75   PHI(I,I,N)=PH(I,N)
           CALL DELTA(NSEG,NJNT,JNT,DM,SR,CK,PHI,G,W,RW,LP)
     WRITE(LP,66)
     DO 85 N = 1,NSEG
       DO 80 I = 1,3
         DO 80 J = 1,3
80       PHS(I,J,N)=PHI(I,J,N)
     CALL EIGEN (PHI(1,1,N),D(1,1,N))
     ANG(1,N) = DTAN2(D(2,1,N),D(1,1,N))*RADIAN
     ANG(2,N) = -DASIN(D(1,3,N))*RADIAN
     ANG(3,N) = DTAN2(D(2,3,N),D(3,3,N))*RADIAN
     WRITE(LP,90)N,W(N),((PHS(I,J,N),J=1,3),CK(I,N),PHI(I,I,N),
  *  (D(I,J,N),J=1,3),ANG(I,N),I=1,3)
85   IF(MOD(N,8).EQ.0)WRITE(LP,66)
90   FORMAT(/' SEGMENT',I4,'  WEIGHT',F7.3/
  *  12X,'INERTIA MATRIX',12X,'OFFSET',2X,'EIGENVALUES', 6X,
  *  'DIRECTION COSINE',9X,' Y-P-R'/
  *  3(5F11.5,3F10.6,F11.5/))
     WRITE(LP,95)
95   FORMAT(1H1,
  *  2X,'JOINT',15X,'LOCATION',8X,'SEG(JNT)',
  *              3X,'LOCATION',8X,'SEG(J+1)'/
  *         20X,2(6X,'X',8X,'Y',8X,'Z',3X)/)
     DO 100 J = 1,NJNT
```

```
100   WRITE(LP,105)J,(SR(I,2*J-1),I=1,3),(SR(I,2*J),I=1,3)
105   FORMAT(4X,I3,12X,2(1X,3F9.2))
      GO TO 1
110   WRITE  (LP,111)
111   FORMAT(/'  END OF DELTA PROGRAM.')
      STOP 111
       END
```

```
C
      SUBROUTINE DELTA(NSEG,NJNT,JNT,DM,SR,CK,PHI,G,W,RW,LP)
      IMPLICIT REAL*8(A-H,O-Z)
      DIMENSION JNT(21),JT(21),IG(22)
      DIMENSION PHI(3,3,22),CK(3,22),W(22),RW(22),DM(22),SR(3,42)
      WRITE(LP,1)
    1 FORMAT(' COMPUTATIONS OF DELTA ALGORITHM'/)
      SUM = 0.0
      DO 5 N = 1,NSEG
      W(N)  = W(N) + DM(N)
      RW(N) = G/W(N)
      SUM   = SUM + DM(N)
        DO 5 I =1,3
    5   CK(I,N)=0.
C     DELTA ALGORITHM
C
      DO 90 N = 1,NSEG
C
C     COPY JOINT ARRAY
C
        DO  10  J=1,NJNT
   10   JT(J) = JNT(J)
      SUMT  = 0.0
        DO 35 J = 1,NJNT
C
C     CHECK DIRECT REFERENCE TO JOINT
C
        IF  (JT(J).NE.N)  GO TO 35
        K = N
        M = 1
        IG(M) = J + 1
        JM =  2*J - 1
        JT(J) = 0
        SUM   = DM(J+1)
        SUMT  = SUMT + SUM
        WRITE (LP,100)N,J,K,DM(J+1),SUM,SUMT
  100   FORMAT(1X,3I4,3F10.4)
   15     DO  20  K=1,NJNT
C
C     CHECK FOR STRING
C
          IF  (JT(K).NE.IG(M))  GO TO 20
          M = M + 1
          IG(M) = K + 1
          SUM   = SUM  + DM(K+1)
          SUMT  = SUMT + DM(K+1)
          WRITE(LP,100)N,J,K,DM(K+1),SUM,SUMT
          JT(K) = 0
   20     CONTINUE
        M = M - 1
```

```
C
C       CHECK FOR BRANCHES
C
          IF  (M.GT.0)  GO TO 15
C       **  PROCESS JOINT JM FOR RK ODD **
          SRR = SR(1,JM)**2 + SR(2,JM)**2 + SR(3,JM)**2
            DO 30 L = 1,3
            CK(L,N)  = CK(L,N) + SUM*SR(L,JM)
              DO 25 I = 1,3
   25         PHI(I,L,N) = PHI(I,L,N) + SUM*SR(I,JM)*SR(L,JM)/G
   30       PHI(L,L,N) = PHI(L,L,N) - SUM*SRR/G
   35       CONTINUE
          IF  (N.EQ.1)  GO TO 50
C
C       ALL REMAINING SEGMENTS
C
          SUM   = -(SUMT+DM(N))
C       **  PROCESS  JOINT N-1 FOR RK EVEN **
          JM=2*(N-1)
          SRR=SR(1,JM)**2+SR(2,JM)**2+SR(3,JM)**2
            DO 45 J = 1,3
            CK(J,N)  =CK(J,N)+SUM*SR(J,JM)
              DO 40 I = 1,3
   40         PHI(I,J,N) = PHI(I,J,N) + SUM*SR(I,JM)*SR(J,JM)/G
   45       PHI(J,J,N)=PHI(J,J,N)-SUM*SRR/G
   50     CKK =0.
            DO 55 J = 1,3
            CK(J,N)=CK(J,N)/W(N)
   55       CKK=CKK+CK(J,N)**2
          CKK=CKK/RW(N)
            DO 60 I = 1,3
            PHI(I,I,N)=PHI(I,I,N)-CKK
              DO 60 J = 1,3
   60         PHI(I,J,N) = PHI(I,J,N)+CK(I,N)*CK(J,N)/RW(N)
            DO 65 I = 1,3
   65       IF(N.NE.1)SR(I,JM)=SR(I,JM)+CK(I,N)
            DO 75 J = 1,NJNT
            IF(JNT(J).NE.N)GO TO 75
              DO 70 I=1,3
   70         SR(I,2*J-1)=SR(I,2*J-1)+CK(I,N)
   75       CONTINUE
   90     CONTINUE
          RETURN
          END
```

```
C
      SUBROUTINE EIGEN (A,D)
C
C     COMPUTES EIGENVALUES AND EIGENVECTORS OF A 3X3 SYMMETRIC MATRIX A
C     EIGENVALUES ARE IN A(I,I), A(I,J)=0 FOR I#J.
C     EIGENVECTORS ARE THE COLUMNS OF D(I,J).
C     D IS THE DIRECTION COSINE MATRIX RELATING THE ORIGINAL A MATRIX
C     TO THE PRINCIPAL SYSTEM OF COORDINATES.
C     A SUCCESSIVE ROTATION ALGORITHM IS USED.
C
      IMPLICIT REAL*8(A-H,O-Z)
      DIMENSION A(3,3) , D(3,3) , TEMP(3,3)
      TEST = 0.0
      DO  11  I=1,3
        DO  10  J=1,3
        TEST = TEST + DABS(A(I,J))
10      D(I,J) = 0.0
11    D(I,I) = 1.0
      TEST = TEST*1.0D-16
12    J = 2
      K = 3
13    I = 6-K-J
      IF  (DABS(A(I,J)).LT.TEST)  GO TO 15
      B = A(I,I) - A(J,J)
      R = DSQRT(B**2 + 4.0*A(I,J)**2)
      S = DABS(0.5*B/R)
      C = DSQRT(0.5+S)
      S = DSQRT(0.5-S)
      IF  (B*A(I,J).GT.0.0)  S = -S
      T1     = C*A(I,I) - S*A(I,J)
      T2     = S*A(I,I) + C*A(I,J)
      A(I,I) = C*T1 - S*(C*A(I,J)-S*A(J,J))
      A(J,J) = S*T2 + C*(S*A(I,J)+C*A(J,J))
      T1     = C*A(I,K) - S*A(J,K)
      A(J,K) = S*A(I,K) + C*A(J,K)
      A(I,K) = T1
      DO  14  L=1,3
      T1     = C*D(L,I) - S*D(L,J)
      D(L,J) = S*D(L,I) + C*D(L,J)
14    D(L,I) = T1
      A(K,I) = A(I,K)
      A(K,J) = A(J,K)
15    A(I,J) = 0.0
      A(J,I) = 0.0
      IF  (DABS(A(I,K))+DABS(A(J,K)).LT.TEST)  GO TO 21
      J = 3
      K = K-1
      IF  (K-1)  12,13,13
21    DO  23  ITER=1,10
      CALL CFACTT (D,TEMP,DET)
```

```
        DO  22  I=1,3
          DO  22  J=1,3
          D(I,J) = 0.5*(D(I,J)+TEMP(J,I)/DET)
22        IF  (DABS(D(I,J)).LT.1.0D-15)  D(I,J)=0.0
      IF  (DABS(DET-1.0).LT.1.0D-6)  GO TO 25
23    CONTINUE
      WRITE (1,24) DET
24    FORMAT('0 EIGEN RENORMALIZATION DID NOT CONVERGE, DET ='
     X  ,1PD25.15)
25    RETURN
      END
```

```
C
      SUBROUTINE CFACTT (A,B,D)
C
C        GIVEN 3X3 MATRIX A
C        COMPUTE B TRANSPOSE OF COFACTORS (SIGNED MINORS)
C        AND D THE VALUE OF THE DETERMINANT OF A.
C        INVERSE OF A IS B(J,K)/D
C
      IMPLICIT REAL*8 (A-H,O-Z)
      DIMENSION A(3,3),B(3,3)
       M = 4
       L = 2
       N = 3
       D = 0.0
      DO 20 J=1,3
       B(J,J) = A(L,L)*A(N,N)-A(L,N)*A(N,L)
       IF (J.EQ.3) GO TO 20
       L = N
       N = J
       KK = J+1
        DO 15 K=KK,3
        M = M-1
        B(K,J) = A(K,M)*A(M,J)-A(K,J)*A(M,M)
   15   B(J,K) = A(J,M)*A(M,K)-A(J,K)*A(M,M)
   20  D = D+A(1,J)*B(J,1)
       RETURN
      END
```